Strategies for molecular structure elucidation in static and dynamic systems

Strategies for molecular structure elucidation in static and dynamic systems

Darya Hadavi

Doctoral thesis, Maastricht University—Faculty of Health, Medicine & Life Sciences

Cover design: Elahe Hadavi, Darya Hadavi

Print: ProefschriftSpecialist, www.proefschriftspecialist.nl

ISBN: 978-94-93330-05-4

Strategies for molecular structure elucidation in static and dynamic systems

Dissertation

To obtain the degree of Doctor at Maastricht university on the authority of the Rector Magnificus,

Prof. Dr. Pamela Habibović

In accordance with the decision of the Board of Deans to be defended in public on

Tuesday, 30th of May 2023 at 10:00 hrs.

By

Darya Hadavi

Promoter:
Prof. Dr. Maarten Honing
Co-promoters:
Dr. Tiffany Porta Siegel
Dr. Eva Cuypers

Assessment committee:
Prof. Dr. Ron Heeren (chair)
Prof. Dr. Edwin De Pauw, University of Liège, Belgium
Dr. Ingrid Dijkgraaf
Prof. Dr. Lorenzo Moroni
Dr. Tim Causon, University of Natural Resources and Life Sciences, Vienna

Dedication

This thesis is dedicated to my sister and brother, who are my friends and role models

Dr. Elahe Hadavi

&

Ir. Rashed Hadavi

You are the primary reason that I could be where I am standing now.

Table of Contents

General introduction

Strategies for molecular structure elucidation in static and dynamic systems

General introduction

As the substances of life, molecules exist in a wide range of sizes from a few nanometres to greater than 1 micrometer. In such a broad range, one can find small molecules like water and drugs or large molecules like DNA, proteins, or even viruses (Figure 1). Interestingly, any type of feeling thought and health state largely stems from these chemical units of life, molecules [1]. The intrinsic features of a molecule, the way molecules interact with each other, their existence or not, and even the speed of their transportation or interaction govern their function and eventually the process of life. Knowing this fact highlights the importance of characterizing molecules.

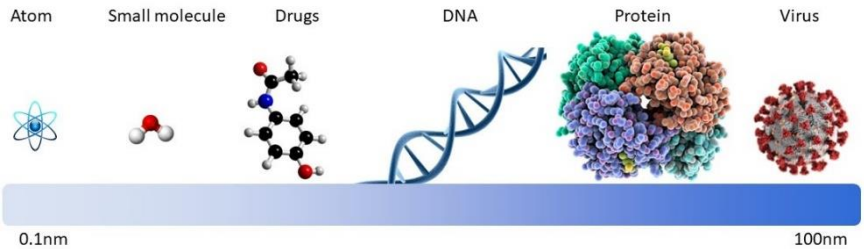

Figure 1. Molecular size chart.

In the field of life science, whether it is about understanding a natural biological mechanism or a disease pathway or about drug discovery and development, one must first elucidate the composition, structure, and properties of natural? or synthesized molecules. It is because there is a close relationship between the behavior and function of a molecule with its constituent, configuration, and conformation [1]. While the chemical constitution represents the elements of a molecule, the chemical configuration and conformation give information regarding the coordination of atoms and their 3-dimensional (3D) spatial arrangements. These factors determine the physiochemical properties of a molecule. In addition, these factors enable us to unravel the mechanisms underlying molecular interactions between each other and with the biological microenvironment.

There are multiple analytical techniques for compositional and structural elucidation of a molecule such as ultraviolet-visible (UV-Vis), infrared (IR), Raman, or nuclear magnetic resonance (NMR) spectroscopy, X-ray crystallography, mass spectrometry (MS) and ion mobility spectrometry (IMS). While a true chemist will never rely on only one technique, mass spectrometry is one of the prime techniques of choice to tentatively characterize a molecule. This is due to the capability of MS to simultaneously detect, identify and quantify a molecule in a pure or a large number of molecules at low concentrations in a complex sample [2].

Usually, MS works as follows [3]; Molecules are introduced to MS through an ionization source, which ionizes molecules with a positive or negative charge. This is followed by a

mass analyzer to separate ions based on their mass-over-charge ratio (*m/z*). Ions are then detected based on their time of travel or frequency of motion in a magnetic or electrostatic field. Depending on the type of ionization source, one can analyze liquid or solid samples enabling a user to collect time resolved or spatially resolved information.

In general, from the molecular mass limited structural information can be derived, other than double bond and cyclic equivalents and an estimation of the elemental composition [4]. Nonetheless, due to the disposition of excess energy in the molecules as a result of the ionization processes, fragmentation of the molecules allows for elaboration on the constitution and rarely the configuration of molecular structures. In so-called soft ionization techniques like electrospray, fragmentation hardly occurs. Thus, to generate fragment ions, a variety of tandem mass spectrometry (MS/MS) approaches are used to for instance fragment a precursor ion upon collision of the molecules with inert gasses (e.g. Ar, N_2). The detected fragment ions are like pieces of a puzzle, which could then be used to study the fragmentation energy and pathway. These data provide compositional and structural information regarding the original precursor ion and increase the specificity and confidence of identification.

Mass spectrometry alone lacks the capacity of discriminating between isomeric or even isobaric compounds. Molecules with identical molecular formulas but different spatial arrangements (isomers) and molecules with similar masses but different molecular formulas and geometry (isobars) show overlapping *m/z* peaks in MS (Figure 2). Even though isobaric compounds could be discriminated by high-resolution mass spectrometry and/or with unique fragmentation patterns obtained from tandem mass spectrometry, discrimination of isomeric molecules only by MS remains challenging.

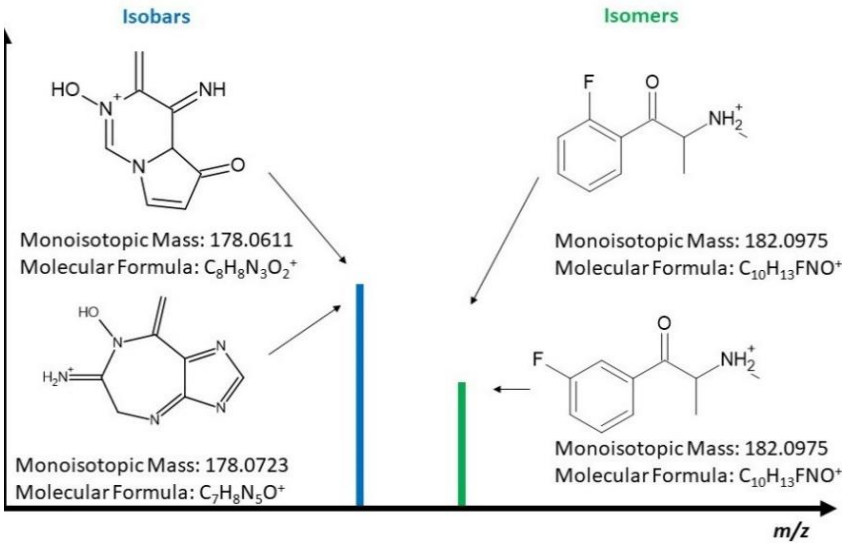

Figure 2. MS profile of isobars and isomers. Overlapping m/z value of isomeric molecular ions that have identical molecular formulae and mass but distinct spatial arrangements

of atoms (green line). Overlapping m/z value of isobaric molecular ions that have similar mass but consisted of different elements and geometry (blue line).

Here, ion mobility spectrometry is expected to play a pivotal role. It enables the separation of ions in the gas phase not only based on their mass and charge but also based on their 3D shape [5]. The principle of IMS is based on the separation of gas-phase ions in the electric field (E) due to collisions with the inert gas particles (e.g. N_2) [6]. The output is the mobility (K), a ratio of the terminal drift velocity v_d (the constant velocity ions reach driven by E) to the electric field [7].

$$K=\frac{v_d}{E} \qquad \text{Eq.1}$$

To correct for the difference in experimental parameters, reduced mobility K_0 is commonly used (Eq.2), where N is the neutral gas number density, p is the pressure, T is the temperature, and N_0, p_0, and T_0 are considered to be standard conditions [5, 8].

$$K_0=\frac{N}{N_0}=\left(\frac{p}{p_0}\right)\left(\frac{T_0}{T}\right) \qquad \text{Eq.2}$$

Smaller ions or ions with higher charge will have higher mobility values and reach the detector fast. IMS also introduces a new variable – momentum transfer collision integral usually called collisional cross section (CCS or Ω) to differentiate among isomers of different sizes and shapes [9, 10]. Even though CCS values could be deduced by different methods, for instance for large molecules by measuring the energy loss of protein ions while passing through a collision cell [9, 11], this thesis relies on ion mobility derived CCS values. This value can be calculated using the fundamental low-field ion mobility equation:

$$\Omega=\frac{3}{16}\left(\frac{2\pi}{\mu k_B T}\right)^{\frac{1}{2}}\frac{zeE}{Nv_d} \qquad \text{Eq.3}$$

Where z and e are the molecular and electronic charge, μ is the reduced mass and k_B is the Boltzmann constant [7, 8]. While this equation is considered to be an approximation, it is still widely used to calculate the CCS values [12]. Obtaining CCS data has the potential to identify and assess the configuration and constitution of unknown molecular structures; for instance by comparing the experimental values to the theoretically computed CCS values. Unlike the arrival time, which depends on the experimental conditions and the used instrument, K_0, and CCS values can be compared across all measurements performed in the low-field limit (where E/N is small enough not to affect the K_0) [5].

There are multiple commercial ion mobility instruments with diverse working principles. For instance, in traveling wave ion mobility spectrometry (TWIMS) ions are propelled by a sequence of symmetric potential waves occurring continuously in a gas-filled ion guide. In this setting, ions are separated based on the mobility of ions in the gas phase, the velocity and amplitude of the traveling wave, and the gas pressure (buffer gas) (Figure 3a) [13]. While trapped ion mobility spectrometry (TIMS) has a different

separation mechanism. In this instrument, radially confining radio frequency voltages along with an axial electric field are created in the ion mobility cell, where ions are "trapped" for a few milliseconds. In the meantime, a continuous flow of neutral gas (buffer gas) exerts a drag force on ions toward the detector. The magnitude of the electric field is then lowered in a stepwise fashion eluting ions based on their mobility, from a large to a small size-to-charge ratio (Figure 3b) [14].

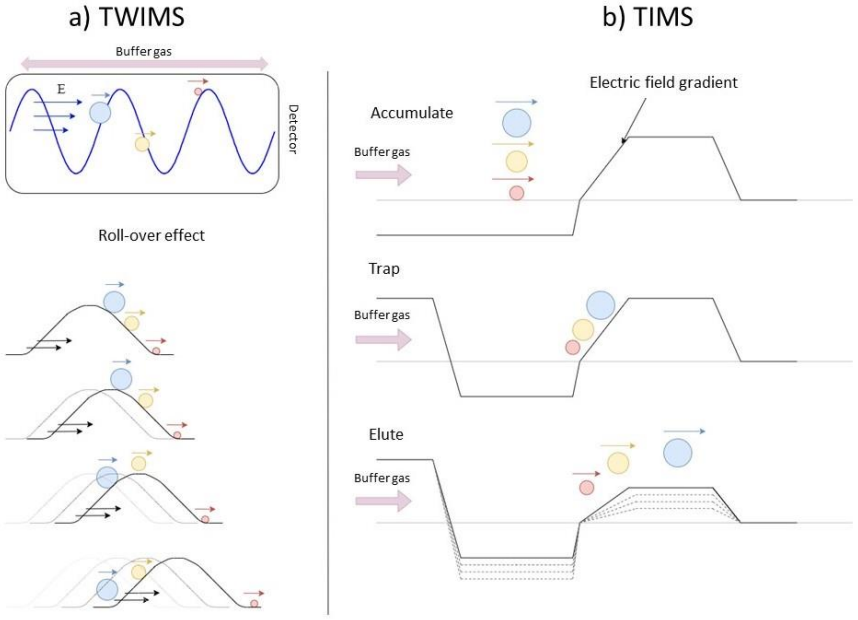

Figure 3. Schematic representation of the separation mechanisms of TWIMS and TIMS instruments (adapted from[15, 16]).

Regardless of the working mechanism of each instrument the mutual feature of them is in their capacity to separate ions with the same mass but different geometry, some instruments separate with better resolution than others. Over the years, ion mobility spectrometry, mass spectrometry, and tandem mass spectrometry (IMS-MS-MS/MS) have been used in combination, which affords higher identification and characterization capacity as well as greater specificity [17]. The capacity of IMS-MS-MS/MS is not just limited to molecular detection, identification, and characterization. Using this combinatorial analytical technique, one can also study the molecular interactions and kinetics, which is of special importance for life science discoveries, such as protein-protein or drug-protein interactions. However, one major uncertainty in the application of IMS-MS-MS/MS for molecular interaction studies is related to the gas phase nature of the analysis, as ionized molecules traverse through the vacuum chamber of MS and IMS until they hit the detector. While biological events happen in a liquid phase. Hence, there is an ever-standing question of whether the ionized molecules in the gas phase of MS and IMS behave the same as in the liquid phase of the biological microenvironment.

To study molecular interactions in a liquid phase, one might utilize analytical techniques such as co-immunoprecipitation, pull-down, and enzyme-linked immunosorbent assays (ELISA). Even though these techniques provide information such as the occurrence of a binding and binding affinity, they are static, and their detection is label dependent. In contrast, the newly emerged technique of surface plasmon resonance (SPR) can overcome the mentioned limitations and offer even more advantages.

SPR is a label-free optical technique, which provides information on binding affinity, association and disassociation rates of molecular interactions and most importantly enables time-resolved analysis [18]. The technique is based on the principle of Krestchmann configuration (Figure 4a). The incoming p-polarized light goes through a prism at an incident angle (θ) and reflects from an electrically conductive surface to the photodetector [19]. The energy from the incoming light couples with the electrons presents on the metal sensor causing the excitation of electrons which propagate parallel to the sensor surface [19, 20]. The metal sensor chips used in the SPR experiments are usually gold coated and can be functionalized by the addition of desired molecules. When there is a molecular interaction at the sensor surface, the refractive index of the surrounding medium changes, which concomitantly changes the angle of the reflected light [19]. These changes could be plotted in the time domain as a sensorgram, from which baseline, association, dissociation, and regeneration phases can be detected (Figure 4b). These data are then used to quantify the quality of molecular interactions.

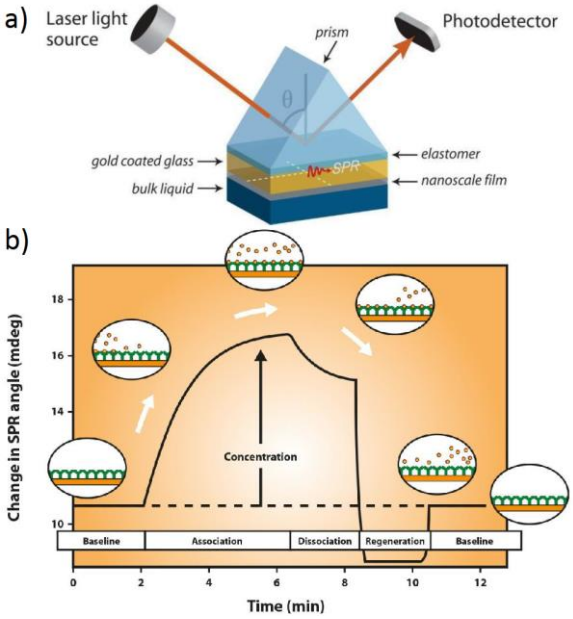

Figure 4. Figure 3: surface plasmon resonance measurement based on Kretschmann configuration (Adapted from BioNavis).

Time-resolved analysis by SPR along with its high sensitivity opens windows for real-time measurements of dynamic biological systems. For instance, one could mimic blood flow and analyze cell-molecule interactions. Alternatively, one could couple a microflow reactor or an organ-on-a-chip platform to SPR and analyze dynamic molecule-molecule/cell interactions of produced chemicals or excreted metabolites.

This thesis explores the potential of innovative techniques (i.e., IMS-MS-MS/MS and SPR, but not limited to) to answer fundamentally relevant questions. It exploits the dynamic nature of molecules when interacting with each other (either in the gas phase or liquid phase) to separate and study their structural properties. This is expected to improve our understanding of molecules of interest for various fields such as biology and pharmaceutical development. This thesis is composed of three chapters, that are articulated around the following curiosity-driven hypotheses.

Challenges & scientific approaches

Chapter 1 – Dynamics of small molecules in ion mobility spectrometry

Section 1- Adduct ion formation as a tool for the molecular structure assessment of ten isomers in traveling wave and trapped ion mobility spectrometry

Nature is filled with isomeric molecules, which serve different physiological effects despite having the same mass [21]. This is also true for engineered small molecules like drugs and similarly important, drug metabolites. This reality raises the concern of identifying and separating these isomeric molecules. The main challenge in characterizing these molecules emerges when the mass and/or tandem mass spectrum of isomeric molecules are not sufficient to differentiate these molecules. Ion mobility spectrometry, on the other hand, adds another differentiation dimension based on the charge, size, and ultimately conformation (shape) of molecules. However, even with IMS, it is not trivial to distinguish molecules that have only slight spatial differences. The reported solutions for this challenge were to use adducts such as sodium (Na) [22, 23]. Based on the localization of an adduct on each isomer, ions adopt different 3D-conformation and shapes. For instance, imagine a molecule with an open structure. As soon as an adduct ion is in proximity, the molecule hugs that adduct and forms ball like structure. Such conformational changes potentially enable isomers' separation in the gas phase of ion mobility. However, this approach does not always aid in separation, because the adduct itself might induce only a minimal spatial difference, insufficient for differentiation. To overcome this challenge, **the assumption was that adducts with different sizes, as well as adduct salt ions (such as $[M+2Na-H]^+$), could impose more degree of conformational differences between the isomeric ions. In addition, it was hypothesized that by fragmenting away the identical parts of an adduct ion by performing MS/MS before the ion mobility cell, it will be possible to highlight the small conformational differences and enable discrimination.** Hence, these hypotheses are investigated in Chapter 1- Section 1.

Section 2- Uncovering the behavior of ions in the gas phase to predict the ion mobility separation of isomeric steroid compounds

Utilizing solely MS for separating complex (pre-)clinical samples is often not sufficient [24]. This is mainly because such complex biological matrices are composed of a diverse range of molecules, including those with similar structures but the same mass. For instance, bile acids that are highly involved in different physiological processes exist in various structural isomeric forms [25]. Even though ion mobility offers a solution for this complexity, the majority of previous studies have only focused on ion mobility examinations on a single isomer rather than a mixture of them. Thus, **a challenge was set to test our previous hypotheses on the mixture of isomers.** To this end, the molecules of choice were clinically important bile acid isomers. This approach could open possibilities to translate a working separation strategy on actual complex (pre-) clinical samples.

In addition, despite having a fast-growing number of papers in the field of ion mobility separations, there is very limited knowledge on interpreting complex ion mobility data and understanding the fate of a molecule after ionization until it reaches a detector. Therefore, it was needed to understand the behavior of ions in the gas phase. To do so, **the assumption was that, by extracting experimental collision cross sections and comparing them to the theoretical molecular modelling, it will be possible to shed light on the fate of ions in the ion mobility cell.** It was hypothesized that it will give the insight to predict the possibility of separating isomeric molecules. This in turn allows smart planning, such as applying necessary pre-treatment strategies for effective analysis of complex (pre-) clinical samples. Hence, these hypotheses are investigated in Chapter 1-Section 2.

Chapter 2- Dynamics of biopolymers by ion mobility spectrometry and Surface plasmon resonance

Section 1- Buffer 4-ethylmorpholine/acetate maintains solution-phase folding for native mass spectrometry of proteins and proteins complexes

Next to small molecules' conformational changes, understanding the 3D structure of large molecules (e.g. proteins) is essential. This can enable us to elucidate their function and explain molecule-molecule interactions. Mass spectrometry and ion mobility have proven their potential for interaction studies [26]. However, there is an important challenge in utilizing IMS-MS to investigate protein-protein interactions. This challenge is about preserving the natural geometry of proteins in the gas phase. One approach to address this challenge is to keep the structural integrity of proteins in the liquid phase just before their introduction into MS and IMS [27]. This highlights the importance of buffer type (liquid phase) and sample preparation before MS analysis. The commonly used buffers have some limitations such as lacking a buffer capacity around the physiological pH. Thus, it was important to find an alternative. To do so, **it was hypothesized that 4-ethylmorpholine/acetate (4EM/A) buffer with pK_a of 7.72/4.76 could preserve the spatial arrangement of proteins and could be eventually used for interaction studies. In addition, it was assumed that the commonly used protein sample preparation process of centrifugal filtration impacts the 3D conformation of proteins, which can only be elucidated by IMS rather than MS.** The assumptions tested on standard proteins as well as the biologically and clinically important protein complex,

cardiac troponin complex. Hence, these hypotheses are investigated in Chapter 2- Section 1.

Section 2- Investigating the protein-protein interactions of cardiac troponin subunits using surface plasmon resonance

Considering the important role of the cardiac troponin complex in one of the leading causes of death, myocardial infarction (MI), it is of special value to elucidate the protein-protein interaction of its subunits [28]. Despite in-depth studies on the structure of this complex, there are some controversies regarding the orientation of each subunit [29, 30]. This is due to the structural heterogeneity and dynamic nature of subunits interactions, which emphasizes the importance of studying the quality and kinetics of subunits interactions. Such information can aid in unraveling the contraction mechanisms of cardiac cells and potentially be used for the prevention of MI. Apart from IMS-MS which enables interaction studies in the gas phase, SPR allows the performing of kinetic investigations in the liquid phase [31]. However, SPR has been mainly used to study the interaction of only 2 molecules with each other [32]. Since the cardiac troponin complex consists of three subunits, **it was hypothesized that by immobilizing each subunit on the SPR sensor in a stepwise fashion, it will be possible to elucidate the association and disassociate rate of all three subunits and unravel their interaction strength**. Hence, this hypothesis is investigated in Chapter 2- Section 2.

Chapter 3- Hyphenation of ion mobility and mass spectrometry to dynamic microfluidic systems

Section 1- Technological advances for analyzing the content of organ-on-a-chip by mass spectrometry

Alongside numerous advantages of IMS-MS-MS/MS in analyzing static systems, this combinatorial analytical tool also offers the possibility of studying dynamic systems. The high sensitivity, selectivity, and speed of IMS-MS-MS/MS make it an ideal analytical approach for time-resolved studies. This can be either monitoring a chemical reaction or cells' response to their microenvironment [33, 34]. Such investigations require an effective connection between the primary chemical or cellular reactor and to IMS-MS-MS/MS instrument. However, in the case of micro-sized cellular reactors (i.e., organ-on-a-chip), the coupling process is not always a very straightforward approach [35]. Hence, **a thorough review was performed on the possibilities of coupling organ-on-a-chip to a mass spectrometer in Chapter 3- Section 1.**

Section 2- Ion mobility spectrometry-tandem mass spectrometry strategies for the on-line monitoring of a continuous microflow reaction

Flow chemistry as one of the promising approaches in the synthesis of active pharmaceutical ingredients has attracted a lot of attention from pharmaceutical industries [36, 37]. Compared to classical batch synthesis, it allows green production due to better heat dispensation, reduction of solvent consumption and costs, and even high-quality (purity) productions. Coupling a flow reactor with an analytical technique enables on-line and real-time reaction monitoring, largely improving the process

analytical technologies capabilities [38]. The on-line detection of low abundant synthesis by-products, reaction intermediates and structural isomers remains a challenge with techniques such as UV/Vis, (N)IR, and NMR. Hence, **the potential of IMS-MS-MS/MS for monitoring a model Diels-Alder reaction was investigated. Furthermore, it was assumed that by performing computational modeling on the fragment ions of isomeric products after acquiring their mobility, it will be possible to annotate mobility peaks without requiring standard molecules.** Hence, these hypotheses investigated in Chapter 3- Section 2.

I encourage you to read researched approaches and findings with these hypotheses in mind.

References

1. Council, N.R., *Opportunities in biology.* 1989.
2. Desiderio, D.M., N.M. Nibbering, and A. Kraj, *Mass spectrometry: instrumentation, interpretation, and applications*. 2008: John Wiley & Sons.
3. De Hoffmann, E. and V. Stroobant, *Mass spectrometry: principles and applications*. 2007: John Wiley & Sons.
4. McLafferty, F.W. and F. Turecek, *Interpretation of mass spectra*. 1993: University science books.
5. Gabelica, V. and E. Marklund, *Fundamentals of ion mobility spectrometry.* Current Opinion in Chemical Biology, 2018. **42**: p. 51-59.
6. Viehland, L.A. and E.A. Mason, *Gaseous Ion mobility in electric fields of arbitrary strength.* Annals of Physics, 1975. **91**(2): p. 499-533.
7. Siems, W.F., L.A. Viehland, and H.H. Hill, Jr., *Improved Momentum-Transfer Theory for Ion Mobility. 1. Derivation of the Fundamental Equation.* Analytical Chemistry, 2012. **84**(22): p. 9782-9791.
8. Revercomb, H.E. and E.A. Mason, *Theory of plasma chromatography/gaseous electrophoresis. Review.* Analytical Chemistry, 1975. **47**(7): p. 970-983.
9. Covey, T. and D.J. Douglas, *Collision cross sections for protein ions.* Journal of the American Society for Mass Spectrometry, 1993. **4**(8): p. 616-623.
10. Hoaglund-Hyzer, C.S., A.E. Counterman, and D.E. Clemmer, *Anhydrous protein ions.* Chem Rev, 1999. **99**(10): p. 3037-80.
11. Chen, Y.L., B.A. Collings, and D.J. Douglascor, *Collision cross sections of myoglobin and cytochrome c ions with Ne, Ar, and Kr.* Journal of the American Society for Mass Spectrometry, 1997. **8**(7): p. 681-687.
12. Dodds, J.N. and E.S. Baker, *Ion Mobility Spectrometry: Fundamental Concepts, Instrumentation, Applications, and the Road Ahead.* J Am Soc Mass Spectrom, 2019. **30**(11): p. 2185-2195.
13. Shvartsburg, A.A. and R.D. Smith, *Fundamentals of traveling wave ion mobility spectrometry.* Anal Chem, 2008. **80**(24): p. 9689-99.
14. Michelmann, K., et al., *Fundamentals of trapped ion mobility spectrometry.* J Am Soc Mass Spectrom, 2015. **26**(1): p. 14-24.
15. May, J.C. and J.A. McLean, *The Influence of Drift Gas Composition on the Separation Mechanism in Traveling Wave Ion Mobility Spectrometry: Insight from Electrodynamic Simulations.* Int J Ion Mobil Spectrom, 2003. **16**(2): p. 85-94.
16. Ridgeway, M.E., et al., *Trapped ion mobility spectrometry: A short review.* International Journal of Mass Spectrometry, 2018. **425**: p. 22-35.

17. Kanu, A.B., et al., *Ion mobility–mass spectrometry.* Journal of Mass Spectrometry, 2008. **43**(1): p. 1-22.
18. Douzi, B., *Protein-Protein Interactions: Surface Plasmon Resonance.* Methods Mol Biol, 2017. **1615**: p. 257-275.
19. Pattnaik, P., *Surface plasmon resonance.* Applied Biochemistry and Biotechnology, 2005. **126**(2): p. 79-92.
20. Prabowo, B.A., A. Purwidyantri, and K.-C. Liu, *Surface Plasmon Resonance Optical Sensor: A Review on Light Source Technology.* Biosensors, 2018. **8**(3): p. 80.
21. Chhabra, N., M.L. Aseri, and D. Padmanabhan, *A review of drug isomerism and its significance.* Int J Appl Basic Med Res, 2013. **3**(1): p. 16-8.
22. Fernandez-Maestre, R., D. Meza-Morelos, and C. Wu, *Mobility shifts when buffer gas temperature increases in ion mobility spectrometry are affected by intramolecular bonds.* International Journal of Mass Spectrometry, 2016. **407**: p. 113-117.
23. Zietek, B.M., et al., *Adduct-ion formation in trapped ion mobility spectrometry as a potential tool for studying molecular structures and conformations.* International Journal for Ion Mobility Spectrometry, 2018. **21**(1): p. 19-32.
24. Burnum-Johnson, K.E., et al., *Ion mobility spectrometry and the omics: Distinguishing isomers, molecular classes and contaminant ions in complex samples.* TrAC Trends in Analytical Chemistry, 2019. **116**: p. 292-299.
25. Monte, M.J., et al., *Bile acids: chemistry, physiology, and pathophysiology.* World J Gastroenterol, 2009. **15**(7): p. 804-16.
26. Ben-Nissan, G. and M. Sharon, *The application of ion-mobility mass spectrometry for structure/function investigation of protein complexes.* Curr Opin Chem Biol, 2018. **42**: p. 25-33.
27. Leney, A.C. and A.J. Heck, *Native Mass Spectrometry: What is in the Name?* J Am Soc Mass Spectrom, 2017. **28**(1): p. 5-13.
28. Mozaffarian, D., et al., *Heart disease and stroke statistics—2015 update: a report from the American Heart Association.* Circulation, 2015. **131**(4): p. e29-e322.
29. Oda, T., H. Yanagisawa, and T. Wakabayashi, *Cryo-EM structures of cardiac thin filaments reveal the 3D architecture of troponin.* J Struct Biol, 2020. **209**(3): p. 107450.
30. Takeda, S., et al., *Structure of the core domain of human cardiac troponin in the Ca2+-saturated form.* Nature, 2003. **424**(6944): p. 35-41.
31. Schasfoort, R.B., *Handbook of surface plasmon resonance*. 2017: Royal Society of Chemistry.
32. Karlsson, R., *SPR for molecular interaction analysis: a review of emerging application areas.* Journal of Molecular Recognition, 2004. **17**(3): p. 151-161.
33. Marasco, C.C., et al., *Real-Time Cellular Exometabolome Analysis with a Microfluidic-Mass Spectrometry Platform.* PLOS ONE, 2015. **10**(2): p. e0117685.
34. Ray, A., et al., *On-line reaction monitoring by mass spectrometry, modern approaches for the analysis of chemical reactions.* Mass Spectrometry Reviews, 2018. **37**(4): p. 565-579.
35. Wang, X., et al., *Microfluidics-to-mass spectrometry: a review of coupling methods and applications.* J Chromatogr A, 2015. **1382**: p. 98-116.
36. Baumann, M. and I.R. Baxendale, *The synthesis of active pharmaceutical ingredients (APIs) using continuous flow chemistry.* Beilstein journal of organic chemistry, 2015. **11**(1): p. 1194-1219.
37. May, S.A., *Flow chemistry, continuous processing, and continuous manufacturing: a pharmaceutical perspective.* Journal of Flow Chemistry, 2017. **7**(3-4): p. 137-145.
38. Holmes, N., et al., *Online quantitative mass spectrometry for the rapid adaptive optimisation of automated flow reactors.* Reaction Chemistry & Engineering, 2016. **1**(1): p. 96-100.

Chapter 1 - Dynamics of small molecules in ion mobility spectrometry

Section 1 - Adduct ion formation as a tool for the molecular structure assessment of ten isomers in traveling wave and trapped ion mobility spectrometry

Darya Hadavi[1], Erik de Lange[1], Jan Jordens[2], Ynze Mengerink[2], Filip Cuyckens[3], Maarten Honing[1]

[1]Maastricht Multimodal Molecular Imaging (M4i) Institute, Maastricht University, Universiteitssingel 50, 6229 ER, Maastricht, The Netherlands
[2]DSM Materials Science Center, Urmonderbaan 22, 6167 MD, Geleen, The Netherlands
[3]Janssen Pharmaceutica, Janssen PR&D, Turnhoutseweg 30, 2340, Beerse, Belgium

Based on

Hadavi, D., de Lange, E., Jordens, J., Mengerink, Y., Cuyckens, F., & Honing, M. (2019). Adduct ion formation as a tool for the molecular structure assessment of ten isomers in traveling wave and trapped ion mobility spectrometry. Rapid Communications in Mass Spectrometry, 33(S2), 49-59. doi:https://doi.org/10.1002/rcm.8419

Abstract

Rationale

The separation of isomeric compounds with major differences in their physiochemical and pharmacokinetic properties is of particular importance in pharmaceutical R&D. However, the structural assessment and separation of these compounds with current analytical techniques and methods are still a challenge. In this study, we describe strategies to separate the various structural and stereo-isomers.

Methods

The separation of ten structural and stereo-isomers was investigated using Trapped and Travelling Wave ion mobility spectrometry (TIMS and TWIMS). Different strategies including adduct ion formation with Na, Li, Ag and Cs as well as fragmentation before and after the ion mobility cell were applied to separate the isomeric compounds.

Results

All the counter ions (in particular Na) strongly coordinated with the test analytes in all the IMS systems. The highest resolving power was achieved for the sodium and lithium adducts using TIMS-time-of-flight (TOF). However, some separation was attained on a Synapt HDMS system with its unique potential to monitor the ion mobility of the product ions. The elution order of the adduct ions was the same in all instruments, in which, unexpectedly, the para-substituted isomer of the $[M + Na]^+$ species had the lowest collision cross section followed by the meta- and ortho-isomers.

Conclusion

The formation of adduct ions could facilitate the separation of structural and even stereo-isomers by generating different molecular conformations. In addition, fragmenting isomers before or after the ion mobility cell is a valuable strategy to separate and also to assess the structures of adducts and different conformers.

Introduction

Ion mobility spectrometry (IMS) has received tremendous attention over the last decade. It is applied in nearly all fields of science primarily focusing on the molecular structure assessment of (bio)polymers, lipids and endogenous metabolites but also for drug lead compound libraries [1-3]. It separates ions based on their size, shape and charge. IMS combined with mass spectrometry (MS) and tandem mass spectrometry (MS/MS) has proven to be an efficient method in the detailed structural assessment of isomeric forms of small molecules [4, 5]. Such a combination can generate detailed insight into the configuration or even conformation of a small molecule.

Over the last decade, various commercial IMS devices have been extensively researched. In these devices, alternative separation mechanisms have been employed in order to compensate for the highly reduced length of the classical drift tube. However, the commercially available IMS devices exhibit a lower resolving power than classical drift tube IMS devices, hampering the separation of structural and stereo-isomers [6]. To compensate for this shortcoming and for successful separation of small molecules, alternative approaches along with integration of tandem mass spectrometry are required.

The use of adduct ions has been proven to be such an alternative for the separation of structural and even stereo-isomers [7-17]. As an example, Na, Li, Ag or even Cs coordinates to molecules with different conformers of the isomeric forms, leading to an improved separation. Moreover, the ions can coordinate at different positions within one molecule and give rise to multiple peaks in the mobilogram, which can generate insight into the different complexation mechanisms [7]. As an example, our previously validated approach led to the separation of the isobaric and structural isomers of tetrahydrocannabinol and cannabidiol in a Trapped ion mobility spectroscopy (TIMS) setup [7]. Furthermore, Huang et al studied the separation of carbohydrate isomers by Traveling Wave ion mobility spectrometry (TWIMS) using the Synapt high-definition (HD) mass spectrometer, and reported more than one mobility peak for trisaccharide maltotriose upon cesium adduct formation. All these articles explained that the different binding sites of adducts on the target analytes result in better separation of isomers. Diversity in the binding sites results in the formation of different conformations of ions in the gas phase and thus separation of isomeric compounds.

TIMS and TWIMS are the commonly used types of ion mobility cells for the separation of isomers. These two ion mobility cells have different separation mechanisms. In TWIMS, a sequence of symmetric potential waves continually propagates through the drift tube, which drives ions to move along the drift tube, while the drift gas flows against the direction of movement of the ions. The applied electric field and the collision of ions with drift gas result in the separation of ions (Figure 1) [18]. In the TIMS system, on the other hand, a linearly increasing electric field is applied, which counteracts the drag force exerted on ions toward the detector by a continuous flow of neutral gas. In TIMS, after a certain accumulation time, ions are eluted by lowering the magnitude of the electric field, leading to separation of the ions (Figure 1) [19]. Between the Synapt HDMS (equipped with TWIMS) and TIMS-time-of-flight (TIMS-TOF) instruments, in

addition to the mentioned differences in the ion mobility cells, there are other configuration differences. In the Synapt HDMS system, it is possible to fragment ions before and after the ion mobility cell; fragmenting ions in the trap collision cell, which is situated before the IMS cell, allows the ion mobility of the product ions to be monitored. In a mass spectrometer hyphenated with TIMS, however, the collision cell is only placed after the IMS cell, which limits the ion mobility separation on intact ions.

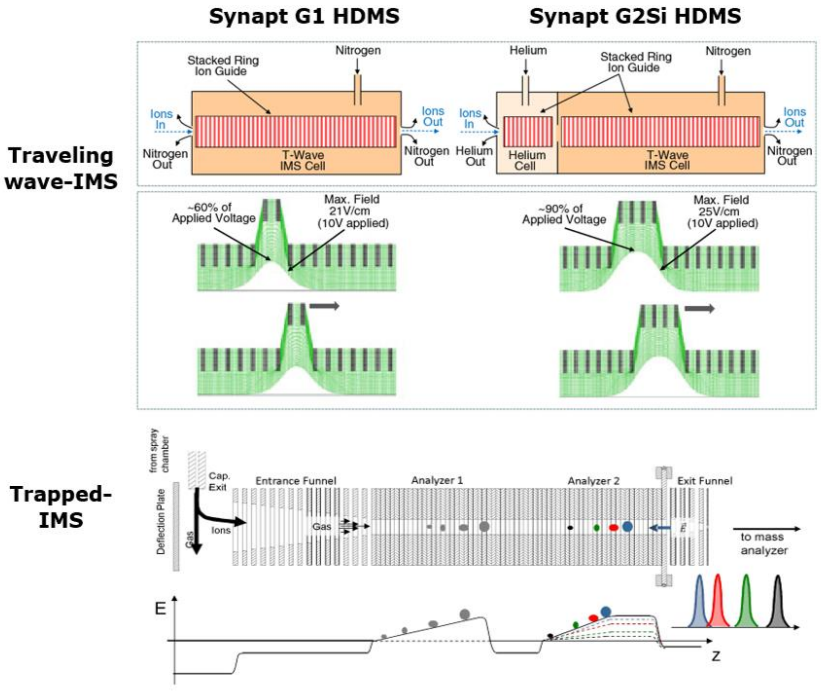

Figure 1 .Schematics of the ion mobility cells for TWIMS in Synapt G1 and G2Si HDMS and TIMS. Adapted from Giles et al [20] and Silveira et al [21].

In this study, we aimed to separate ten structural and stereo-isomers of epilepsy drug metabolites (Figure 2) [22] by adduct ion formation. The influence of counter ions on the tendency of analytes to form new conformations was studied on both the Synapt HDMS and the TIMS-TOF systems. Since these two IMS-MS devices have major instrumental differences, we expected to observe different behavior of the adduct ions, and this could assist in separating the isomers. Thus, we compared and evaluated the separation power of the TIMS and TWIMS systems by means of IMS, MS/MS-IMS and IMS-MS/MS approaches. We also explored the capability of the Synapt HDMS instrument to separate isomers based on the mobility of their product ions.

Experimental

Chemicals

The mercapturic acid conjugates of 1,2-ethanediol, [1–2-chlorophenyl]-, 2-carbamate (RWJ-333369) with molecular mass of 376.05 Da (Figure 2), were obtained from Janssen Pharmaceutica (Beerse, Belgium). Ten isomers, five structural isomers each with both S- and R-enantiomers (denoted A and B, respectively), were tested. The solvents methanol (MeOH), acetonitrile (ACN), water (H_2O) and formic acid (FA) were obtained from Biosolve BV (Valkenswaard, The Netherlands). Lithium chloride (LiCl), silver nitrate ($AgNO_3$) and cesium chloride (CsCl) were obtained from Sigma-Aldrich (Steinheim, Germany). Sample preparation was performed using solvents with high purity (>98%).

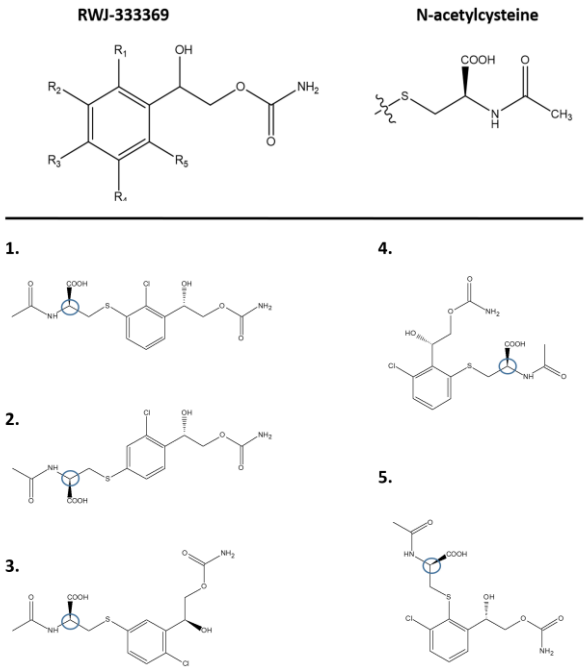

Figure 2.Chemical structures of mercapturic acid conjugates of RWJ-333369. Five structural isomers (ortho-, meta- and para-substituted isomers) each with the S- and R-enantiomers (blue circles).

Sample preparation

The ten individual mercapturic acid samples, a mixture containing all ten isomers (10-mix) and a mixture containing isomers 2A, 3A, and 4A (3-mix) were prepared and tested. The working concentrations of these compounds were 0.1, 1 and 10 µM prepared in MeOH/ACN/H_2O/FA in the ratio 40/40/20/0.1%. An aqueous solution of LiCl, $AgNO_3$, or CsCl with a concentration of 25 µM was prepared to introduce the counter ions.

IMS-MS operational modes and parameters

This study was performed using two series of the Synapt HDMS system, known as G1 and G2Si (Waters, Milford, MA, USA), as well as a Trapped-Ion Mobility Spectrometry-

Time-Of-Flight (TIMS-TOF) instrument (Bruker Daltonics Inc., Billerica, MA, USA). All measurements were performed in the TOF, MS/MS and IMS modes. Direct infusion, with a Chemyx fusion 100 syringe pump (Stafford, TX, USA) coupled to an electrospray ionization (ESI) interface operated in positive ion mode, was used for sample introduction. The MS experimental parameters are presented in Table 1. Fragmentation of the ions obtained from the mercapturic acids (10- and 3-mix samples) was performed in the trap collision cell of the Synapt HDMS instruments and in the collision cell of the TIMS-TOF instrument in the presence or absence of Li, Ag or Cs counter ions. The quadrupole analyzer was used to select ions with the desired *m/z* value. Following the fragmentation, the ion mobility was measured using a wave velocity of 900 m/s and a wave height of 35 V.

Data evaluation

All data from the Synapt HDMS instruments were processed in Masslynx v4.1 and Drifscope v2.8 (Waters), and the data from the TIMS-TOF system were processed using Compass Data Analysis v5.0 software (Bruker). Data obtained with the Synapt systems were exported to Matlab and Excel for reconstruction of the mobilogram and for further data analysis.

Table 1. Settings used in the Synapt HDMS G1, G2Si and the TIMS-TOF.

Parameter	Synapt G1	Synapt G2Si	TIMS-TOF
Syringe pump flow rate (µL/min)	5	5	3
Capillary voltage (kv)	3	3	4.5
Sampling cone voltage (v)	50	50	-
Extraction cone voltage (v)	5		-
Source temperature (°c)	100	90	-
Desolvation gas temperature (°c)	400	250	200
Desolvation gas flow (N_2) (L/h)	350	400	210
Nebulizer gas (N_2) (bar)	-	2.5	0.5
Wave velocity (m/s)	800	500	-
Wave height (v)	11.5	40	-
IMS rate (mL/min)	20	90	-

Results and discussion

The ten test compounds in this study are the metabolites of novel neuromodulators, used for the treatment of epilepsy [22]. Five of them differ in the positioning of "side groups" along the central aromatic ring (*ortho*, *meta* and *para*), and for each of them the *S*- and *R*-enantiomers are present; adding up to ten structural and stereo-isomers (Figure 2). Moreover, the side chains are rather "long" and are expected to form intra-molecular bonds. As a result, they serve as an ideal "molecular platform" for more detailed research into adduct ion formation and their separation by IMS.

In previous reports, adduct ion formation has been shown to have an effect on ion conformations and to facilitate the separation of isomeric compounds; however, the

separation of stereo-isomers remains challenging. Here, the separation of ten pharmaceutically important molecular structures upon adduct ion formation was studied, using both the Traveling Wave and the Trapped-IMS technologies. In addition, "upfront" and post IMS tandem mass spectrometry approaches show their added value in assigning the structures of the "adduct ions".

Mass spectra of analytes

The mass spectra of the analytes were generated at three different concentrations (0.1, 1 and 10 µM) in both the MS-TOF and IMS-TOF modes. The mass spectrometers demonstrated a linear concentration dependency, consistent with a previous ESI-MS study [23]. However, on changing from the TOF to the IMS-TOF mode, the MS sensitivity reduced by three orders of magnitude, being most pronounced for the TWIMS system (Figure S1, supporting information). This dramatic loss in ion transmission upon use of IMS probably occurs in the high-pressure region [24].

Rather high abundance "cluster" ions ($[xM + Na]^+$ and $[xM - H + 2Na]^+$) of all test compounds were encountered when using a concentration of 10 µM, and they were most abundant in the TIMS instrument. The IMS data of clusters and their identities, which were confirmed by performing MS/MS experiments, are discussed in Figure S2 (supporting information). Due to the low ion abundances obtained at 0.1 µM and the extensive cluster formation at 10 µM concentration, all further experiments were performed at 1 µM concentration.

The ESI-MS spectra of all ten test compounds for both the Synapt HDMS and the TIMS-TOF systems showed a base peak at *m/z* 399.03 corresponding to $[M + Na]^+$, and an $[M - H + 2Na]^+$ ion at *m/z* 421.01 (Figure S3, supporting information). No abundant $[M + H]^+$ ion was observed at *m/z* 377, even without the addition of the sodium, lithium, silver or cesium salts. This can be explained by the excess of sodium in the glassware that was used (the syringe or reagent bottles), which favors the formation of sodiated adducts. Because the protonated molecules were not observed in either of the IMS-MS systems, all further experiments were focused on the separation of the $[M + Ad]^+$ and $[M - H + 2Ad]^+$ ions, where "Ad" represents any of the employed adduct ions (Na^+, Li^+, Ag^+, Cs^+).

Separation based on ion mobility spectrometry

Here, the ability of the Synapt HDMS (both series of G1 and G2Si) and the TIMS-TOF systems to separate and study adduct ions using the ten isomers was investigated in detail. At first, the optimal conditions for the separation of the sodiated adducts, $[M + Na]^+$ and $[M - H + 2Na]^+$, in the "10-mix" was studied. The obtained data from all the instruments demonstrated a similar trend in regard to the transition time of the $[M + Na]^+$ and $[M - H + 2Na]^+$ species in the ion mobility cells; the $[M - H + 2Na]^+$ ions had higher transition times than ions with a single Na adducted ($[M + Na]^+$) (Figure 3) and larger collision cross sections (CCSs) were obtained for $[M - H + 2Na]^+$ ions than for $[M + Na]^+$ ions (Table 2). The second Na ion possibly prevents the structural folding (intra-molecular bridge between the two antennae) of ions due to intra-molecular interactions and thus increases their transition time in an ion mobility cell. Similar

differences in the mobility of the sodium adducts have been reported by Haler et al for polyethylene oxide polymers complexed by one to four Na cations [25]. It is worth noting that in the Synapt HDMS instrument the transition time of ions is proportional to their mobility and their CCS ($t \propto K_0 \propto CCS$), whereas in the TIMS-TOF setup the time of detection is proportional to the CCS and to the inverse of the ion mobility ($t \propto CCS \propto 1/K_0$) [19].

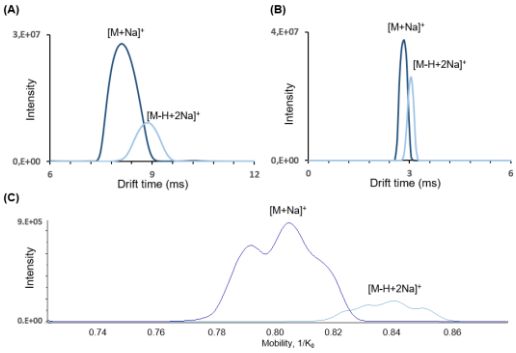

Figure 3.Mobilograms of $[M+ Na]^+$ and $[M - H+ 2Na]^+$ species from the 10-mix sample with A, Synapt G1 HDMS; B, Synapt G2Si HDMS; and C, TIMS-TOF.

Table 2. Collision cross section of $[M+Na]^+$ and $[M-H+2Na]^+$ calculated from Synapt HDMS.

Isomer	CCS (Å²) of $[M+Na]^+$	SD (%)	CCS (Å²) of $[M-H+2Na]^+$	SD (%)
1a	176.67	± 0.3%	185.46	± 0.3%
1b	176.66	± 0.5%	186.87	± 0.2%
2a	176.42	± 0.5%	187.05	± 0.2%
2b	176.01	± 0.5%	186.36	± 0.2%
3a	178.39	± 0.1%	185.82	± 0.1%
3b	179.25	± 0.4%	184.93	± 0.2%
4a	180.76	± 0.5%	182.97	± 0.1%
4b	179.05	± 0.1%	181.78	± 0.1%
5a	178.53	± 0.5%	184.89	± 0.1%
5b	178.31	± 0.4%	183.66	± 0.1%

When it comes to the separation power of the instruments, not unexpectedly significant differences between the Synapt HDMS and TIMS-TOF systems were observed, while in general the performance of the Synapt HDMS G1 and G2Si was rather similar (Figure 3).

In both the Synapt HDMS G1 and G2Si one unresolved peak for both $[M + Na]^+$ and $[M – H + 2Na]^+$ species was observed. However, the Synapt HDMS G2Si showed a greatly reduced (by a factor > 2) full width at half-maximum (FWHM) resolution (Figure 3B and A). This finding is consistent with an earlier study, where the resolution of the Synapt G2Si HDMS instrument improved up to fourfold in comparison with the Synapt G1 HDMS system [20]. Despite this gain, the resolving power remained rather insufficient, as no clear separation of the structural and stereo-isomers in the 10-mix could be observed. In contrast, the ion mobility peak in the TIMS instrument was partly resolved, indicating the separation of at least three to four isomers (Figure 3).

In order to assign the partially resolved ion mobility peaks to their isomers, experiments on all three systems, injected with the individual solutions of ten isomers, were performed. This could also allow the one ion mobility peak to be assigned to the isomers and the distribution of the isomers in the unresolved mobilograms of the Synapt HDMS systems to be studied. Figure S4 (supporting information) shows the ion mobility of ten isomers individually. It can be seen that the *S*- and *R*-enantiomers had the same elution trend in all IMS systems. Therefore, in the further studies of structural isomers, only the *S*-isomers were investigated. Their structures are depicted in figure 2.

The most significant separation was observed for the *para*-, *meta*- and *ortho*-constitutional isomers for both the $[M + Na]^+$ and $[M – H + 2Na]^+$ adducts (Figure 4A). However, the elution order of the structural isomers illustrated an unexpected trend for the $[M + Na]^+$ ions, while the $[M – H + 2Na]^+$ species showed the expected profile that was in line with literature reports.

The *para*-substituted isomer of the $[M + Na]^+$ species is generally expected to have the longest drift time due to its bulky conformation. However, the acquired IMS data from all the IMS systems displayed an opposite trend, in which the *para*-isomer of the $[M + Na]^+$ species had the lowest transition time followed by the *meta*- and then the *ortho*-isomers (Figure 4). Barnett et al also observed such an unexpected trend in an attempt to separate *para*-, *meta*-, and *ortho*-phthalic acids by FAIMS [14]. They applied mixed carrier gases of N_2 and CO_2 (95:5) for separation and the observed results were not consistent with the calculated values from Blanc's law. This unexpected trend for $[M + Na]^+$ species could be due to the intra-molecular interaction of chains attached to the aromatic ring. The interaction possibly is caused by the coordination of sodium with e.g. the oxygen atoms or via hydrogen bonding. For the *para*-substituted isomers, this interaction could result in an intra-molecular ring formation and thus boost the mobility and transition time that is caused by Brownian motion. It can be argued that where the *N*-acetylcysteine is located in the *meta*- or *ortho*-position, the tendency of the formed ring by alkyl chains to move outwards increases. This hypothesis needs further study and density functional theory (DFT) calculations.

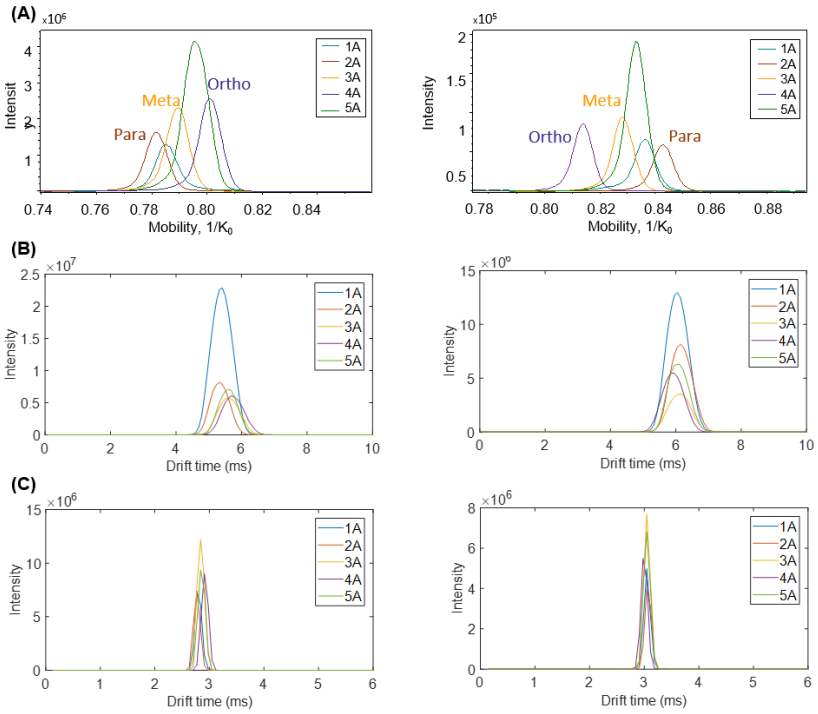

Figure 4.Mobilograms of [M+ Na]⁺ (right) and [M − H+ 2Na]⁺ (left) of the S-enantiomers, obtained with A, TIMS-TOF; B, Synapt G1 HDMS; and C, Synapt G2Si HDMS.

On the other hand, the $[M - H + 2Na]^+$ isomers showed a clear and expected trend of *ortho*- having the lowest drift time followed by the *meta*- and *para*-isomers (Figure 4). This trend is probably caused by sodium-hydrogen ion exchange at the carboxylic group of the molecule, forming the sodium salt. The sodium ion is coordinated between the conjugated carboxylic acid and the sulphur atom, thereby inhibiting the intra-molecular interaction between the alkyl chains. This, in turn, results in the *para*-substituted isomers of $[M - H + 2Na]^+$ having higher transition times than the *ortho*- and *meta*-isomers.

In addition to these findings, the data from the TIMS-TOF system demonstrated significant differences in the ion mobility of some diastereomers (Figure S4, supporting information). The separation of the stereo-isomers of the *meta*- (compounds 1A and 1B) and *ortho*- (compounds 5A and 5B) substituted isomers was also studied in more detail with the TIMS system. Only for the $[M - H + 2Na]^+$ complexes a clear shift in the mobility of the diastereoisomers was observed (Figure 5). As was explained for the structural isomers, the formation of the sodium salt on stereo-isomers could result in different conformers, and thus separation. It could be clearly seen that the formation of cation-adduct complexes with the analytes influences the conformation of the analytes and thus facilitates their separation. As mentioned above, these small differences in

molecular conformations, and consequently in the CCSs, can only be detected with the TIMS instrument with its increased resolving power.

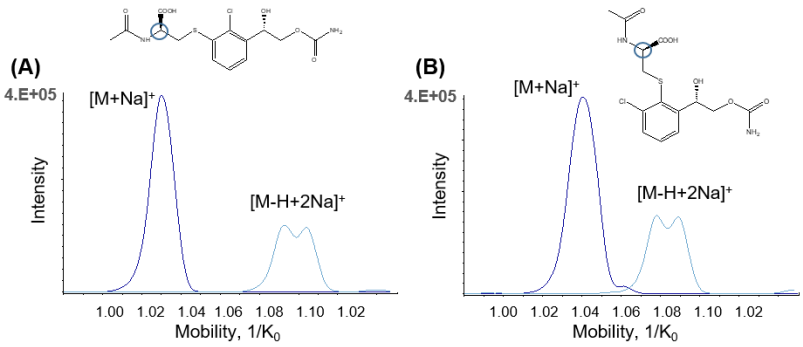

Figure 5.Mobilograms of the stereo-isomers by TIMS-TOF. A, Compounds 1A and 1B and B, compounds 5A and 5B.

Separation after counter ion addition

The addition of metal cations has been shown to be a valuable approach in forcing molecules into more rigid conformations, thus introducing 'detectable" differences in the CCS and allowing the IMS separation of different conformers (potamers) [8, 26]. More specifically, previous studies have reported improved mobility separation upon the addition of Ag, Li and Cs cations [7, 9], which are the same metal cations that were used in this study. It was assumed that the size of the counter ions (radius of Li = 76, Ag = 138, Cs = 167 picometers) can improve the separation of isomers in the ion mobility cells. Furthermore, with the assumption that in all IMS technologies adduct formation is not extensively hampered by "declustering effects", the "stability" and separation power upon addition of Li, Ag and Cs to the isomers with the Synapt G2Si TWIMS and TIMS systems were investigated.

Because the best separation was observed for compounds 2, 3 and 4 (Figure 4), we performed these experiments on the mix of compounds 2A, 3A and 4A (3-mix) and the 10-mix. Compounds 2, 3 and 4 have the mercapturic acid respectively positioned para, meta and ortho to the side chain (Figure 2).

The acquired mass spectra of all samples with added metal cations showed the presence of $[M + Ad]^+$ and $[M - H + Na + Ad]^+$ ions (where Ad refers to Na, Li, Ag or Cs). This observation, which was seen in both IMS systems, demonstrates that the mercapturic acid conjugates of RWJ-333369 coordinated well with the counter ions. The analytes also coordinated strongly with sodium since both $[M + Na]^+$ and $[M - H + 2Na]^+$ ions were observed in the spectra of all samples with various counter ions. This is despite the fact that an excess of the counter ions (Li, Ag, Cs) was used in the sample solutions.

Upon analyzing the ion mobility spectra of all the cation adducts measured on the TIMS-TOF instrument, some level of separation could be detected in both the 3- and the 10-mix samples (Figure 6). Formation of adduct ions containing both Na and the additional counter ion ($[M - H + Na + Li]^+$, $[M - H + Na + Ag]^+$ and $[M - H + Na + Cs]^+$) resulted in better separation than the $[M + Li]^+$, $[M + Ag]^+$ and $[M + Cs]^+$ species, particularly in the 3-mix sample. For both the 3- and the 10-mix samples, the greatest separation was observed for Li adducts and the poorest for Ag adducts (Figure 6). Overall, however, the mobility shift was more pronounced as a result of the formation of the sodium adducts ($[M + Na]^+$ and $[M - H + 2Na]^+$), detected by TIMS.

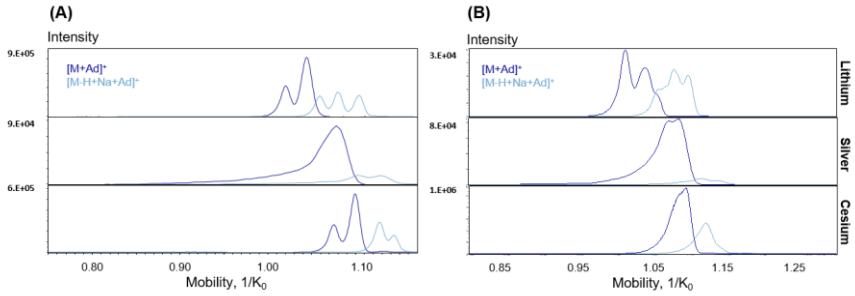

Figure 6.Mobilograms of A, 3-mix sample and B, 10-mix sample after cation adduct formation acquired by TIMS-TOF.

In contrast to TIMS, the conformational changes caused by the addition of cations (Li, Ag and Cs) did not shift the mobility of the $[M + Ad]^+$ and the $[M - H + Na + Ad]^+$ species sufficiently enough for them to be detected by the Synapt G2Si instrument (Figure 7). However, the MS and IMS data of all the formed cation adducts could be detected on the Synapt HDMS instrument, which shows strong coordination of these cations with the test analytes. In the Synapt HDMS instrument, it is expected that intra-molecular heating due to the high electrical field could lead to fragmentation of the analytes. Consequently, the abundance of adduct ions would be reduced in the Synapt HDMS instrument compared with the TIMS-TOF system in which a rather "soft" separation mechanism is operating [27]. Thus, our findings demonstrate the stability of the cation ions on the target isomers in both the TIMS-TOF and the Synapt HDMS instruments. As hypothesized, one of the notable similarities of the data acquired by both IMS systems was the slight increase in drift time upon increasing the ionic radii for Li^+, Ag^+ and Cs^+ [28]. Hence, the elution time of the cation adducts corresponds with the radius of the cations, with the shortest drift time being obtained for the smallest cation (Li) and the longest drift time for the largest cation (Cs) (Figures 6 and 7). A similar observation was reported by Huang et al in which the drift time of carbohydrates increased upon adding counter ions with larger atomic radii [9].

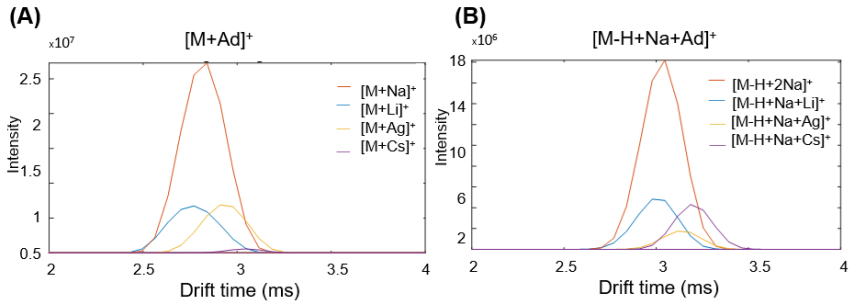

Figure 7.Mobilograms of a mix of 10 mercapturic acid conjugates after cation adduct formation acquired with a Synapt G2Si instrument: A, [M + Ad]⁺ and B, [M − H + Ad]⁺.

Combining IMS and MS/MS for structural assessment of adduct ion

In addition to the strategies applied to separate isomers based on their ion mobility, other strategies can be employed to separate isomers based on their fragmentation patterns: IMS-MS/MS and MS/MS-IMS.

Separation based on fragmentation pathway (IMS-MS/MS)

Traditionally, MS/MS generates valuable data on the molecular structures of small molecules. It could be argued that MS/MS experiments on different molecular conformations might also result in the formation of "unique" product ion(s) relating to one specific conformation, especially when using TIMS. MS/MS data could also support the explanation of differences in mobility, by generating different fragmentation pathways. Hence, in order to gain more information on the fragmentation pathways of the $[M + Na]^+$ and $[M - H + 2Na]^+$ species, MS/MS experiments were performed on the ten individual isomers.

For both commercial tandem MS systems, no differences in the collision-induced dissociation mass spectra of any of the compounds could be observed, hampering the unique identification of the isomers. On the other hand, and in line with common knowledge on the MS/MS of alkali metal adducts, the fragmentation pathways of $[M + Na]^+$ and $[M - H + 2Na]^+$ ions were quite different (Figure 8). Fragmentation of $[M + Na]^+$ species starts with the fragmentation of the *N*-acetylcysteine group resulting in the $[M + Na - CH_2CO]^+$ product ion, whereas fragmentation of $[M - H + 2Na]^+$ species is initiated through a loss from the carbamate group $[M - H + 2Na - HNCO]^+$ from the other substituted chain. This could suggest the coordination of the second sodium ion to the carboxylic acid (sodium salt), causing "stabilization" and redirecting the fragmentation to the loss of HNCO. This interesting finding supports another hypothesis, that the second sodium ion is exchanged for the acidic proton, thus stabilizing this group in the IMS of $[M - H + 2Na]^+$. Such differences in the fragmentation of adduct ions were also observed by Harvey for *N*-linked carbohydrates [29]. Altogether, these findings convey the ability to use MS/MS to assess the coordination position of cation adducts on analytes, as shown previously [30] and to generate valuable data to correctly

interpret trends in IMS. Nonetheless, MS/MS alone does not allow the straightforward distinguishing of structural isomers.

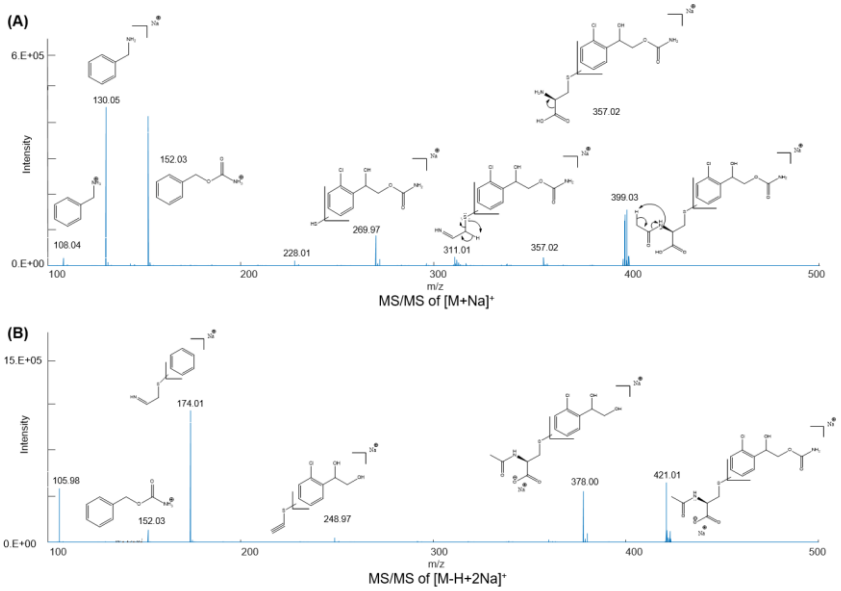

Figure 8.MS/MS of test analytes. Product ion spectrum and tentative fragmentation pathway of A, $[M + Na]^+$ and B, $[M - H + 2Na]^+$.

Separation based on MS/MS-IMS

Reversing the previous approach, by monitoring the ion mobility of the product ions of the isomeric molecules, with the TWIMS system opens new windows in the structural assessment [20]. Samples with a mixture of compounds (10- and 3-mix) and ten individual isomers with and without counter ions (Li, Ag, and Cs) were studied. Ion mobility measurements were performed on the product ions produced in the trap collision cell. The extracted ion mobilogram (EIM) of most of the product ions showed only one mobility peak. Fragmentation of the Cs adducts was not observed regardless of the applied collision energy. Similar observations were made in a study on the fragmentation of sucrose complexed with Rb and Cs [31], which suggests weak coordination of relatively large Cs cations with mercapturic acid. Thus, the metal cations were easily separated from the neutral isomers. For a few product ions, more than one ion mobility peak could be observed. However, these multiple peaks for a same nominal mass could also be found in the product ions of the individual compounds. This observation shows that either a single product ion has multiple conformations or that multiple product ions have exactly the same nominal mass. Thus, isomeric separation based on those product ions was not feasible. Interestingly, the mobilogram of product ions, fragmented from $[M + Ag]^+$ or $[M + Li]^+$ at *m/z* 353.98 and 280.06, respectively, showed more than one ion mobility peak (Figure 9). Multiple ion mobility peaks for these product ions could only be found in the mixture of compounds and not in the IMS

spectrum of an individual compound. This shows that different coordination of a counter ion on isomers results in the formation of “unique” product ions, which could facilitate the separation of isomers. In conclusion, despite the limited resolving power of TWIMS, the MS/MS-IMS configurations allow the distinction of the structural isomers based on the ion mobility of their product ions.

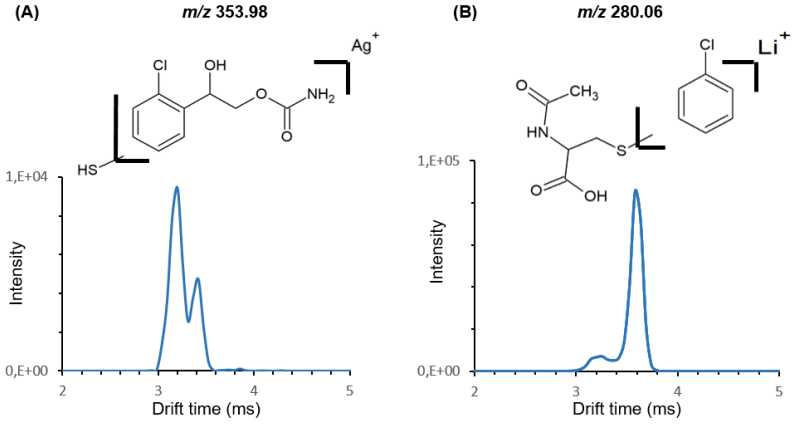

Figure 9.Mobilograms of product ions at m/z 353.98 and 280.06 fragmented from A, $[M + Ag]^+$ and B, $[M + Li]^+$.

Conclusions

In this research we focused on the use of adduct ions as an approach to the separation of a well-designed set of structural and stereo-isomers, with both Traveling Wave and Trapped ion mobility spectrometry. In contrast to TIMS, and in line with common knowledge and previous reports, the addition of counter ions does not lead to a significant increase in the separation power for the Traveling Wave-IMS systems. Although the selected molecules are “rather similar”, the TIMS system is able to distinguish among structural isomers and even between stereo-isomers. When studying the ten individual compounds, all the IMS systems showed the same trend regarding the transition time (CCS) of the structural isomers in the ion mobility cells, where the *para*-$[M + Na]^+$ ions showed the lowest transition time. This observation can be regarded as somewhat counter-intuitive and needs more attention by e.g. DFT or *ab initio* calculations. The same trend was obtained when using lithium, silver and cesium counter ions. The $[M – H + 2Na]^+$ species, however, led to the reverse and expected ‘gas-phase mobility”. As expected, TIMS showed better resolving power and allowed structural and stereo-isomers to be separated. Use of other metal adduct ions did not lead to significant gains in terms of separation power.

Overall, evaluating the different cations, the optimal separation was observed with Li and Na adducts, showing the influence of cations in generating different conformations of molecules and in facilitating separation. Thus, MS/MS combined with IMS, either upfront or downstream of the IMS cell, is a valuable tool to understand the

"coordination of adducts" in the different conformers, and a valuable tool for the structural identification of compounds.

Acknowledgment

The authors would like to thank Dr R.J. Vreeken for fruitful discussions and sharing of knowledge.

References

1. Ridgeway, M.E., et al., *Trapped ion mobility spectrometry: A short review.* International Journal of Mass Spectrometry, 2018. **425**: p. 22-35.
2. Creaser, C.S., et al., *Ion mobility spectrometry: a review. Part 1. Structural analysis by mobility measurement.* Analyst, 2004. **129**(11): p. 984-994.
3. Sans, M., C.L. Feider, and L.S. Eberlin, *Advances in mass spectrometry imaging coupled to ion mobility spectrometry for enhanced imaging of biological tissues.* Current Opinion in Chemical Biology, 2018. **42**: p. 138-146.
4. Lanucara, F., et al., *The power of ion mobility-mass spectrometry for structural characterization and the study of conformational dynamics.* Nature Chemistry, 2014. **6**: p. 281.
5. Williams, D.M. and T.L. Pukala, *Novel insights into protein misfolding diseases revealed by ion mobility-mass spectrometry.* Mass Spectrometry Reviews, 2013. **32**(3): p. 169-187.
6. Haler, J.R.N., et al., *Comprehensive Ion Mobility Calibration: Poly(ethylene oxide) Polymer Calibrants and General Strategies.* Analytical Chemistry, 2017. **89**(22): p. 12076-12086.
7. Zietek, B.M., et al., *Adduct-ion formation in trapped ion mobility spectrometry as a potential tool for studying molecular structures and conformations.* International Journal for Ion Mobility Spectrometry, 2018. **21**(1): p. 19-32.
8. Huang, Y. and E.D. Dodds, *Ion-neutral collisional cross sections of carbohydrate isomers as divalent cation adducts and their electron transfer products.* Analyst, 2015. **140**(20): p. 6912-6921.
9. Huang, Y. and E.D. Dodds, *Ion Mobility Studies of Carbohydrates as Group I Adducts: Isomer Specific Collisional Cross Section Dependence on Metal Ion Radius.* Analytical Chemistry, 2013. **85**(20): p. 9728-9735.
10. Fenn, L.S. and J.A. McLean, *Structural resolution of carbohydrate positional and structural isomers based on gas-phase ion mobility-mass spectrometry.* Physical Chemistry Chemical Physics, 2011. **13**(6): p. 2196-2205.
11. Jackson, S.N., et al., *A study of phospholipids by ion mobility TOFMS.* Journal of the American Society for Mass Spectrometry, 2008. **19**(11): p. 1655-1662.
12. Chen, L., Y.Q. Gao, and D.H. Russell, *How Alkali Metal Ion Binding Alters the Conformation Preferences of Gramicidin A: A Molecular Dynamics and Ion Mobility Study.* The Journal of Physical Chemistry, 2012. **116**(1): p. 689-696.
13. Clowers, B.H. and H.H. Hill, *Influence of cation adduction on the separation characteristics of flavonoid diglycoside isomers using dual gate-ion mobility-quadrupole ion trap mass spectrometry.* Journal of Mass Spectrometry, 2006. **41**(3): p. 339-351.
14. Barnett, D.A., et al., *Separation of o-, m- and p-phthalic acids by high-field asymmetric waveform ion mobility spectrometry (FAIMS) using mixed carrier gases.* Journal of Mass Spectrometry, 2000. **35**(8): p. 976-980.
15. Fernández-Maestre, R., D. Meza-Morelos, and C. Wu, *Shift reagents in ion mobility spectrometry: the effect of the number of interaction sites, size and interaction energies*

on the mobilities of valinol and ethanolamine. Journal of Mass Spectrometry, 2016. **51**(5): p. 378-383.
16. Howdle, M.D., et al., *The Use of Shift Reagents in Ion Mobility-Mass Spectrometry: Studies on the Complexation of an Active Pharmaceutical Ingredient with Polyethylene Glycol Excipients.* Journal of the American Society for Mass Spectrometry, 2009. **20**(1): p. 1-9.
17. Fernandez-Maestre, R., D. Meza-Morelos, and C. Wu, *Mobility shifts when buffer gas temperature increases in ion mobility spectrometry are affected by intramolecular bonds.* International Journal of Mass Spectrometry, 2016. **407**: p. 113-117.
18. Shvartsburg, A.A. and R.D. Smith, *Fundamentals of Traveling Wave Ion Mobility Spectrometry.* Analytical Chemistry, 2008. **80**(24): p. 9689-9699.
19. Michelmann, K., et al., *Fundamentals of Trapped Ion Mobility Spectrometry.* Journal of The American Society for Mass Spectrometry, 2015. **26**(1): p. 14-24.
20. Giles, K., J.P. Williams, and I. Campuzano, *Enhancements in travelling wave ion mobility resolution.* Rapid Communications in Mass Spectrometry, 2011. **25**(11): p. 1559-1566.
21. Silveira, J.A., et al., *Parallel accumulation for 100% duty cycle trapped ion mobility-mass spectrometry.* International Journal of Mass Spectrometry, 2017. **413**: p. 168-175.
22. Mannens, G.S.J., et al., *The Absorption, Metabolism, and Excretion of the Novel Neuromodulator RWJ-333369 (1,2-Ethanediol, [1-2-Chlorophenyl]-, 2-carbamate, [S]-) in Humans.* Drug Metabolism and Disposition, 2007. **35**(4): p. 554-565.
23. Han, X. and R.W. Gross, *Electrospray ionization mass spectroscopic analysis of human erythrocyte plasma membrane phospholipids.* Proceedings of the National Academy of Sciences, 1994. **91**(22): p. 10635-10639.
24. D'Atri, V., et al., *Adding a new separation dimension to MS and LC–MS: What is the utility of ion mobility spectrometry?* Journal of Separation Science, 2018. **41**(1): p. 20-67.
25. Haler, J.R.N., et al., *Comparison of Different Ion Mobility Setups Using Poly (Ethylene Oxide) PEO Polymers: Drift Tube, TIMS, and T-Wave.* Journal of The American Society for Mass Spectrometry, 2018. **29**(1): p. 114-120.
26. Zheng, X., et al., *Enhancing glycan isomer separations with metal ions and positive and negative polarity ion mobility spectrometry-mass spectrometry analyses.* Analytical and Bioanalytical Chemistry, 2017. **409**(2): p. 467-476.
27. Morsa, D., V. Gabelica, and E. De Pauw, *Effective Temperature of Ions in Traveling Wave Ion Mobility Spectrometry.* Analytical Chemistry, 2011. **83**(14): p. 5775-5782.
28. Shannon, R.D., *Revised effective ionic radii and systematic studies of interatomic distances in halides and chalcogenides.* Acta Crystallographica, 1976. **32**(5): p. 751-767.
29. Harvey, D.J., *Collision-induced fragmentation of underivatized N-linked carbohydrates ionized by electrospray.* Journal of Mass Spectrometry, 2000. **35**(10): p. 1178-1190.
30. Smith, G. and J.A. Leary, *Mechanistic Studies of Diastereomeric Nickel(II) N-Glycoside Complexes Using Tandem Mass Spectrometry.* Journal of the American Chemical Society, 1998. **120**(50): p. 13046-13056.
31. Paek, J., et al., *MALDI-MS Analysis of Sucrose Using a Charcoal Matrix with Different Cationization Agents.* Bulletin of the Korean Chemical Society, 2018. **39**(6): p. 750-756.

Section 2 - Uncovering the behaviour of ions in the gas-phase to predict the ion mobility separation of isomeric steroid compounds

Darya Hadavi, Marina Borzova, Tiffany Porta Siegel, Maarten Honing

Maastricht Multimodal Molecular imaging (M4i) Institute, Division of Imaging Mass Spectrometry Maastricht University, Universiteitssingel 50, 6229ER, Maastricht, The Netherlands.

Based on

Hadavi, D., Borzova, M., Porta Siegel, T., & Honing, M. (2022). Uncovering the behaviour of ions in the gas-phase to predict the ion mobility separation of isomeric steroid compounds. Analytica Chimica Acta, 1200, 339617. doi:10.1016/j.aca.2022.339617

Abstract

Bile acids are steroid compounds involved in biological mechanisms of neurodegenerative diseases making them potential biomarkers for diagnosis or treatment. These compounds exist as structural and conformational isomers, which hinder distinguishing them in physiological processes. We aimed to develop tandem mass spectrometry-ion mobility spectrometry (MS/MS-IMS) methodologies to explore and understand the behaviour of isomeric steroids in the gas-phase and rapidly separate them. Unlike previously published ion mobility data, various isomers were investigated in mixtures to better mimic complex (pre-) clinical samples. The experimental collision cross sections (CCS)s were compared to the theoretical CCS values for an in-depth analysis of isomeric ions' behaviour in the gas-phase. Based on density-functional theory, we identified the impact of adduct positioning on the 3D conformation of enantiomers, diastereomers and structural isomers. The curling of the large side chains hedged the small differences among the isomers and lowered the CCS values. On the other hand, fragmenting off the identical side branches as well as imposing the bending of the steroid ring resulted in ion mobility differentiation. Careful data evaluation revealed the tendency of isomers to form homo-cluster in the mixture solutions and assist the separation. Our fundamental and experimental findings enable the ion mobility separation of isomeric steroids to be predicted. The introduced rapid and optimal MS/MS-IMS analytical methodology can be applied to distinguish isomeric bile acids both in a solution and potentially in patients' tissue samples, and consequently, reveal their molecular pathways.

Keywords: ion mobility, density functional theory, collision cross section, bile acids, gas-phase molecular ion, traveling wave ion mobility.

Introduction

Primary bile acids are steroids and metabolites of cholesterol produced in the liver that can further be metabolized to secondary bile acids by gut microbiota. These amphipathic molecules have been the centre of attention due to their involvement in a wide range of physiological processes, rendering them as suitable biomarker candidates, as well as potential molecules to improve drug performance [1-4]. There are numerous pieces of evidence on the diagnostic and treatment application of bile acids for neurodegenerative diseases such as Parkinson and Alzheimer's [5-9]. Despite the significant importance of bile acids, there are still uncertainties on mechanisms modulated by bile acids that derive the pathological abnormalities. The uncertainty partly comes from the deviation of bile acid profile between human and animal models, which renders the translation challenging. Furthermore, the detection and discrimination of bile acids throughout the (pre-)clinical studies pose a challenge for research. This is due to the complexity of (pre-)clinical samples that include a diverse range of bile acid molecules with nearly identical molecular structures. Therefore, there is an urgent need for a rapid analytical technique, sensitive and selective enough to detect trace levels of bile acids and to distinguish the large variety of structural isomers, to gain a deeper insight regarding the origin, function, and impact of bile acids in various metabolic disorders. To this end, ion mobility mass spectrometry (IMS) especially in combination with tandem mass spectrometry methodologies, is an enabling technology to address all aforementioned challenges for evaluation of bile acids.

IMS separates ions in the gas-phase, based on their size, shape, and charge [10]. It became popular in a broader scientific community due to its significantly reduced analysis time (milliseconds) compared to the other analytical techniques such as gas and liquid chromatography (GC and LC) [11, 12]. In addition, IMS limits the extensive efforts required to achieve maximal liquid chromatographic separation. While IMS is a powerful technique on its own, its combination to mass spectrometry (MS) allows for molecular discrimination based on their mass-over-charge ratio *(m/z)* and further structural analysis by tandem mass spectrometry (MS/MS). MS together with the ion mobility values collected increases the selectivity and sensitivity of the measurement [13]. Moreover, the hyphenation of IMS with MS is potentially a valuable tool for the direct analysis of human patient samples and biopsies for spatial localisation of bile acids in sample tissue by mass spectrometry imaging [14-16].

With the development of the theoretical methods for molecular modelling, it became possible to estimate the structural conformation of an ion and predict its mobility in the gas-phase [17-19]. This provides an opportunity for in-depth research of molecular structural behaviour and interactions [20]. The principle of IMS is explained in supporting information. Collision cross section (CCS) data has the potential to identify and describe unknown structures by comparing the experimental values to the theoretically predicted CCS database. Unlike the arrival time, that depends on the experimental conditions and the IMS instrument, K0 and CCS values can be compared across all measurements performed in the low-field limit (where E/N is small enough to not affect the K0) [21].

Critical investigation on the ion mobility results is an utmost step for predicting ions fate in the gas-phase chamber of IMS and applying necessary strategies for (pre-)treatment of the samples. In addition, during the (pre-)clinical studies the separation of bile acids with similar structures has been a challenge [22, 23], which is due to the high complexity of bile acids behaviour and interactions in the gas-phase. Hence, considering the significant importance of bile acids as potential biomarkers, precise identification and characterization of these molecules will enable researchers to increase understanding of their biological pathways and their role in disease progression.

Here, we report an integrated MS/MS-IMS study designed to separate isomeric bile acids. Different strategies including clustering and collision induced dissociation before the ion mobility cell of traveling wave ion mobility spectrometry (TWIMS) applied. In addition metal adducts analysed whether they promote the separation of bile acids in complex samples and in individual injections. Furthermore, the lowest energy conformers of each isomer were thoroughly investigated by density functional theory (DFT). The optimal data from DFT used to theoretically calculate CCS of analytes and compare to the experimental $^{TW}CCS_{N_2}$ results to reveal the ions behaviour

Materials and methods

Chemicals and sample preparation

Analytes of interest consisted of colic acid (CA, Sigma-Aldrich, Zwijndrecht, Netherlands), Allocholic acid (AlloCA, Santa Cruz Biotechnology, Heidelberg, Germany), Taurine conjugated deoxycholic acid (TDCA, Sigma-Aldrich, Zwijndrecht, Netherlands), Taurine conjugated chenodeoxycholic acid (TCDCA, Sigma-Aldrich, Zwijndrecht, Netherlands), Glycodeoxycholic acid-3-sulfate sodium salt (GDCA, IsoSciences, Ambler, Pennsylvania), Glycochenodeoxycholic acid-3-sulfate sodium salt (GCDCA, Toronto Research Chemicals, Toronto, Canada), alfa-, beta- and omega- muricholic acid (α-, β-, and ω-MCA respectively, Steraloids, Rhode Island, USA), gamma- muricholic acid (γ-MCA, Sigma-Aldrich, Zwijndrecht, Netherlands), Taurine conjugated α-, β- and ω-MCA (Tα, Tβ- and Tω-MCA respectively, Toronto Research Chemicals, Toronto, Canada) and Taurine conjugated γ-MCA (Tγ-MCA, Sigma-Aldrich, Zwijndrecht, Netherlands) (Fig.S1). The HPLC grade solvents methanol (MeOH), water (H2O) and acetic acid (AcOH) of purity >98% were purchased from Biosolve BV (Valkenswaard, The Netherlands). The total bile acid concentrations in human liver is usually in the nmol/gram range [24], which is a detectable range as evidenced by Flinders et al.,[25]. However, for the fundamental ESI investigations performed in this paper standard solutions were prepared at a concentration of 10 µM dissolved in MeOH/H2O/AcOH with the ratio of 50/50/0.1 (v/v/v). Isomers infused and analysed in triplicate es, individually and/or in mixtures.

IMS-MS analysis and data evaluation

TWIMS measurements performed on a Synapt G2-Si HDMS instrument (Waters, Milford, MA, USA). The operation system of TWIMS have been discussed in detail before 12. A Helium cell is placed just before the ion mobility cell, hence the gas composition of TWIMS should be a mixture of He and N2. However the major gas flowing directly into the TWIMS cell is pure N2 with the fixed flow rate of 90 ml/min and pressure read out

of 2.87mbar. All experiments performed in a thermo-controlled laboratory, with a stable temperature read-out of 19°C. Samples were directly infused through ESI source with a Chemyx fusion 100 syringe pump (Stafford, TX, USA). Both positive and negative ion modes were tested. The $[M-H]^-$ ions did not show separation (Fig.S15), while the positive mode was found to be optimal as it showed abundant adduct formation, and hence used for all analysis. Mass spectrometry data was analysed with MassLynx v4.1. Arrival time data was analysed with DriftScope v2.8 software, mobilities of the ion of interest extracted and plotted in Excel for further analysis. Mass spectra were acquired within a mass-to-charge m/z range of 50-1500. Prior to the measurements, the instrument was calibrated with a sodium formate solution, and TWIMS was calibrated with polyalanine (Sigma-Aldrich, Zwijndrecht, Netherlands). All measurements were performed in the high-resolution mode. Applied MS and IMS parameters are presented in table S6. The cluster content confirmed by MS/MS to observe individual constituents. All experimental CCS values were obtained from TWIMS instruments ($^{TW}CCS_{N_2}$). All the IMS data were reported in accordance with the latest recommendations [26].

Theoretical calculations

The most optimal (lowest internal energy) molecular structure of the test compounds was obtained using DFT calculations on SPARTAN '18 software (v1.3.0 - Wavefunction, Inc. & Q-Chem, Irvine, CA, USA). Acquiring the global energy minimum was attempted by performing a Conformer Distribution calculation with Density Functional ω B97X-D and basis set 6-31G*. This functional was chosen instead of the commonly used B3LYP because it accounts for long-range nonbonded interactions. The geometry used was the molecular mechanics, Merck Molecular Force Field (MMFF). The software considered 100 conformers from which 10 conformers with the lowest energy were calculated with the DFT method. As it cannot be known whether the conformation represents the local or the global minimum, an adduct (Na^+ or K^+) was placed manually close to the oxygen atoms of hydroxyl or ketone groups and the energies of such isomer were compared. For the deprotonated sodium adducts, the ionic salt interactions of the Na^+ with the deprotonated site assumed. Theoretical CCS calculations were performed with the IMoS software package (v1.10) 2. Trajectory Method (TM) was applied for 3 orientations and 300.000 nitrogen gas molecules per orientation. Mulliken charges were used as partial atomic charges, they were automatically calculated by Spartan. CCS_{N_2} calculations were done for each conformer with Boltzmann weight above 5% and the weighted average of the CCS of the conformers is presented. Full dataset with each individual conformer is presented in the supporting information section (Table S5).

Results and discussion

Different approaches of combined IMS and MS/MS methodologies for the separation and structural characterization of fourteen clinically relevant bile acids (Fig.S1) were investigated by ESI-TWIMS. A comprehensive view on the performance of the MS/MS-IMS methodologies was achieved by combining and comparing the experimental $^{TW}CCS_{N_2}$ findings with the theoretical molecular modelling data obtained by SPARTAN '18 and IMoS modelling data was obtained by SPARTAN '18 and IMoS [18]. The analytes were separated in 3 groups: i) non-conjugated muricholic acids (α-, β-, ω- and γ-MCA),

ii) Taurine conjugated muricholic acids (Tα-, Tβ-, Tω- and Tγ-MCA), and iii) cholic acid and its derivatives (CA, AlloCA, TDCA, TCDCA, GDCA, GCDCA).

Mass spectra of analytes of interest

The ESI mass spectra of all analytes demonstrated a significant tendency of molecules to form sodium and potassium adducts and clustering with more than one analyte molecule (Fig.S2-6). The base peak of all non-conjugated MCA isomers (α-, β-, ω- and γ-MCA) was $[M+Na]^+$ ion at m/z 431. Despite the mild ionization conditions (Table S6), water loss was found to be favoured, as such a sequence of peaks at m/z 391, 373 and 355 (minus 1, 2, and 3H2O respectively) was detected (Fig.S2). At a higher mass range, adduct clusters were identified at m/z 632, 839 and 883, respectively relating to $[3M+2Na]^{2+}$, $[2M+Na]^+$ and $[2M+3Na-2H]^+$ ions. In the positive ion mode, deprotonation of the carboxylic acid group led to the formation of adduct ions containing multiple sodium atoms (e.g. $[M+2Na-H]^+$). Such adducts were of interest as adduct formation promotes the separation of isomers in IMS [27, 28].

Taurine conjugated MCA isomers displayed three major abundant peaks at m/z 538 for $[M+Na]^+$, m/z 554 for $[M+K]^+$, and m/z 560 for $[M+2Na-H]^+$ ions (Fig.S3). Similar to the non-conjugated MCA isomers, clusters containing two analyte molecules were also formed. However, the intensity of these dimers appeared to be very low. This could be due to the bulky taurine chain, which hampers the formation of clusters.

The CA and AlloCA mainly appeared in sodium adduct form (Fig.S4). However, TDCA and TCDCA isomers favoured potassium adduct formation (Fig.S5). According to Kruve et al., [29] in the absence of additives (e.g. Na) in a sample solution, the excessive surface charge of formed nanoparticles in ESI is defined by the impurities. These impurities can change on a daily basis and based on solvent quality and sample purity, which could explain the abundance of $[M+K]^+$ ions. In addition, the presence of more electron pair donators in TDCA and TCDCA favours the positioning of a bigger cation (K^+ versus Na^+) adjacent to the molecule to stabilize them. A different trend was observed for GDCA and GCDCA. These isomers readily lost a $SO3H^-$ group even under soft ionization conditions, without exerting collision energy (Fig.S6). Comparing the loss of sulfonate group among taurine and glycol-conjugated groups suggests the greater tendency of steroid ring A to stabilise by losing a $SO3^-$ group. Nevertheless, intact GDCA and GCDCA isomers mainly appeared in the form of $[M+2Na-H]^+$ ions or very low abundant dimers, $[M+Na]^+$ and $[M+H]^+$ ions.

Theoretical and experimental ion mobility separation of analytes

Besides arrival time comparison, the experimentally derived ${}^{TW}CCS_{N_2}$ values were compared to the theoretically calculated ones. For theoretical calculation of CCS, the Trajectory Method (TM) was selected because it was found to be one of the most precise methods available [30]. In addition, TM output is in greater agreement with the experimental CCS [19, 31] compared to the projection approximation (PA) [30] and exact hard-sphere scattering (EHSS) [19] methods. Prior to CCS calculations, the minimal energy conformation of an ion was optimized by DFT.

Ion mobility separation of non-conjugated MCAs

The effect of adduct formation and clustering on the mobility separation of non-conjugated α-, β-, ω- and γ-MCAs isomers were investigated. No separation was achieved for the $[M+K]^+$, $[2M+Na]^+$ (Fig.S7), and $[M+Na]^+$ ions (Fig.1). On the other hand, ions containing two and three sodium atoms ($[M+2Na-H]^+$, $[3M+2Na]^{2+}$, $[2M+3Na-2H]^+$) could be more readily differentiated (Fig.1).

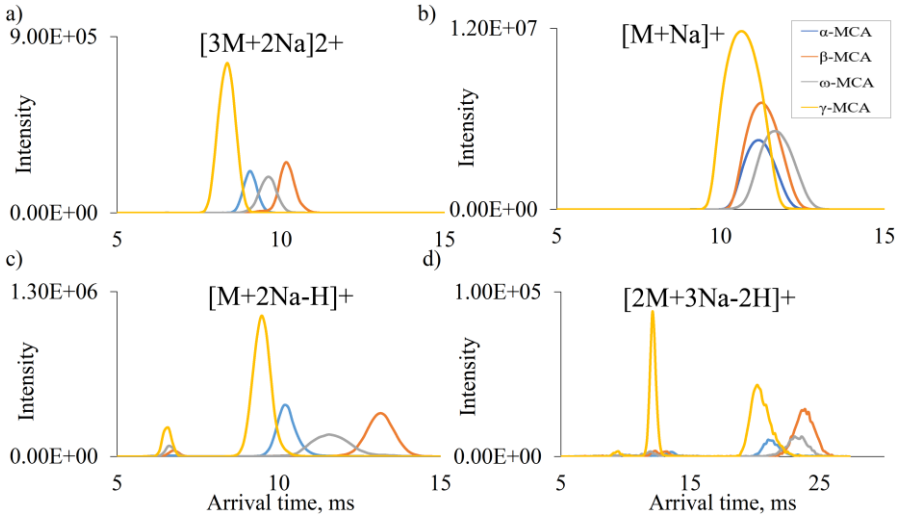

Figure 1. Arrival time distributions of non-conjugated MCAs for a) $[3M+2Na]^{2+}$, b) $[M+Na]^+$, c) $[M+2Na-H]^+$, and d) $[2M+3Na-2H]^+$ ions.

One of the major factors that promotes the separation is enhancing the structural differences in the analyte ions and reducing their similarity. Several explanations were derived in support of the experimental data based on the performed search via DFT calculations to find the most stable conformers. The low degree of separation for ions with only one metal adduct might be because the first adduct resides in between –OH groups so that either planar conformation is formed or curling of the molecule occurs around the Na^+ (Fig.2a). In the case of latter event, the central localization of Na^+ among OH-C6, OH-C7 and carboxyl group creates the opposite of the desired effect, as the adduct residing on the isomeric -OH groups (on C6 and C7) may hedge the differences in the orientation of these groups among isomers. The curled form of this ion species was found to be a more stable conformer compared to the planar one (Table S1), which could be due to the optimal charge distribution as the sodium atom is surrounded by several –OH groups. In addition, the order of experimental $^{TW}CCS_{N_2}$ values of 4 isomers were identical to the theoretical CCS values of the curled conformation rather than the planar. The theoretically obtained values (for both curled and planar conformations) were also compared to the previously measured CCS values of α-, β- and ω-MCAs isomers by drift tube IMS ($^{DT}CCS_{N2}$) [32]. Based on this comparison, only the curled conformations were within close agreement (ΔCCS<5 %) with $^{DT}CCS_{N2}$. Consequently, the

ions most likely formed curled conformation and hence due to their very close CCS values no clear separation was observed for $[M+Na]^+$ ions.

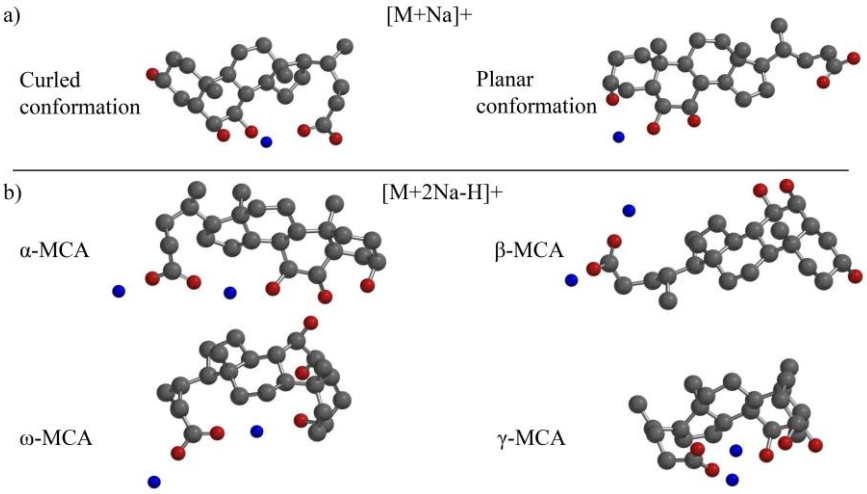

Figure 2. Molecular ion conformation of non-conjugated MCAs obtained via DFT calculations. a) Curled and planar conformations of β-MCA for the $[M+Na]^+$ ion. b) Isomers α-, ω-, γ-MCA showed similar trend. Conformations change among isomers for $[M+2Na-H]^+$ ion (Red – oxygen, grey – carbon, blue – sodium).

The $[M+2Na-H]^+$ ion displayed a different trend. According to the DFT calculations, the positioning of the two sodium adducts differed greatly among the non-conjugated α-, β-, ω- and γ-MCA isomers (Fig.2b), which led to differentiation. Furthermore, there is a shift in the relative mobility of isomers upon the addition of the second sodium. As such, that γ-MCA opts highest mobility, while β-MCA has lowest mobility (Fig.1c). This suggests that the second sodium atom on the isomers decreases the CCS of γ-MCA, making it more compact, whilst increasing the CCS of β-MCA. The CCS changes arise possibly because the side branch curls in the same plane with the -OH groups for γ-MCA, making it ball-like, whereas on β-MCA the two adducts are probably on the acidic group leading to a planar conformer and increasing the ion's surface (Fig.2).

It is expected that compounds with narrow peaks in the arrival time distributions have fewer conformers compared to the ones showing broader peaks. This appeared true for the $[M+2Na-H]^+$ ion as DFT results yielded one conformer for γ-MCA and two conformers for β-MCA with more than 5% Boltzmann weight (Table S5 and Fig.1c). The opposite was observed for the ω-MCA. The broadness of the ω-MCA peak on Figure.1c could be explained by having multiple conformers with similar and high (>30%) Boltzmann weights, found by DFT calculations (Table S5). This implies that the molecule has several stable conformations with slightly different mobilities, which leads to the broadening of the mobility peaks. The DFT calculation of α-MCA unexpectedly showed high number of conformers, which was not reflected in the experimental results. This may be explained either by the fact that the experimental conditions affect the conformers' abundance,

or that the conformers with lower abundance do not significantly affect the overall arrival time to broaden the peak. Most α-MCA conformers were less than 10% abundant (Table S5).

The theoretically calculated CCS values were in close agreement (less than 5%) with the experimentally extracted $^{TW}CCS_{N_2}$ values (with RSD% of less than 2%), which is a common range for TWIMS experiments (Table S2-4) [33]. This discrepancy might indicate that conformers calculated in DFT differ from those adopted in real life measurement conditions. Alternatively, the DFT calculation method lacked precision, which is likely since the investigated molecules have many rotational bonds and relatively bulky side chains [20]. Such a discrepancy in values was observed for most of the ions calculated in this study, suggesting that this is a systematic error. Nevertheless, the order of the least mobile to the most mobile ions was comparable between theoretical and experimental calculations. This suggests that the conformations obtained with molecular modelling are relevant and can be used for further investigations of the ion behaviour.

Arrival time distribution of the $[M+2Na-H]^+$ ion displayed two sets of peaks (Fig.1c); the first one appeared at 6.0-7.0 ms and the second one at 8.5-14.5 ms. The latter represents the arrival time of the selected ion ($[M+2Na-H]^+$ at m/z 453). The peak at 6.0-7.0 ms is related to a more mobile metastable ion, which probably undergoes structural changes en route from the ion source to the MS detector, after its arrival time has been recorded, as explained before [34, 35]. By the time it hits the TOF mass analyser, the modified ion has the same mass as the analyte of interest, resulting in two arrival time peaks. A possible theory, in line with the study conducted by Chouinard et al.,[36] is that some species tend to fragment to a seeking m/z upon leaving the ion mobility cell. In the case of this study, both ion species of $[M+2Na-H]^+$ and $[2M+4Na-2H]^{2+}$ were possibly formed in the liquid phase or in the ionization source. Bearing multiple charges by $[2M+4Na-2H]^{2+}$ ion makes it more mobile than $[M+2Na-H]^+$ and shortens its arrival time (Fig.S8). The doubly charged ion species could either directly reach the detector or its additional charge gets fragmented away during the traverse from the ion mobility cell to the detector. In the latter case, the ion could also adopt the $[M+2Na-H]^+$ structure, m/z of which will be recorded by the MS. This was confirmed by performing MS/MS before of the IMS cell (in the trap cell of TWIM). As a result of MS/MS-IMS the low abundant $[2M+4Na-2H]^{2+}$ ions fragmented, consequently no arrival time distribution at the lower time scale (6.0-7.0 ms) observed (Fig.S8). A similar phenomenon was also observed for the $[2M+3Na-2H]^+$ ion (Fig.1d), which illustrated the tendency of the molecule to form doubly charged clusters of $[2M+6Na-2H]^{2+}$.

Figure 1a displays the arrival time graph for the $[3M+2Na]^{2+}$ ion of the non-conjugated isomers with clear differentiation. This ion species had faster arrival time compared to the other ion species due to its double charge. Currently, it is not possible to obtain the lowest energy structure of such large clusters through DFT as this will require numerous manual alterations and lead to extremely high computational costs [36]. Individual injection of each isomer forced them to form homo-trimer, which resulted in having distinguishable mobility values and differentiation (Fig.1a). However, when four isomers were injected in a mixture solution, their arrival time distribution resulted in one broad

peak with no separation (Fig.S9). This means that the trimer ion ($[3M+2Na]^{2+}$) consists of a random combination of 4 isomers (α-, β-, ω- and γ-MCA), and this ion is not an optimal choice for isomeric separation in a complex sample.

Direct injection of individual analytes to ESI-TWIMS resulted in a clear differentiation of several adduct ions of the stereoisomers (Fig.1). However, the challenge in the clinical analysis is to distinguish among the isomers in a complex and mixture solution. Besides insufficient resolution of an analytical tool, matrix effect and gas-phase interaction of ions may cause peaks to fuse together in one broad peak. It can also be challenging to separate a mixture of isomers by analysing the cluster peaks containing more than one molecule. This is because such clusters may consist of a random combination of isomers and form hetero - dimer/trimer [23]. Nevertheless, an interesting trend was observed for the $[2M+3Na-2H]^{+}$ ion species, where the α- vs ω- MCAs or α- vs β- MCAs could be differentiated (Fig.S10a). The bimodal peak, that was formed when a mix of β-MCA and γ-MCA was injected, indicates that ions mainly tend to form homo-dimer, instead of forming a hetero-dimer. While this way of homo- clustering may not occur for other ions such as $[3M+2Na]^{2+}$ (Fig.S9). The 2M clusters were found to show good discrimination between the isomers. In this trend, isomers can only be differentiated in pairs as β-MCA overlaps with ω-MCA. Between these molecules, only the 6-hydroxyl isomeric group promotes separation, while the different orientations of the 7-hydroxyl group do not influence the arrival time distributions. A similar trend for steroid dimers was also seen in prior research [36].

In order to investigate a mixture of non-conjugated MCA analytes in pre-clinical studies, the $[M+2Na-H]^{+}$ ion species is the most optimal ion of choice. The trimodal peak of $[M+2Na-H]^{+}$ ion shows a clear differentiation among α-, β- and ω-MCAs (Fig.S10b). This finding suggests that the minimum ${}^{TW}CCS_{N_2}$ differences of about 10 $Å2$ is required to enable differentiating the bile acid isomers. However, discrimination of α- and γ-MCA isomers in a clinical sample, namely patients' material, remains a challenge, which could be address by means of a high resolution IMS.

Ion mobility separation of Taurine conjugated MCAs

The ion mobility separation of the taurine conjugated MCAs was investigated. Unlike non-conjugated MCAs, the individual injection of Tα-, Tβ-, Tω- and Tγ- MCA isomers resulted in more overlapped peaks (Fig.S11a, b, c). The large taurine group of these isomers contributed to the structural similarity by forming an intermolecular bridge with the C3-OH, hence the collisional cross section values were too close to each other for separation. The separation of these set of MCAs has been a challenge even when another traveling wave based mobility separation module: structures for lossless ion manipulations-serpentine ultralong path with extended routing- ion mobility (SLIM-SUPER-IM) was utilized [37]. These isomers could be separated only after addition of cyclodextrin to form noncovalent complexed with MCA isomers.

The arrival time distribution of three types of adduct ions ($[M+Na]^{+}$, $[M+K]^{+}$ and $[M+2Na-H]^{+}$) had two distinct high and low mobile peaks in a similar order to the non-conjugated MCA ions. The highly mobile peaks, which were observed at 6-7 ms (Fig.S11),

were subjected to the same outcome both in conjugated and non-conjugated MCA isomers and were formed by doubly charged cluster ions ($[2M+2Na]^{2+}$, $[2M+2K]^{2+}$ and $[2M+4Na-2H]^{2+}$). Notably, only the $[M+Na]^{+}$ of the Tβ- MCA isomer showed an extra peak with lower arrival time, unlike the other two ions ($[M+K]^{+}$ and $[M+2Na-H]^{+}$), where all isomers displayed two distinct peaks (Fig.S11c).

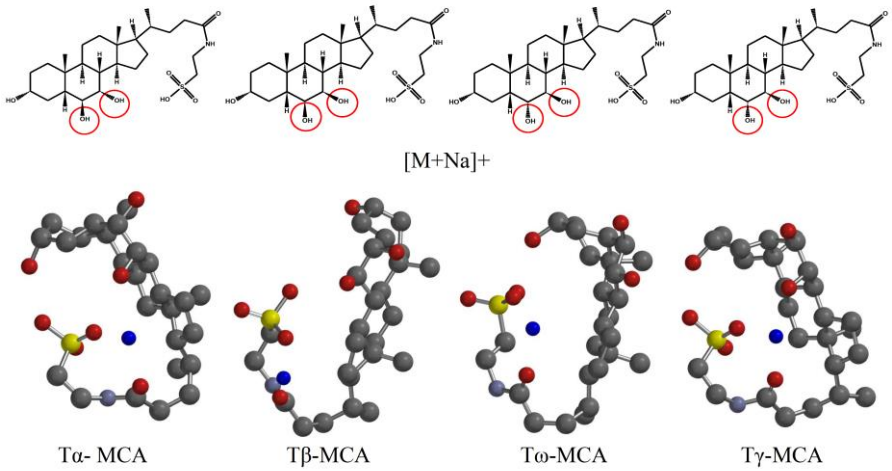

Figure 3. Molecular ion conformations of $[M+Na]^{+}$ ions for taurine conjugated MCA isomers obtained via DFT calculations (Red – oxygen, grey – carbon, blue – sodium, purple – nitrogen, bright yellow – sulphur).

As shown on Figure 3, the conformation of $[M+Na]^{+}$ ion differs for each isomer, with the Tγ-MCA being the most compact and the Tβ-MCA having the largest surface area. These theoretical differences were consistent with the experimental $^{TW}CCS_{N_2}$ (Table S3) and the arrival time data (Fig.S11b). A similar trend was observed for the $[M+K]^{+}$ adduct, though here the CCS of the Tβ-MCA was relatively low, compared with the experimental findings. Among the conjugated MCA isomers, experimental $^{TW}CCS_{N_2}$ values differed by maximum 6.1 Å2, whilst $^{TW}CCS_{N_2}$ value differences could reach almost 30 Å2 for the non-conjugated MCAs. Consequently, the inability to separate taurine conjugated MCAs is due to the resolution of the instrument, as the peaks with $^{TW}CCS_{N_2}$ values of less than ≈10 Å2 difference will have fused arrival time distributions and hence will not show clear separation. Thus, it is possible to discriminate among the taurine conjugated MCA isomers when measured individually but not in a complex sample.

Ion mobility separation of CA and its derivatives

Cholic acid and its derivatives have also exhibited measurable ion mobility differences upon investigation by ESI-TWIMS. The IMS of CA with 5β configuration was comparable to that of AlloCA with 5α configuration. Although there was no baseline ion mobility separation, each isomer eluted with slightly different arrival times (Fig.S11d and e). Prior research has shown that steroids containing 5α groups tend to have a planar ring

structure, while those containing 5β groups appear to adopt a bent conformation [38]. Hence, there was a notable difference in the experimental $^{TW}CCS_{N_2}$ values between CA and AlloCA enantiomers (5.22 Å2). However, this difference was not significant enough to separate them in a mixture solution. Similar to MCA ions, CA and AlloCA ions tended to form doubly charged clusters of $[2M+2Na]^{2+}$, which appeared as a highly mobile peak at 6 ms arrival time (Fig.S11d).

The energy comparison between the planar and curled conformers (Table S1) showed that the curled conformer of $[M+Na]^+$ ions was more stable, especially for AlloCA. However, the CCS value for the curled conformer of AlloCA was not consistent with the experimental data (Table S4). Experimentally, AlloCA had higher CCS than CA (206.61 and 201.39 Å2 respectively), which is theoretically comparable only if AlloCA adopts a planar conformation. This suggests that AlloCA isomers form a less energetically favourable structure in the gas-phase of IMS, which is the bioactive conformation of this bile acid [39].

The only structural difference between GDCA and GCDCA isomers is related to the position of hydroxyl group on C7 and C12, respectively. Under the soft ionization conditions of ESI-TWIMS, the SO3H- group of GDCA and GCDCA was lost upon collisional activation. When the IMS of the mono-sodiated fragment ions ($[M1+Na]^+$) of these isomers was investigated, two separable arrival time distributions (Fig.S11f) were obtained with CCS differences of 8.37 Å2 (Table S4). The DFT conformers of $[M1+Na]^+$ ions for these structural isomers were found to differ significantly in their folding orientation (Fig.4). It might be explained by the carboxyl branch of each isomer, which tended to curl over its –OH group, positioned on either C7 or C12. Poland et al., investigated the molecular model of glycocholic acid and they also reported about the tendency of carboxyl side chain to fold over the steroid ring to form a bridge with –OH group [40]. In addition, the steroid ring of GDCA isomer adopted a more planar conformation than GCDCA. Consequently, the gas-phase conformation of each isomer had a unique CCS value.

The presence of multiple sodium adducts on the fragment ion ($[M1+2Na-H]^+$), on the other hand, formed a bulky conformation, that brought the CCS values very close to each other (Fig.S13, Table S4). Positioning a sodium adduct and a sodium salt on the molecule prohibited the fragmentation of the sulphate group and preserved the original molecular structure. Multiple sodium adducts on GDCA and GCDCA molecules (e.g. $[M+2Na-H]^+$, and $[M+3Na-2H]^+$), curled the side chains located on C3 and C17, on the steroid ring skeleton, forming a ball-like structure. Adopting such a bulky conformation reduced the impact of the -OH group orientation on the CCS of the whole molecular ion and inhibits ion mobility separation (Fig.S14). Therefore, the presence of multiple adducts does not necessarily increase the collision cross sectional differences; however, it is a molecular structure dependent property.

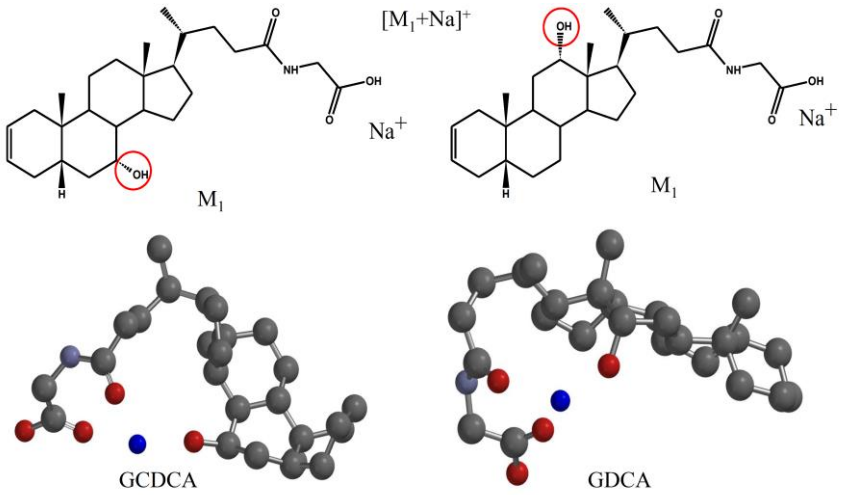

Figure 4.Molecular ion conformations of [M1+Na]⁺ ion for GCDCA and GDCA isomers obtained via DFT calculations (Red – oxygen, grey – carbon, blue – sodium, purple – nitrogen).

On TDCA and TDCDA isomers, the potassium was positioned such that the large carboxyl branch of the molecular ion was curled on its rings and the 3-OH group led into the bending of the steroid ring towards potassium (Fig.S12a). This curling concealed the small difference of TDCA and TCDCA that is the position of OH group on C12 and C17, respectively. The structural prediction by DFT was also reflected by the experimental $^{TW}CCS_{N_2}$ differences of 3.29 Å2 (Table S4), which is a small value for the IMS separation of taurine conjugated CAs by TWIMS. To partially fragment off the large branches of TDCA and TCDCA, the trap collision cell energy was increased. Although the MS/MS-IMS approach formed smaller sodiated fragment ions of M1 (Fig.S12b), $[M1+Na]^+$ ions did not enhance the IMS separation. The ΔCCS of $[M1+Na]^+$ ions of TDCA and TCDCA isomers was even below 1 Å2 (Table S4), which made them very challenging isomers to be separated compared to the intact adduct ions. This trend was unlike the observed results for GDCA and GCDCA isomers, where the fragment ions pronounced the differences of two isomers and thus the differentiation was promoted. The main reason for this alternating result relies on the steroid ring conformation. The lowest energy conformer of $[M1+Na]^+$ ions was predicted to adopt the curled conformation (Table S1). Curling of the side branch along with bending of the steroid ring towards an adduct hedged the small differences between isomers. This was further supported by experimental $^{TW}CCS_{N_2}$values, where the theoretical value will be comparative to the experimental data if only TDCA and TCDCA have curled conformations (Table S4). Adopting bent ring conformation by both isomers brought their CCS values very close to each other.

Comparing the molecular model of CA and its derivatives, it is suggested that one of the promoting factors in the ion mobility separation of bile acids is to adopt the bent or planar conformation on the steroid ring. The presence of a functional group with high

electron density on the steroid ring A and B (e.g. on C3 and C7) increases the possibility of forming a bent ring conformation. Along with the ring conformation, fragmenting off the large identical functional groups of isomers further exposes their small structural differences to the neutral gas of IMS cell. Hence, MS/MS-IMS is another method to facilitate IMS discrimination of isomers.

Conclusion

The molecular ion structure and ion mobility separation of 14 clinically relevant bile acids were studied by ESI-TWIMS. The gas-phase behaviour of these molecules was thoroughly explained by DFT predations and theoretical CCS calculations. These findings enabled to predict the gas-phase behaviour of steroid compounds. Multiple adducts' localization on the non-conjugated MCA enabled the differentiation of these isomers in a complex sample. In addition, the tendency of each isomer to form multiple conformers with high abundance broadened the ion mobility peaks. Taurine conjugated MCA isomers showed very close collision cross section values, which was the consequence of having a large taurine chain, contributing to the conformational similarities. The bent and planar ring structures of respectively CA and AlloCA were confirmed by both experimental $^{TW}CCS_{N_2}$ and theorical predictions. Consequently, the 3D-shape differences of these enantiomers enabled their ion mobility differentiation. The formation of fragment ions before the ion mobility cell led to significant differences in the mobility of isomers and thereafter promoted the differentiation of CA derivatives. Another enabling factor to separate molecules with a steroid ring skeleton was to impose formation of bend and planar ring structures. According to the findings of this study, the $^{TW}CCS_{N_2}$ difference of ≈10 Å 2 is suggested as the minimal required value to obtain ion mobility differentiation of bile acids in a complex sample by TWIMS. Combining the ion mobility and mass spectrometry data with theoretical studies deepens researchers' knowledge regarding the gas-phase behaviour of molecular ions. This knowledge allows smart planning for (pre-) treatment of complex clinical samples of bile acids.

Acknowledgement

We would like to thank Dr. Frank G Schaap (Department of General Surgery, Maastricht University) for fruitful discussion and for providing the bile acid standards. Tiffany Porta Siegel would like to thank the financial support from the Dutch Province of Limburg.

Declaration of competing interest

The authors declare that there is no conflict of interest.

References

1. Guddat, S., et al., *Application of FAIMS to anabolic androgenic steroids in sport drug testing.* Drug Testing and Analysis, 2009. **1**(11-12): p. 545-553.
2. Gouveia, M.J., et al., *Mass spectrometry techniques in the survey of steroid metabolites as potential disease biomarkers: a review.* Metabolism: clinical and experimental, 2013. **62**(9): p. 1206-1217.
3. Nozaki, O., *Steroid analysis for medical diagnosis.* Journal of Chromatography A, 2001. **935**(1): p. 267-278.

4. Pavlović, N., et al., *Bile Acids and Their Derivatives as Potential Modifiers of Drug Release and Pharmacokinetic Profiles.* Frontiers in Pharmacology, 2018. **9**(1283).
5. Hasuike, Y., et al., *Bile acid abnormality induced by intestinal dysbiosis might explain lipid metabolism in Parkinson's disease.* Medical Hypotheses, 2020. **134**: p. 109436.
6. McMillin, M. and S. DeMorrow, *Effects of bile acids on neurological function and disease.* FASEB journal : official publication of the Federation of American Societies for Experimental Biology, 2016. **30**(11): p. 3658-3668.
7. Baloni, P., et al., *Identifying differences in bile acid pathways for cholesterol clearance in Alzheimer's disease using metabolic networks of human brain regions.* bioRxiv, 2019: p. 782987.
8. Ackerman, H.D. and G.S. Gerhard, *Bile Acids in Neurodegenerative Disorders.* Frontiers in aging neuroscience, 2016. **8**: p. 263-263.
9. Hadavi, D. and A.A. Poot, *Biomaterials for the Treatment of Alzheimer's Disease.* Frontiers in Bioengineering and Biotechnology, 2016. **4**(49).
10. Karasek, F., *Plasma Chromatography.* Analytical Chemistry - ANAL CHEM, 2008. **46**.
11. Asbury, G. and H. Hill, *Evaluation of Ultrahigh Resolution Ion Mobility Spectrometry as an Analytical Separation Device in Chromatographic Terms.* Journal of Microcolumn Separations, 2000. **12**.
12. Kyle, J.E., et al., *Uncovering biologically significant lipid isomers with liquid chromatography, ion mobility spectrometry and mass spectrometry.* Analyst, 2016. **141**(5): p. 1649-1659.
13. Kanu, A.B., et al., *Ion mobility–mass spectrometry.* Journal of Mass Spectrometry, 2008. **43**(1): p. 1-22.
14. Genangeli, M., et al., *MALDI-Mass Spectrometry Imaging to Investigate Lipid and Bile Acid Modifications Caused by Lentil Extract Used as a Potential Hypocholesterolemic Treatment.* J Am Soc Mass Spectrom, 2019. **30**(10): p. 2041-2050.
15. Rzagalinski, I., et al., *MALDI Mass Spectral Imaging of Bile Acids Observed as Deprotonated Molecules and Proton-Bound Dimers from Mouse Liver Sections.* Journal of The American Society for Mass Spectrometry, 2018. **29**(4): p. 711-722.
16. Brock, W.J., et al., *Bile Acids as Potential Biomarkers to Assess Liver Impairment in Polycystic Kidney Disease.* International journal of toxicology, 2018. **37**(2): p. 144-154.
17. Frisch, M., et al., *Gaussian 16 Rev. C. 01, Gaussian 16 Rev C01.* 2016.
18. Wu, T., et al., *Optimization of long range potential interaction parameters in ion mobility spectrometry.* The Journal of Chemical Physics, 2018. **148**(7): p. 074102.
19. Mesleh, M.F., et al., *Structural Information from Ion Mobility Measurements: Effects of the Long-Range Potential.* The Journal of Physical Chemistry, 1996. **100**(40): p. 16082-16086.
20. Boschmans, J., et al., *Combining density functional theory (DFT) and collision cross-section (CCS) calculations to analyze the gas-phase behaviour of small molecules and their protonation site isomers.* Analyst, 2016. **141**(13): p. 4044-4054.
21. Gabelica, V. and E. Marklund, *Fundamentals of ion mobility spectrometry.* Current Opinion in Chemical Biology, 2018. **42**: p. 51-59.
22. Ahonen, L., et al., *Separation of steroid isomers by ion mobility mass spectrometry.* Journal of Chromatography A, 2013. **1310**: p. 133-137.
23. Rister, A.L., T.L. Martin, and E.D. Dodds, *Formation of multimeric steroid metal adducts and implications for isomer mixture separation by traveling wave ion mobility spectrometry.* Journal of Mass Spectrometry, 2019. **54**(5): p. 429-436.
24. Setchell, K.D., et al., *Bile acid concentrations in human and rat liver tissue and in hepatocyte nuclei.* Gastroenterology, 1997. **112**(1): p. 226-35.

25. Flinders, B., et al., *Cross-Species Molecular Imaging of Bile Salts and Lipids in Liver: Identification of Molecular Structural Markers in Health and Disease.* Anal Chem, 2018. **90**(20): p. 11835-11846.
26. Gabelica, V., et al., *Recommendations for reporting ion mobility Mass Spectrometry measurements.* Mass spectrometry reviews, 2019. **38**(3): p. 291-320.
27. Hadavi, D., et al., *Adduct ion formation as a tool for the molecular structure assessment of ten isomers in traveling wave and trapped ion mobility spectrometry.* Rapid Communications in Mass Spectrometry, 2019. **33**(S2): p. 49-59.
28. Zietek, B.M., et al., *Adduct-ion formation in trapped ion mobility spectrometry as a potential tool for studying molecular structures and conformations.* International Journal for Ion Mobility Spectrometry, 2018. **21**(1): p. 19-32.
29. Kruve, A. and K. Kaupmees, *Adduct Formation in ESI/MS by Mobile Phase Additives.* Journal of The American Society for Mass Spectrometry, 2017. **28**(5): p. 887-894.
30. Shvartsburg, A.A. and M.F. Jarrold, *An exact hard-spheres scattering model for the mobilities of polyatomic ions.* Chemical Physics Letters, 1996. **261**(1): p. 86-91.
31. Shvartsburg, A.A., G.C. Schatz, and M.F. Jarrold, *Mobilities of carbon cluster ions: Critical importance of the molecular attractive potential.* The Journal of Chemical Physics, 1998. **108**(6): p. 2416-2423.
32. Zheng, X., et al., *Evaluating the structural complexity of isomeric bile acids with ion mobility spectrometry.* Analytical and Bioanalytical Chemistry, 2019. **411**(19): p. 4673-4682.
33. Kune, C., J. Far, and E. De Pauw, *Accurate Drift Time Determination by Traveling Wave Ion Mobility Spectrometry: The Concept of the Diffusion Calibration.* Analytical Chemistry, 2016. **88**(23): p. 11639-11646.
34. Pettit, M.E., et al., *Collision-energy resolved ion mobility characterization of isomeric mixtures.* Analyst, 2015. **140**(20): p. 6886-6896.
35. Pettit, M.E., et al., *Broadband ion mobility deconvolution for rapid analysis of complex mixtures.* Analyst, 2018. **143**(11): p. 2574-2586.
36. Chouinard, C.D., et al., *Experimental and Theoretical Investigation of Sodiated Multimers of Steroid Epimers with Ion Mobility-Mass Spectrometry.* Journal of The American Society for Mass Spectrometry, 2017. **28**(2): p. 323-331.
37. Chouinard, C.D., et al., *Rapid Ion Mobility Separations of Bile Acid Isomers Using Cyclodextrin Adducts and Structures for Lossless Ion Manipulations.* Analytical Chemistry, 2018. **90**(18): p. 11086-11091.
38. Mendoza, M.E., et al., *Physiological characteristics of allo-cholic acid.* J Lipid Res, 2003. **44**(1): p. 84-92.
39. Shiffka, S.J., M.A. Kane, and P.W. Swaan, *Planar bile acids in health and disease.* Biochimica et Biophysica Acta (BBA) - Biomembranes, 2017. **1859**(11): p. 2269-2276.
40. Poland, J.C., et al., *Collision Cross Section Conformational Analyses of Bile Acids via Ion Mobility–Mass Spectrometry.* Journal of the American Society for Mass Spectrometry, 2020. **31**(8): p. 1625-1631.

Chapter 2 - Dynamics of large molecules and biopolymers by ion mobility spectrometry and Surface plasmon resonance

Section 1 - Buffer 4-ethylmorpholine/acetate maintains solution-phase folding for native mass spectrometry of proteins and proteins complexes

Darya Hadavi, Che yee Ng, Yuandi Zhao, Anjusha Mathew, Ian G. M. Anthony, Eva Cuypers, Tiffany Porta Siegel, Maarten Honing

Maastricht MultiModal Molecular Imaging (M4i) Institute, Division of Imaging Mass Spectrometry (IMS), Maastricht University, Maastricht, The Netherlands.

Based on

Submitted paper to the journal of Angewandte Chemie.

Section 2 - Investigating the protein-protein interactions of cardiac troponin subunits using surface plasmon resonance

Yuandi Zhao[1], Nika Šimičić[1], Martin Albers[2,3], Maarten Honing[1], Darya Hadi[1]

[1]Maastricht Multimodal Molecular Imaging (M4i) Institute, Division of Imaging Mass Spectrometry Maastricht University, Universiteitssingel 50, 6229ER, Maastricht, The Netherlands
[2]BioNavis Ltd., Hermiankatu 6-8 H, 33720 Tampere, Finland
[3]Technex B.V., Industrieweg 35, 1521 NE Wormerveer, The Netherlands

Based on

In preparation paper for submission.

Chapter 3 - Hyphenation of ion mobility and mass spectrometry to dynamic microfluidic systems; study of small and large molecules

Section 1 - Technological advances for analyzing the content of organ-on-a-chip by mass spectrometry

Darya Hadavi, Ilona Tosheva, Tiffany Porta Siegel, Eva Cuypers, Maarten Honing

Maastricht Multimodal Molecular Imaging (M4i) Institute, Division of Imaging Mass Spectrometry Maastricht University, Universiteitssingel 50, 6229ER, Maastricht, the Netherlands

Based on

Submitted paper to the journal of Frontiers in Bioengineering and Biotechnology.

Abstract

Three-dimensional (3D) cell cultures, including organ-on-a-chip (OOC) devices, offer the possibility to mimic human physiology conditions better than 2D models. The OOC devices have a wide range of applications, including mechanical studies, functional validation, and toxicology investigations. Despite many advances in this field, the major challenge with the use of OOCs relies on the lack of online analysis methods preventing the real-time observation of cultured cells. Mass spectrometry is a promising analytical technique for real-time analysis of cell excretes from OOC models. This is due to its high sensitivity, selectivity, and ability to tentatively identify a large variety of unknown compounds, ranging from metabolites, lipids, and peptides to proteins. However, the hyphenation of OOC with MS is largely hampered by the nature of the media used, and the presence of nonvolatile buffers. This in turn stalls the straightforward and online connection of OOC outlet to MS. To overcome this challenge, multiple advances have been made to pre-treat samples right after OOC and just before MS. In this review, we summarised these technological advances and exhaustively evaluated their benefits and shortcomings for successful hyphenation of OOC with MS.

Keywords: mass spectrometry, organ-on-a-chip, interface, analytical technique, online, real-time analysis

Introduction

The use of three-dimensional (3D) cell cultures has been growing due to their widespread application ranging from studying drug efficacy and toxicity to creating disease models [1]. By using a 3D-culture model, one can mimic the *in vivo* environment of human physiology more accurately than two-dimensional (2D) models, such as standard cell culture [2, 3]. Therefore, the quality of the conducted experiments improves. The progress of 3D devices and technologies has advanced to the development of microfluidic chips to capture organ-level function known as organ-on-a-chip (OOC) [4, 5]. The design of the OOC devices is made to mimic the human cellular microenvironment. It includes the flow of fluids through micro-channels to mimic the vasculature network for providing nutrients and transporting waste and metabolites. The OOC models could also simulate the physical environment of human organs (e.g. lung, gut, and kidney) by mimicking the structural features [6-8]. This can eventually facilitate the translation of the *in vitro* findings to the human condition.

The use of OOCs has the potential to make the drug discovery process fast and cheaper (with a cost reduction of up to 26%) [9]. However, despite many advances, its applicability is hampered by the lack of online detection schemes, allowing the real-time observation of cellular behaviors [10, 11]. This shortage limits our understanding of cellular mechanism as a function of time and consequently prevents us from correcting the deficiencies of the OOC models created. The analytical techniques that have been used so far include optical imaging, electrochemical sensors, fluorescence- or label-free assays such as photonic crystal in a total internal reflection [12], capillary electrophoresis, and mass spectrometry (MS) [13].

Among these techniques, MS offers high sensitivity and specificity to analyze changes in metabolites, proteins, and lipids [14-16]. Utilizing MS for the in-situ monitoring of 3D cell systems in OOC can provide insight into the molecular composition of culture media, excreted metabolites, and waste products [17]. Despite the multiple advantages of MS, it cannot be directly coupled with OOC for online and real-time analysis of molecules of interest (e.g. cytokines, proteins, chemokines) [11]. This problem occurs mainly due to the presence of cell media in the chambers of OOC, which is rich in salts, non-volatile buffers, and compounds that can hamper the MS analysis by creating ion suppression [13]. Currently, offline sample preparation methods are used to manipulate cell excretes before MS analysis. However, with these approaches, the time-resolved detection of metabolites is largely reduced, which is an essential factor for unraveling cellular mechanisms.

Considering multiple advantages that MS offers for biomedical applications in this review, the main attention is given to the investigated and tested approaches to directly couple OOC with MS and their capabilities and shortcomings for real-time analysis are exhaustively reviewed. The review begins with an introduction to OOC and used analytical techniques to evaluate the mimetic tissue models. After a brief discussion on the techniques of phase contrast microscopy, enzyme-linked immunosorbent assays (ELISA), transepithelial electrical resistance (TEER), the review is mainly focused on MS. To this end, MS introduction is followed by hyphenation techniques that bridge OOC

with MS, namely electrophoresis, solid phase extraction, liquid chromatography and droplet-based chips, and their limitations are discussed. This article provides an exhaustive review of relatively new developments that would potentially enable the development of a robust and reliable interface for analyzing OOC content with MS as a rapid, sensitive, and specific analytical technique.

Introduction to organ-on-a-chip

Organ-on-a-chip devices simulate human micro-physiological systems, which is a powerful alternative to conventional 2D *in vitro* testing [2, 3, 10, 18]. The OOC field emerged almost 25 years ago starting with microfluidic-associated microfabrication techniques and moving toward more physiologically relevant cell cultures [19]. The common composition of an OOC is a flexible polymer the size of a computer USB stick, that contains microfluidic channels lined by living human organ-specific cells, interconnected with human endothelial artificial vasculature (Figure 1a) [20]. This design provides the scientist with a window into the inner working condition of human cells in living tissues. Consequently, it allows them to study the molecular- and cellular-scale activities that drive human organ function [20]. The OOC is at the frontier of microfluidics, tissue engineering, and stem cell biology [18, 21]. As OOC devices attempt to replicate human physiology, they have been implemented in mechanical studies as well as functional validation [22]. Furthermore, they can be potentially implemented in molecular pharmacology testing during the drug discovery phase, giving information on the mode of action, efficacy, and toxicity of the drug candidates in lead libraries [23]. The fast advances in this field can not only decrease the costs of pharmacological studies [24] but possibly enables the testing of drug combinations at different concentration levels facilitating the design of treatments in personalized medicine. For example, cancer patients have different responses to the given treatment. The use of OOC for the growth and observation of patient-specific cells can assess the most convenient treatment and drug concentrations for each patient [25]. Additionally, OOCs can also be used as neural-systems-on-a-chip for target-based or phenotypic screenings using patient-specific disease models, establishing highly effective treatments [26].

Thus far many OOCs have been developed, including specific conditions for the organ or tissue of interest. These conditions include pressure, flow rate, pH, osmotic pressure, nutrient content, and toxins' presence or absence [2]. Amongst the many OOCs, one can find lung-, liver-, kidney-, gut-, skin-, brain-, heart- and even placenta-on-a-chip [6, 25]. With the new studies conducted in the past years, researchers are aiming to bring this field a step further by developing a human-on-a-chip, leading to mimicking the whole-body physiology in multiple connected OOCs [5, 7, 20]. Therefore, this would allow for the observation and analysis of how different agents influence the physiological functioning of the body as a whole. Eventually, it can also allow for progress in personalized medicine [4, 24], prediction of quantitative pharmacokinetic parameters [27], and examination of metastasis processes by metastasis-on-a-chip devices [25].

With this goal to simulate the physiological environment of human organs as accurately as possible [7], OOC devices are widely claimed as a potential tool in replacing animal studies [28]. However, with current knowledge, this replacement seems very

challenging. One of the obstacles in this transition is the lack of analytical technologies, able to selectively detect low concentrations of a large diversity of molecules in a time-resolved manner, and both in or outside the cells. It seems obvious that the availability of real-time measurements will serve to monitor the dynamic behavior of the cellular microenvironment. In the upcoming sections, the analysis method of OOC is evaluated.

Organ-on-a-chip analytical techniques

Some of the challenges that come along with the implementation of OOCs in research include the analytical techniques that have been commonly used for chip analysis [10, 11]. Evaluating the tissue behavior in OOC devices requires accurate, non-invasive, and real-time measurement of cell functions [17]. (17). Some of the analytical techniques that have been implemented for on-/off-chip analysis include phase contrast microscopy, ELISA, TEER and MS compared in table 1[13, 19].

Microscopy

Various optical imaging techniques have been used to monitor OOC platforms. Amongst them are, bright-field microscopy, phase contrast microscopy, and fluorescent and confocal microscopy [29]. To monitor the cellular level activities in an OOC by optical microscopies, high magnifications (e.g., 400x – 1500x) and a resolution of 0.25 µm are preferred. One of the general disadvantages under these conditions is related to a low field of view at high magnifications and resolutions [29, 30]. The limited field of view obscures observing the total area of micron-sized chips. This limitation becomes more concerning when dynamic cellular mechanisms are under investigation. Another aspect to consider when utilizing microscopes is the required low working distance between the objective lens and the surface of the sample for better resolution and magnification [29]. This requirement imposes the fabrication challenge to OOC devices, which must have a similar thickness and refractive index to those of the used objectives. This in turn dramatically restricts the choice of material for chip manufacturing and inhibits the fabrication of complex designs. Additionally, the use of either fluorescent or confocal microscopy in OOC analysis faces the researchers with challenge of attaching fluorescent molecules to the appropriate biological agents [29]. Furthermore, although confocal microscopy is a technique of high quality for the analysis of OOC, the intensity of the laser beam should be carefully controlled to prevent phototoxicity of the cells on the chip, thus the optical setup has to be highly precise [29].

Enzyme-linked immunosorbent assays (ELISA)

ELISA enables measuring the enzymatic activity of analytes, antigens, and antibodies. The process is based on the application of enzymes as labels and the subsequent detection of the occurring enzymatic reactions [31, 32]. Nestorova and colleagues presented the use of thermoelectric direct sandwich ELISA as an analytical technique for OOC (Figure 1b). Their microfluidic device included a channel wall with immobilized primary antibody and an inlet to introduce unmodified analyte. The same inlet was used to supply enzyme-linked reporter to form primary antibody-analyte-reporter antibody complex. A separate inlet was used to provide a laminar flow of substrate for the enzymatic reaction. This reaction releases heat which was detected by a thermopile

sensor implemented in the microfluidic device. This relatively new approach relies on the determination of the analyte concentration based on the produced heat from the enzymatic reaction between the substrate and the enzyme-linked reporter. Although successful, this approach hides the down point of heat loss, thus decreasing the sensitivity and the magnitude of the signal received from the OOC [31]. Generally, one of the main concerns regarding biosensors is related to the risk of detecting non-specific proteins due to their overabundance compared to the analytes of interest.

Transepithelial electrical resistance (TEER)

TEER is an electrochemical sensing technique, which measures the barrier integrity of epithelial and endothelial layers [33]. This approach is usually used as an analytical technique for disease models, or as a toxicology marker. The TEER measurements are non-invasive and real-time. TEER design consists of submerged electrodes in both the top and bottom compartments of the *in vitro* transwell system [33]. Odijk *et al*. tried to implement TEER in OOC analysis, which revealed that the obtained results from OOC are comparable to transwell systems (Figure 1c) [34]. Henry *et al*. also implemented TEER electrodes on an OOC by patterning them on a polycarbonate substrate [35]. The research group explained that their system provided sufficient sensitivity and enabled real-time measurements. However, the location, dimensions, and design of the electrodes could be improved. The slightest displacement of the electrode can significantly impact the TEER results, causing variation in measurements. Generally, the integration of these electrodes in the closed areas of an OOC device is risky due to the smaller cell culture area of OOC compared to transwell systems. Therefore, this complexity makes the fabrication and reliability of TEER on OOCs more challenging. Taking to account the shortcomings of the mentioned analytical techniques, to increase the translational relevance of OOC in a research setting, quantitative analytical techniques offering online and real-time analysis are still missing. Mass spectrometry offers multiple advantages in this regard.

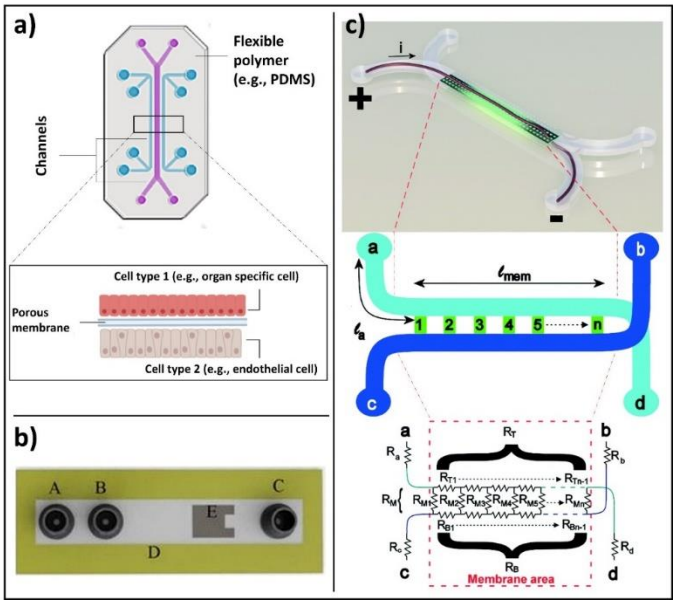

Figure 1. ***(a)*** *Organ-on-a-chip with two parallel channels separated by a porous membrane (Adapted from Zhang et al,.[4]).* ***(b)*** *Schematic of a microfluidic device with integrated thin-film thermopile. A is the first inlet to the supply buffer solution, B is the second inlet to supply the analyte, C is outlet/waste, D is the channel wall, and E is the thermopile to measure the heat of the enzymatic reaction (Adapted from Nestorova et al,.[31]).* ***(c)*** *Artist impression of the organ-on-a-chip with integrated TEER with simplified geometry of the chip. The circuit model presents the working principle of the chip. The inlet and outlet channels la to ld are shown by resistors Ra to Rd. Channels a–d and b–c are connected by the membrane and indicated by lmem (the length of the membrane) and the red dashed square (Adapted from Odijk et al,.[34]).*

Mass spectrometry (MS)

Mass spectrometry is one of the most used analytical tools that offer multiple advantages for OOC analysis [36]. When analyzing the cellular excretes from the 3D cellular environment of an OOC, a diverse range of molecules are encountered. Some of these molecules are already known material through decades of research on cellular mechanisms. However, the quantity of these materials might change to different pathological conditions. Analyzing OOC content by MS enables quantifying these known compounds and comparing healthy versus disease models. On the other hand, not all cellular mechanisms are elucidated yet. One step to unraveling cellular behaviors is to identify the involved unknown compounds. Here again, MS offers the capacity to identify unknown molecules with high sensitivity and confidence. In addition, rapid detection of molecules by MS facilitates online, real-time, and high throughput screenings. Hence, the hyphenation of OOC with MS can assist in understanding the cellular behavior and reaction pathways as well as optimizing an OOC device to be a better representative of natural human physiology. One main concern in connecting

OOC with MS is related to matrix effect that can influence sensitivity and selectivity, subsequently the precision, accuracy, and robustness of results. The matrix effect mainly happens when analysing biological matrices. This effect is caused by either suppression or enhancement of ionization efficiency of target analytes due to the presence of matrix compounds. In the case of analysing OOC content, usually the used cell media include non-volatile compounds, causing matrix effect. Hence, direct connection of OOC to MS requires an interface to reduce this effect before MS analysis.

Table 1. Organ-on-a-chip analytical techniques and their shortcomings.

Organ-on-a-chip analytical techniques	**Shortcomings**
Optical imaging	Low field of view at high magnifications
	Low working distance and fabrication challenges
	Suitable for static analysis
Fluorescent microscopy	Fluorescent labelling is required
Confocal microscopy	Phototoxicity due to laser intensity
Thermoelectrical ELISA	Heat loss
	Decreased sensitivity and received signal magnitude
TEER	Difficulties in integrating electrodes on the OOC
	Electrode displacement influences results
MS	Sample pre-treatment is required

Introduction to mass spectrometry

Every MS instrument is composed of three main components including – an ion source for the ionization of samples, a mass analyzer for the separation of ions (i.e. based on mass-to-charge (*m/z*)), and a detector [37]. The MS devices measure primarily the mass-to-charge ratio of electrically charged ions providing information about the elemental composition of compounds [38, 39]. Thus, the more accurate the *m/z* is, the more confidence there is about the elemental composition of the tested composite. In addition, MS instruments can be used to fragment the precursor ions to generate products or fragment ions. The so-called tandem mass spectrometry (MS/MS), provides structural information on the compound and enables identification [40].

MS has been coupled with various interfaces such as liquid chromatography (LC-MS), and ion mobility spectrometry (IMS-MS) [41-43], expanding the applicability of this analytical tool. Currently, the LC-MS(/MS) is a widely used technology as it enables the separation and sensitive detection of a wide range of molecules, including potential isomers [44, 45]. LC allows for online clean-up of the sample, often a complex biological matrix, and thus opens possibilities to clean up salts and reduce chemical background. Ion mobility MS is a gas-phase separation technique that allows to differentiation of ions with the same *m/z* values but different molecular structures (isomers). Isomeric separation of ions by ion mobility is performed based on their size, shape, and charge state differences.

Several ion sources used for the ionization of the molecules can be interfaced with MS. Amongst these sources one can find electrospray ionization (ESI), atmospheric pressure chemical ionization (APCI), atmospheric pressure photoionization (APPI) and matrix-assisted laser desorption/ionization (MALDI). The ionization sources that are widely used for biological samples include ESI and MALDI. ESI is the commonly used ionization method in MS when studying the excretes of cells from OOC, in either the off – or on-line mode. Therefore, taking the sensitivity, specificity, and structural identification potential of MS into account, its hyphenation to OOC devices is potentially offering online and real-time observation of cell behavior.

Hyphenation of Organ-on-a-chip and mass spectrometry

MS as a sensitive and high-throughput technique can provide molecularly specific information. This analytical tool also can detect short-lived reaction intermediates or labile metabolites [46]. Various research groups have tried to couple OOC and MS, however, there is no established methodology yet. The failures so far are mainly due to the decreased flexibility, clogging, and incompatibility of the solvents when the two systems are connected. This results from the oxygenated medium, consisting of salts and serum that can cause interferences in the MS [47, 48]. Hence, to analyze the biological content of OOC, which contains a complex mixture of components, sample pre-treatment (e.g. purification, extraction, preconcentration) before ionization for MS analysis is essential [49]. To this end, various pre-treatment techniques and chip designs naming electrophoresis, solid-phase extraction, liquid chromatography, and droplet-based chips have been developed to bridge OOC with MS.

Electrophoresis – mass spectrometry for organ-on-a-chip analysis

Electrophoresis is a separation technique, in which an electric field is applied in a running buffer that enables the separation of analytes based on their size and charge. Electrophoresis has been widely used as a separation method in microfluidic chips as it offers high efficiency and requires no stationary phase or high pressure [50, 51]. The high efficiency is due to the separation of molecules through shorter separation channels in a short time. These features enable fast detection of analytes, particularly short-lived molecules, reduce fabrication costs, and aid in miniaturization. Capillary electrophoresis (CE) is an electrophoresis-based separation method, which is performed in micro or nano fluidic channels through submillimetre sized capillaries. Integrated CE within the microfluidic chips contributes to super high-speed performance and high separation efficiency using very low sample volume [52]. CE has been used for the separation of small molecules [53, 54] and large molecules like proteins [55, 56]. Under the high electric field of microchip CE, the separation mechanism and behavior of small molecules will not be harmed. In addition, protein separation by CE occurs in a running buffer, which is similar to physiological conditions without requiring complex additives. As a result, protein structure and functions are preserved through the separation process. The chip-based CE interfaced with MS has been reported by the Karger team and Ramsey group [57-59]. The Karger team introduced glass-based microdevices with an external transfer capillary to connect to the electrospray interface of a MS instrument (Figure 2a). In another design, they also introduced an integrated pneumatic nebulizer

(Figure 2b), which omitted the need for an external electrospray port [57, 58]. The latter design reduced the dead volume and enabled on-chip separation and electrospray of peptides and protein digests to MS. For analysis of proteins, Ramsey and co-workers also reported microchip-based electrophoresis-ESI device to interface with MS [59]. However, their designs were only suitable for analyzing small volumes of samples and were not suitable for multiple uses. Having limited loading capacity raise a concern regarding the detection limit, especially for biological samples that include a scarce amount of analyte per volume. To address this concern, a pre-concentration step has been employed along with CE separation. A concentrator-CE was introduced by Lin and his team, in which a nano-porous membrane was placed between two layers of polydimethylsiloxane (PDMS) microchannels (Figure 2c) [60]. Even though this device contributed to desalting and concentrating analytes from human plasma, the small size of pores filters out proteins. An alternative approach is to integrate the dynamic pH junction preconcentration method with CE-ESI-MS (Figure 2d)[61]. In this method, analytes are prepared in a basic buffer and introduced into a capillary with an acidic buffer. Upon application of an electric field, charged analytes migrated through different zones of the capillary to concentrate and separate. This method has been used by multiple groups [62-64] and proved to be useful for the injection of large volumes and the detection of a large number of proteins and peptides. Nevertheless, this technique requires pre-treatment of samples before injecting them into the capillary, which limits its application for the online analysis required for OOC platforms. Considering the benefits of electrophoresis, new designs based on the same working principle of this technique were developed to address the online analysis shortcoming.

Electromembrane extraction (EME) is another electrokinetic-based miniaturized sample preparation technique for the extraction of molecules in their ionized form from aqueous media [65]. EME system is composed of a donor phase (metabolic reaction mixture) and an acceptor phase, making it compatible with MS detection. The two phases are separated by a supported liquid membrane (SLM), filled with organic solvent (usually polypropylene with immobilized 2-nitrophenyl octyl ether). To drive ionized analytes from one phase to the other, an electric field is applied across the membrane [66, 67]. Petersen *et al*., [68] experimented with an EME-chip made of polymethyl methacrylate (PMMA) for real-time drug monitoring by ESI-MS (Figure 2e). During their experiment a reaction mixture was continuously perfused by a syringe pump, making contact with the SLM inside the EME-chip. On the other side, the acceptor phase with an organic solvent was also pumped continuously. The electric potential was applied across the SLM by a direct current power supply through small platinum wires, located in both the donor and acceptor phases [68]. Once the analytes reach the acceptor phase, they are transferred to MS for detection. The main advantages of EME are the online sample pre-treatment that can remove salts, buffers, and large molecules of the biological samples. In addition, this method enables studying fast reaction kinetics. Nevertheless, one major disadvantage of this design is that before each metabolic experiment, the EME-chip needs to be re-connected with tubing on the acceptor side. Abdossalami *et al*., [69] and Baharfar *et al*., [70] used on-chip EME coupled with high-performance liquid chromatography (HPLC) for the enhancement of extraction efficiency. Similar to Petersen *et al*., these two research groups used PMMA chips, with

a SLM made out of a polypropylene sheet, and two platinum electrodes integrated with the donor and acceptor phases [69, 70]. The experiments conducted by Petersen *et al*., Abdossalami *et al.,* and Baharfar *et al*., demonstrated it was possible to concentrate analytes and analyze them with MS. Nevertheless, a persisting drawback of this method is the discrimination of large biomolecules, which could be resolved by implementing specialized SLMs. The electrophoretic separation method directly connected to MS has also been extensively used for cell analysis as reviewed before [71]. However, these studies require pre-treatment of samples before performing CE-MS analysis. While online analysis of OOC content requires a direct connection of OOC to MS without stalling the process. This can be a possible future direction for scientists to develop an OOC-EME/CE-MS system for online analysis of OOC, a possibility combined with other online pre-treatment methods such as solid phase extraction.

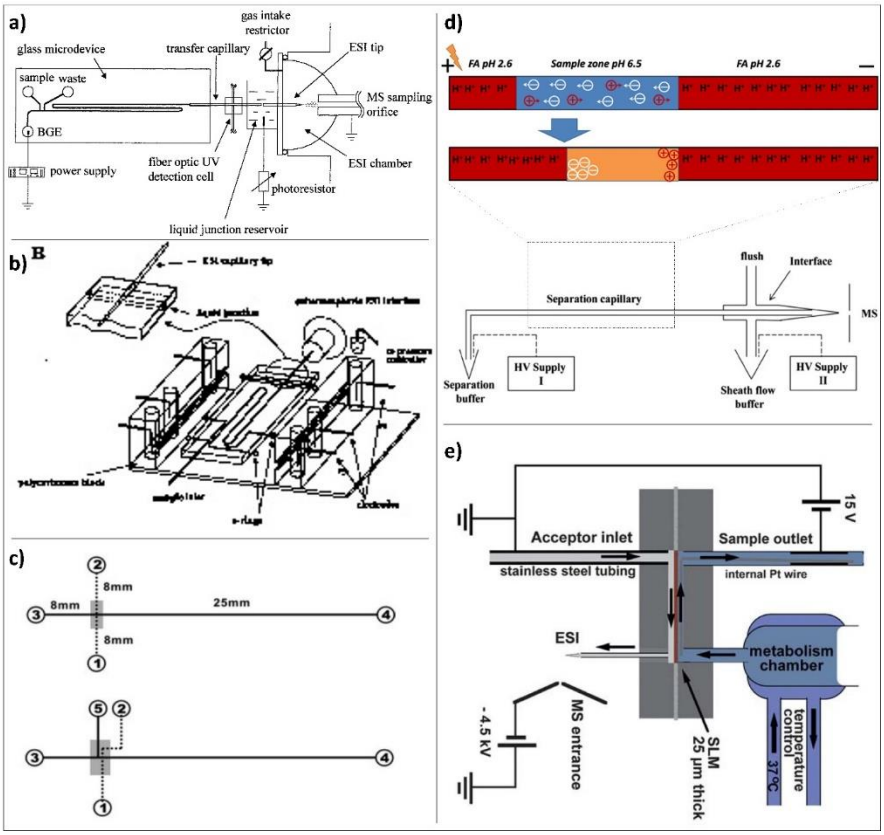

Figure 2. ***(a)*** *Diagram of the chip-based capillary electrophoresis with the capillary transfer line interfaced with the subatmospheric electrospray (Adapted from Zhang et al,.[57]).* ***(b)*** *Diagram of the chip-based capillary electrophoresis with an integrated pneumatic nebulizer (Adapted from Zhang et al.,[58]).* ***(c)*** *Diagram of multilayer microfluidic device (top) the filter-capillary electrophoresis (bottom) the concentrator-*

capillary electrophoresis with a nanoporous membrane (gray area) (Adapted from Long et al,.[60]). ***(d)*** *Diagram of the integrate dynamic pH junction preconcentration method with capillary electrophoresis. The HV supply II drives the electrokinetic flow to pump the sheath liquid. The potential difference between the inlet (HV supply I) and outlet (HV supply II) drives the capillary separation (Adapted from Sun et al., and Zhu et al.,[61, 62]).* ***(e)*** *Schematic illustration of the electro membrane extraction (Adapted from Petersen et al.,[68]).*

Solid-phase extraction – mass spectrometry for organ-on-a-chip analysis

SPE is another method used by various research groups for the sample pre-treatment before MS analysis. Generally, SPE is used for the extraction and concentration of analytes and purification of interfaces from analytical samples from complex matrices such as urine, blood, animal tissue homogenate extracts, and soil [72, 73]. It is a solid-liquid separation method, which relies on affinity differences among compounds present in a liquid mixture to a solid phase in order to separate and extract. The widely used high throughput SPE systems coupled with MS is mainly relying on an integrated autosampler for the injection of samples from multiwell plates as reviewed before [74]. However, such a system does not enable an online analysis of OOC complex content. Jin-Ming Lin and his team introduced a novel method to integrate chip-based SPE between OOC and MS junction for online analysis of cultured cells [73]. In their first design, they fabricated a microfluidic chip made from PDMS with two separate parts, which were connected via polyethylene tubes. The first part of the chip is used for the cultivation of cells and the second part is packed with polymeric SPE beads of 45 µm size (Figure 3a). The outlet of the second part is directly connected to ESI-MS. Before MS analysis, the wash solution of 5% ethanol water was injected into the beads for the removal of unbound materials, proteins, and salts. Subsequently, the purified sample could migrate to the ESI source via fused silica capillary. Using this platform, they could desalt and concentrate the metabolites of interest to study vitamin E metabolism by human lung epithelial cells. The highlight of their design was packing SPE beads in straight microchannels with narrow ends to trap the beads. In addition, this device offers a simplified sample pre-treatment method with high efficiency and potential for high throughput screening of cellular drug metabolism. This group used the same pre-treatment approach for online monitoring of more complex cellular assays by changing the design of the first part of their chip. As such that they could study drug permeability by fabricating two channeled chips separated by a semipermeable membrane to culture cells [75]. In another study, they performed high throughput drug screening by designing a micro-scale gradient generator connected to a micro-sized cell culture chamber followed by an online SPE chip and MS analysis [76]. Lin and his team also reported three section chips for cytotoxicity study. The first section of their chip encapsulated human liver microsomes that metabolized acetaminophen. The following section included a cell culture chamber that was directly exposed to the products of acetaminophen. The third section of their chip consisted of a micro SPE column for desalting and concentrating analytes just before direct injection and online monitoring by MS [77]. Further work has been performed by this work with the same pre-treatment strategy to study cell-cell communications [78]. Even though this design has proven to be applicable for multiple

types of cellular assays, it bears a few drawbacks. This pre-treatment method has a relatively long analysis time, which might not be ideal for real-time analysis of fast reactions and cell responses. In addition, this system consumes high volumes of solvents and reagents. On top of all, it requires an offline washing step, which raises concerns regarding the complexity of experiments and the online nature of the system. Dugan *et al*. designed a chip with the feasibility of performing an online washing step. They fabricated a multilayer PDMS chip, which consisted of a cell cultivation chamber and a series of valves (Figure 3b) [79]. The operation of valves was similar to a six-port valve and enabled the controlling of an on-chip injection loop, placed right after the cell chamber. The injection loop was connected to a PicoClear union, which was packed with 20 µm sized beads to form a ∼1-mm long SPE column. The other end of the column was directly connected to a spray tip to electrospray the analytes into MS. The designed valve system enabled the on-chip washing step without disconnecting the tubing for offline injections. Even though this design enabled online desalting and concentrating to analyze cell secretion by MS, it still bears the similar drawback of long analysis time (30 min). This concern was addressed by Marasco *et al*., by constructing a microfluidic bioreactor coupled online to a SPE desalter and MS detector for near real-time analysis of cocaine metabolism by T-cells (Figure 3c) [80]. In this design, a low temporal resolution of 9 min was achieved by using an online desalter comprised of two C18 columns, three valves, and two sample loops. One main concern about this platform was about clogging of used filters by cells. This is because their microfluidic bioreactor (multi-trap nanophysiometer) was made from U-shaped traps to study unattached cells. Regardless of multiple advances in the application of online SPE for sample pre-treatment of OOC content before MS analysis, this system still suffers from sufficient temporal resolution, the possibility of clogging by large molecules, and the inability to analyze a wide range of analytes (e.g., proteins).

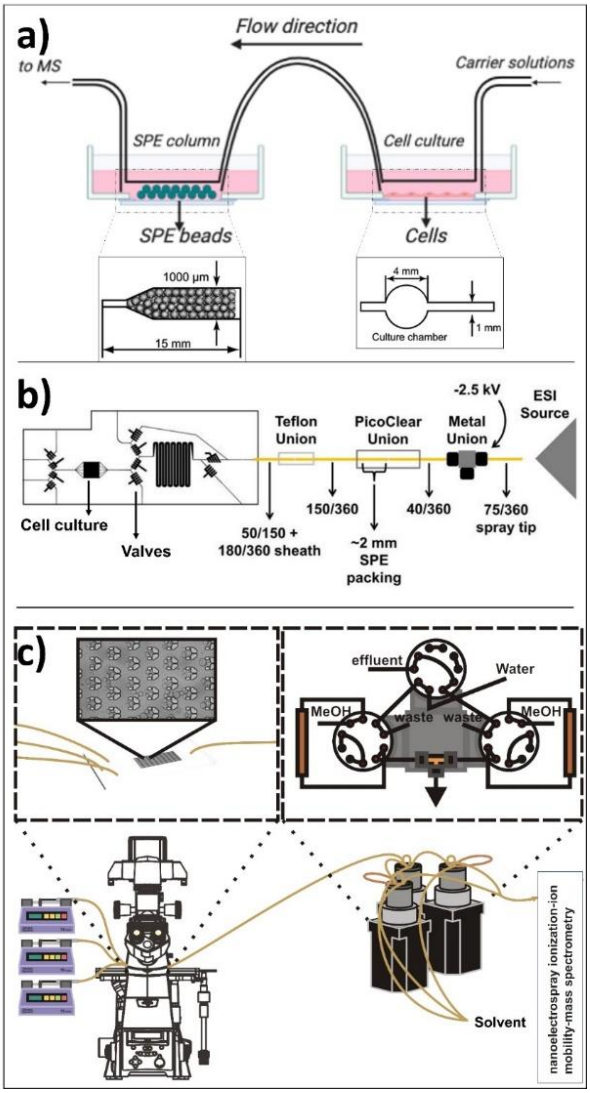

Figure 3. ***(a)*** *Schematic of integrated chip-based solid phase extraction placed between organ-on-a-chip and mass spectrometry with the diagram of the cell culture channel and the narrow-ended microchannel of micro-SPE column (Adapted from Gao et al.,[73]).* ***(b)*** *Schematic of the PDMS-based chip consisted of a cell cultivation chamber and series of the valve to control the on-chip injection loop, which is connected to the SPE column and followed by a spray tip to interface with electrospray ionization source (Adapted from Dugan et al.,[79]).* ***(c)*** *Schematic of the multi-trap nanophysiometer placed on an inverted fluorescence microscope and connected to solid phase extraction using pumps to control the flow. The setup is continuously analyzed by interfacing with the nanoelectrospray ionization source (Adapted from Marasco et al.,[80]).*

Liquid chromatography is the commonly used approach for sample separation before MS. The conventional LC systems with a large internal diameter of 1-2.1 mm are not the ideal approach for bridging OOC with MS. This is due to the large internal diameter of such columns that requires a large sample volume. This condition does not match the working criteria of microfluidic OOC with a small sample size and low flow rates. The development of narrow-sized LC columns, nano-LC, addresses this issue. Nano-LC-MS, with an inner diameter as low as 75 µm, has been widely used for proteomic and metabolomic studies as reviewed before [81]. This technique offers improved sensitivity, lower flow rate, and lesser injection volume compared to conventional LC systems. However, the relatively low flow rate applied in OOC systems requires implementing concentrators in conjunction with multi-port valves of nano-LC systems. Multi-valve connections increase the possibility of flow leakage and blockage at different sites of connections. This is especially true for packed nano-LC columns. The size of packed particles in nano-LC can go down to 2 µm, which results in improved chromatography. However, lowering particle size comes with the cost of high back pressure and frictional heating effects. This is not an ideal approach for online analysis of OOC content. An alternative to packed nano-LC columns is open tubular LC columns with a much smaller inner diameter of 5-10 µm [82]. Open tubular LC columns have proven to improve sensitivity, chromatography results, and back pressure concerns [83], however, they have not been widely used for omics studies and not at all used as the interface of OOC and MS. This might be due to columns poor robustness and reproducibility [84]. As a result of technological development, chip-based LC platforms appear to address the aforementioned shortcomings. Chip-based LC (Chip-LC) is a miniaturized LC system with its components integrated into a micro-sized chip. This design enables hyphenation with a micro-sized OOC from one side and a MS detector from the other end. Interfacing chip-LC to MS could be done either by integrating an electrospray emitter on the same chip or by tubing connection to the ESI source of a MS instrument [85]. As reviewed before [86], chip-LC technology requires low sample volume, reduces reagent consumption and total cycle time (due to its miniaturized nature), and enables high throughput as well as fast analysis. Yin *et al*., [87] used Chip-LC-ESI-MS and developed a microchip integration system on a single-chip device. They established the connection between the two components by laminating the polyimide field with laser-ablated channels, ports, and frit structures. The design contained both enrichment and separation columns, which were packed by the use of conventional reversed-phase chromatography particles. A special face-seal rotary valve was used to switch between sample loading and separation [87]. Overall, such systems performed well on stability, reproducibility, and sensitivity to identify peptides at low abundance. However, as already known, LC-MS analytical tools are not suitable for biological samples, due to their complexity and the thousands of different compounds within a biological specimen, as well as the high abundance of matrix components that can interfere with the LC-MS analysis. The reason behind this is that complete separation is not possible for complex samples, but rather separation by the grouping of compounds would be made. Hence, one should always keep in mind that purification of the sample is needed before LC-MS analysis by for instance SPE integration. In addition, high back pressure is an inevitable concern when working with micro-scaled fluidic systems.

Droplet-based chips – mass spectrometry

Droplet-based microfluidics has been widely used for various biomedical applications. This system enables the performance of cellular assays and chemical reactions in micro- to femtoliters of volumes [88, 89]. Droplet-based microfluidics has been interfaced with ESI-MS for fast, sensitive, and selective analysis of single-cell studies [90] proteomics [91] and peptide tracing [92-94]. Zhu *et al*., [92] presented an integrated droplet system for ESI-MS sampling. The system aimed the minimalization the interferences of the matrix, by separating the water and oil base droplets containing solute analytes by two-phase flow methods. Thus, after the separation, the droplets are brought to the aqueous phase of the ESI and then further detected by ESI-MS (Figure 4a). The separation of droplets is an example of the enrichment of samples, improving the selectivity and sensitivity analysis. The research group of Zhang *et al*., also used a droplet-based method, however, they used it to extract the cellular compounds of a single cell for ESI-MS analysis [90]. The mechanism is similar to the one used by Zhu *et al*. The target cell was wrapped around by a droplet, containing extraction solvent. After an incubation time, the cell content was extracted to the droplet, which was sucked and dried in the ESI emitter. The dried molecules re-dissolved in an organic solvent, which was then electro-sprayed and detected by MS. Their approach showed that it could selectively acquire and detect the cellular components of a single cell without the interference of other components of the matrix. Nevertheless, the method of Zhang *et al*., could not detect and extract ATP, ADP, and AMP, due to the high possibility of contaminating the MS instrument with the cytoplasm. The use of droplet-based sample preparation for OOC platforms can be beneficial for the selective analysis of analytes by MS. However, this method does not provide a full range of molecules and requires multi-step sample handling. To improve this method a sample pre-treatment operation must be integrated, such as SPE, for desalting and chemical derivation for it to be used for direct analysis of real biological samples. Another droplet-based manipulation system used for proteomic sample preparation is digital microfluidics [95]. Using this technique, microdroplets are moved, mixed, reacted, and analyzed on a surface with insulated electrodes (Figure 4b). Leipert *et al*., [47] addressed the mentioned limitations by developing a cell lysing protocol using a digital microfluidic platform for proteome study. On this platform, multiple steps of cell lysis, protein extraction, and protein digestion are performed on a single digital chip. The chip included magnetic beads used as solid phase enhanced sample preparation and clean up. Upon detergent removal, the supernatant was aspirated and pipetted to a LC glass micro insert for LC-MS analysis. This technology enabled the identification of the Jurkat T cells protein profile. However, the complicated fabrication and sample preparation process hinders its application for OOC-MS studies, and it still requires further optimizations for real-time analysis of cellular mechanisms.

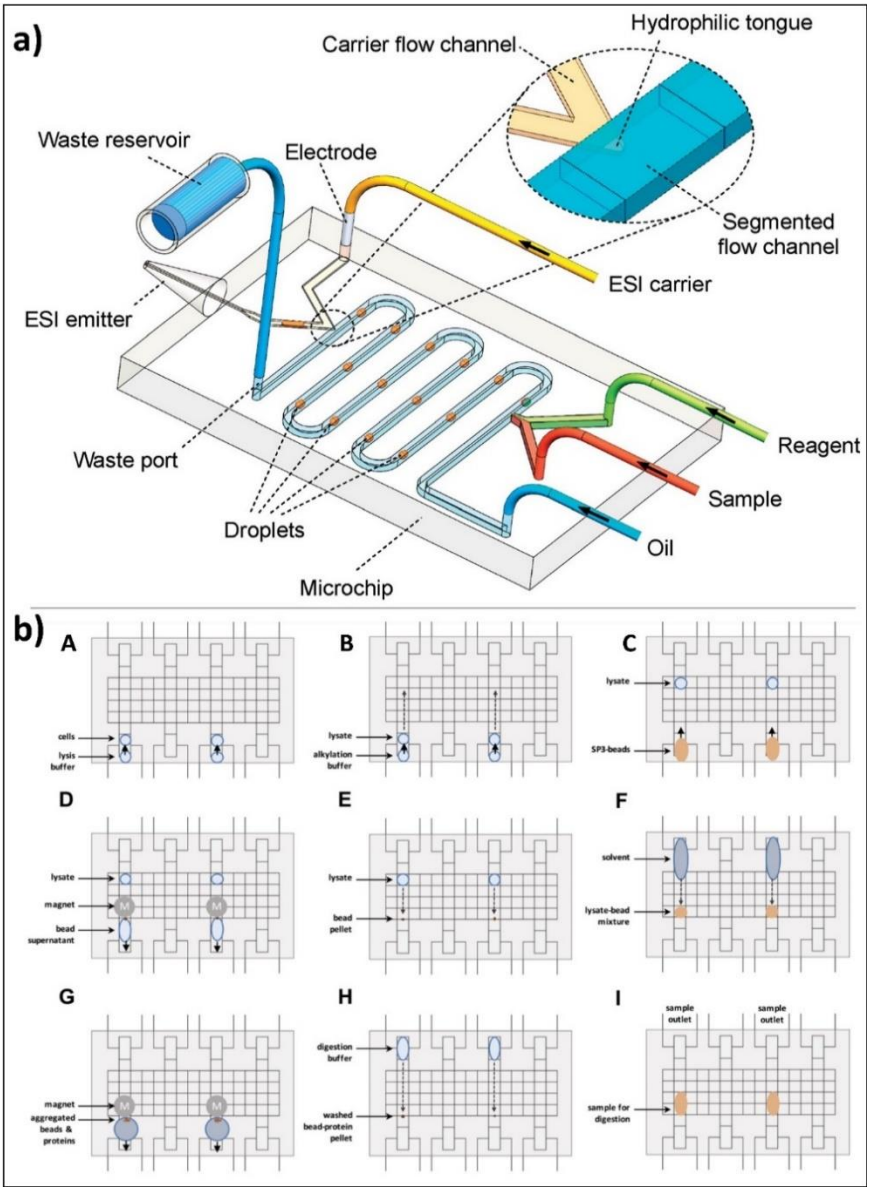

Figure 4. ***(a)*** *Schematic diagram of water and oil droplet-based analysis system interfaced with ESI-MS detection (not to scale) (Adapted from Zhu et at.,[92]).* ***(b)*** *Schematic of the digital microfluidic system for droplet-based sample preparation. (A) The reservoir and transfer electrodes are actuated to directly load cell suspension. In the middle of the reservoir, the sample is loaded towards the transfer electrode. To move the droplet into the transfer electrode, the reservoir electrode is deactivated. (B) The same principle is used to add a buffer. (C) Following buffer loading, the solid-phase-enhanced sample preparation bead mixture is loaded. (E) After moving the lysate into the bead pellet, the solution is mixed. (F) The solvent is added to induce protein bead aggregation.*

(G) The supernatant is removed upon extracting the beads. (H) The bead pellet is mixed with the digestion buffer. (I) For 8 hours the samples were incubated. Aspirated samples were analyzed by LC-MS (Adapted from Leipert et al.,[47]).

Conclusion

This review looked into connecting OOC to different analytical techniques either on- or off-chip to evaluate and analyse biological content of mimetic tissue model of the OOC, focusing on the coupling of OOC to MS. With the ability of OOCs to mimic human physiology *in vivo*, they open another door to a new generation of research. More particularly, the invention of OOCs brings pharmacological research to a level at which "patient-based" studies within the context of personalized medicine and drug tolerance testing can be performed. Nonetheless, the OOCs approach suffers from the absence of well-validated, fast, and universal analytical detection technologies. Mass spectrometry on the bases of its nature is expected to be a suitable detection and monitoring technology. Yet, its hyphenation of OOC is highly hampered by the lack of fast, accurate, and universal sample pre-treatment technologies. Over the years, several attempts have been made to hyphenate OOC with MS for online and real-time analysis of 3D microcellular cultures. The aim of these approaches has been rapid, precise, and sensitive analysis of cellular mechanisms with minimal chance of outside contamination. Solid phase extraction, electrophoresis-based separations, and liquid chromatography have proven to offer multiple advantages for sample handling in the interface of OOC and MS. Albeit substantial progresses to bridge OOC and MS, there is no concrete solution for online analysis of complex OOC content with MS.

Further research focusing on combinatorial approaches that relies on multiple level of extraction and purification could address optimum sample treatment criteria for low flow rate OOC platforms. In addition, particle separation approaches such as acoustic separation could be down sized to molecular level to enable direct connection of OOC with MS.

References

1. Zheng, F., et al., *Organ-on-a-Chip Systems: microengineering to biomimic living systems.* Small, 2016. **12**(17): p. 2253-2282.
2. Mittal, R., et al., *Organ-on-chip models: implications in drug discovery and clinical applications.* Journal of cellular physiology, 2019. **234**(6): p. 8352-8380.
3. Lee, S.H. and J.H. Sung, *Organ-on-a-chip technology for reproducing multiorgan physiology.* Advanced healthcare materials, 2018. **7**(2): p. 1700419.
4. Zhang, B., et al., *Advances in organ-on-a-chip engineering.* Nature Reviews Materials, 2018. **3**(8): p. 257-278.
5. Zhang, B. and M. Radisic, *Organ-on-a-chip devices advance to market.* Lab on a Chip, 2017. **17**(14): p. 2395-2420.
6. Sosa-Hernández, J.E., et al., *Organs-on-a-chip module: A review from the development and applications perspective.* Micromachines, 2018. **9**(10): p. 536.
7. Wu, Q., et al., *Organ-on-a-chip: Recent breakthroughs and future prospects.* Biomedical engineering online, 2020. **19**(1): p. 1-19.
8. Caplin, J.D., et al., *Microfluidic organ-on-a-chip technology for advancement of drug development and toxicology.* Advanced healthcare materials, 2015. **4**(10): p. 1426-1450.

9. Franzen, N., et al., *Impact of organ-on-a-chip technology on pharmaceutical R&D costs.* Drug discovery today, 2019. **24**(9): p. 1720-1724.
10. Probst, C., S. Schneider, and P. Loskill, *High-throughput organ-on-a-chip systems: Current status and remaining challenges.* Current Opinion in Biomedical Engineering, 2018. **6**: p. 33-41.
11. An, F., et al., *Organ-on-a-chip: new platform for biological analysis.* AnAlyticAl chemistry insights, 2015. **10**: p. ACI. S28905.
12. Morales, A.W., et al. *Label-free detection of protein molecules secreted from an organ-on-a-chip model for drug toxicity assays*. in *Frontiers in Biological Detection: From Nanosensors to Systems VIII*. 2016. SPIE.
13. Wikswo, J.P., et al., *Engineering challenges for instrumenting and controlling integrated organ-on-chip systems.* IEEE Transactions on Biomedical Engineering, 2013. **60**(3): p. 682-690.
14. Caballero, B., L.C. Trugo, and P.M. Finglas, *Encyclopedia of food sciences and nutrition*. 2003: Academic.
15. Zhou, M. and T.D. Veenstra, *Mass spectrometry: m/z 1983–2008.* Biotechniques, 2008. **44**(5): p. 667-670.
16. Glish, G.L. and R.W. Vachet, *The basics of mass spectrometry in the twenty-first century.* Nature reviews drug discovery, 2003. **2**(2): p. 140-150.
17. Ahadian, S., et al., *Organ-on-a-chip platforms: a convergence of advanced materials, cells, and microscale technologies.* Advanced healthcare materials, 2018. **7**(2): p. 1700506.
18. Rothbauer, M., et al., *Tomorrow today: organ-on-a-chip advances towards clinically relevant pharmaceutical and medical in vitro models.* Current opinion in biotechnology, 2019. **55**: p. 81-86.
19. Junaid, A., et al., *An end-user perspective on Organ-on-a-Chip: Assays and usability aspects.* Current Opinion in Biomedical Engineering, 2017. **1**: p. 15-22.
20. Lee, J.B. and J.H. Sung, *Organ-on-a-chip technology and microfluidic whole-body models for pharmacokinetic drug toxicity screening.* Biotechnology journal, 2013. **8**(11): p. 1258-1266.
21. Skardal, A., et al., *Multi-tissue interactions in an integrated three-tissue organ-on-a-chip platform.* Scientific reports, 2017. **7**(1): p. 1-16.
22. Huh, D., et al., *Reconstituting organ-level lung functions on a chip.* Science, 2010. **328**(5986): p. 1662-1668.
23. Peel, S., et al., *Introducing an automated high content confocal imaging approach for Organs-on-Chips.* Lab on a Chip, 2019. **19**(3): p. 410-421.
24. Bhise, N.S., et al., *Organ-on-a-chip platforms for studying drug delivery systems.* Journal of Controlled Release, 2014. **190**: p. 82-93.
25. Caballero, D., et al., *Organ-on-chip models of cancer metastasis for future personalized medicine: From chip to the patient.* Biomaterials, 2017. **149**: p. 98-115.
26. Haring, A.P., H. Sontheimer, and B.N. Johnson, *Microphysiological human brain and neural systems-on-a-chip: potential alternatives to small animal models and emerging platforms for drug discovery and personalized medicine.* Stem cell reviews and reports, 2017. **13**(3): p. 381-406.
27. Herland, A., et al., *Quantitative prediction of human pharmacokinetic responses to drugs via fluidically coupled vascularized organ chips.* Nature biomedical engineering, 2020. **4**(4): p. 421-436.
28. Van Der Meer, A.D. and A. Van Den Berg, *Organs-on-chips: breaking the in vitro impasse.* Integrative Biology, 2012. **4**(5): p. 461-470.
29. Arandian, A., et al., *Optical Imaging Approaches to Monitor Static and Dynamic Cell-on-Chip Platforms: A Tutorial Review.* Small, 2019. **15**(28): p. 1900737.

30. Paiè, P., et al., *Microfluidic based optical microscopes on chip.* Cytometry Part A, 2018. **93**(10): p. 987-996.
31. Nestorova, G.G., N.D. Crews, and E.J. Guilbeau, *Theoretical and experimental analysis of thermoelectric lab-on-a-chip ELISA.* Microfluidics and Nanofluidics, 2015. **19**(4): p. 963-972.
32. Premjeet, S., et al., *Enzyme-Linked Immuno-Sorbent Assay (ELISA), basics and it's application: A comprehensive review.* Journal of Pharmacy Research, 2011. **4**(12): p. 4581-4583.
33. Santbergen, M.J., et al., *Online and in situ analysis of organs-on-a-chip.* TrAC Trends in Analytical Chemistry, 2019. **115**: p. 138-146.
34. Odijk, M., et al., *Measuring direct current trans-epithelial electrical resistance in organ-on-a-chip microsystems.* Lab on a Chip, 2015. **15**(3): p. 745-752.
35. Henry, O.Y., et al., *Organs-on-chips with integrated electrodes for trans-epithelial electrical resistance (TEER) measurements of human epithelial barrier function.* Lab on a Chip, 2017. **17**(13): p. 2264-2271.
36. Chen, J., M. Tang, and D. Xu, *Integrated microfluidic chip coupled to mass spectrometry: A minireview of chip pretreatment methods and applications.* Journal of Chromatography Open, 2021. **1**: p. 100021.
37. Awad, H., M.M. Khamis, and A. El-Aneed, *Mass spectrometry, review of the basics: ionization.* Applied Spectroscopy Reviews, 2015. **50**(2): p. 158-175.
38. Choo, K.W. and W.M. Tham, *Tandem mass spectrometry data quality assessment by self-convolution.* BMC bioinformatics, 2007. **8**(1): p. 1-12.
39. El-Aneed, A., A. Cohen, and J. Banoub, *Mass spectrometry, review of the basics: electrospray, MALDI, and commonly used mass analyzers.* Applied Spectroscopy Reviews, 2009. **44**(3): p. 210-230.
40. SUSlick, K.S., *Kirk-Othmer encyclopedia of chemical technology.* J. Wiley & Sons: New York, 1998. **26**: p. 517-541.
41. Hadavi, D., et al., *Adduct ion formation as a tool for the molecular structure assessment of ten isomers in traveling wave and trapped ion mobility spectrometry.* Rapid Communications in Mass Spectrometry, 2019. **33**: p. 49-59.
42. Hadavi, D., et al., *Uncovering the behaviour of ions in the gas-phase to predict the ion mobility separation of isomeric steroid compounds.* Analytica Chimica Acta, 2022. **1200**: p. 339617.
43. Hadavi, D., P. Han, and M. Honing, *Ion mobility spectrometry-tandem mass spectrometry strategies for the on-line monitoring of a continuous microflow reaction.* Journal of Flow Chemistry, 2022. **12**(2): p. 175-184.
44. Theodoridis, G.A., et al., *Liquid chromatography–mass spectrometry based global metabolite profiling: a review.* Analytica chimica acta, 2012. **711**: p. 7-16.
45. Holčapek, M., R. Jirásko, and M. Lísa, *Recent developments in liquid chromatography–mass spectrometry and related techniques.* Journal of Chromatography A, 2012. **1259**: p. 3-15.
46. Wu, J., et al., *Multi-channel cell co-culture for drug development based on glass microfluidic chip-mass spectrometry coupled platform.* Rapid Communications in Mass Spectrometry, 2016. **30**: p. 80-86.
47. Leipert, J. and A. Tholey, *Miniaturized sample preparation on a digital microfluidics device for sensitive bottom-up microproteomics of mammalian cells using magnetic beads and mass spectrometry-compatible surfactants.* Lab on a Chip, 2019. **19**(20): p. 3490-3498.
48. Wink, K., et al., *An integrated chip-mass spectrometry and epifluorescence approach for online monitoring of bioactive metabolites from incubated Actinobacteria in picoliter droplets.* Analytical and bioanalytical chemistry, 2018. **410**(29): p. 7679-7687.

49. Mao, S., et al., *Cell analysis on chip-mass spectrometry.* TrAC Trends in Analytical Chemistry, 2018. **107**: p. 43-59.
50. Chen, D., et al., *Recent advances (2019–2021) of capillary electrophoresis-mass spectrometry for multilevel proteomics.* Mass Spectrometry Reviews. **n/a**(n/a).
51. Wu, D., J. Qin, and B. Lin, *Electrophoretic separations on microfluidic chips.* J Chromatogr A, 2008. **1184**(1-2): p. 542-59.
52. Hamdan, M. and P.G. Righetti, *ELECTROPHORESIS | Capillary Electrophoresis–Mass Spectrometry*, in *Encyclopedia of Separation Science*, I.D. Wilson, Editor. 2000, Academic Press: Oxford. p. 1188-1194.
53. Jacobson, S.C., et al., *High-speed separations on a microchip.* Analytical chemistry, 1994. **66**(7): p. 1114-1118.
54. Jacobson, S.C., et al., *Microchip structures for submillisecond electrophoresis.* Analytical chemistry, 1998. **70**(16): p. 3476-3480.
55. Mao, X., et al., *Analysis of chicken and turkey ovalbumins by microchip electrophoresis combined with exoglycosidase digestion.* Electrophoresis, 2003. **24**(18): p. 3273-3278.
56. Mao, X., et al., *Integrated lectin affinity microfluidic chip for glycoform separation.* Analytical chemistry, 2004. **76**(23): p. 6941-6947.
57. Zhang, B., et al., *Microfabricated devices for capillary electrophoresis− electrospray mass spectrometry.* Analytical chemistry, 1999. **71**(15): p. 3258-3264.
58. Zhang, B., F. Foret, and B.L. Karger, *High-throughput microfabricated CE/ESI-MS: automated sampling from a microwell plate.* Analytical Chemistry, 2001. **73**(11): p. 2675-2681.
59. Lazar, I.M., et al., *Subattomole-Sensitivity Microchip Nanoelectrospray Source with Time-of-Flight Mass Spectrometry Detection.* Analytical Chemistry, 1999. **71**(17): p. 3627-3631.
60. Long, Z., et al., *Integration of nanoporous membranes for sample filtration/preconcentration in microchip electrophoresis.* ELECTROPHORESIS, 2006. **27**(24): p. 4927-4934.
61. Sun, L., et al., *CZE-ESI-MS/MS system for analysis of subnanogram amounts of tryptic digests of a cellular homogenate.* PROTEOMICS, 2012. **12**(19-20): p. 3013-3019.
62. Zhu, G., et al., *Bottom-up proteomics of Escherichia coli using dynamic pH junction preconcentration and capillary zone electrophoresis-electrospray ionization-tandem mass spectrometry.* Analytical chemistry, 2014. **86**(13): p. 6331-6336.
63. Chen, D., X. Shen, and L. Sun, *Capillary zone electrophoresis–mass spectrometry with microliter-scale loading capacity, 140 min separation window and high peak capacity for bottom-up proteomics.* Analyst, 2017. **142**(12): p. 2118-2127.
64. Lubeckyj, R.A., et al., *Single-shot top-down proteomics with capillary zone electrophoresis-electrospray ionization-tandem mass spectrometry for identification of nearly 600 Escherichia coli proteoforms.* Analytical chemistry, 2017. **89**(22): p. 12059-12067.
65. Huang, C., et al., *Electromembrane extraction.* TrAC Trends in Analytical Chemistry, 2017. **95**: p. 47-56.
66. Pedersen-Bjergaard, S., C. Huang, and A. Gjelstad, *Electromembrane extraction–Recent trends and where to go.* Journal of Pharmaceutical Analysis, 2017. **7**(3): p. 141-147.
67. Li, J., et al., *Functional materials and chemicals in electromembrane extraction.* TrAC Trends in Analytical Chemistry, 2022. **150**: p. 116574.
68. Petersen, N.J., H. Jensen, and S. Pedersen-Bjergaard, *On-chip electromembrane extraction for monitoring drug metabolism in real time by electrospray ionization mass spectrometry*, in *Microchip Capillary Electrophoresis Protocols*. 2015, Springer. p. 171-182.

69. Asl, Y.A., et al., *A new effective on chip electromembrane extraction coupled with high performance liquid chromatography for enhancement of extraction efficiency.* Analytica Chimica Acta, 2015. **898**: p. 42-49.
70. Baharfar, M., et al., *Quantitative analysis of clonidine and ephedrine by a microfluidic system: On-chip electromembrane extraction followed by high performance liquid chromatography.* Journal of Chromatography B, 2017. **1068**: p. 313-321.
71. Zhou, W., et al., *Advances in capillary electrophoresis-mass spectrometry for cell analysis.* TrAC Trends in Analytical Chemistry, 2019. **117**: p. 316-330.
72. Płotka-Wasylka, J., et al., *Modern trends in solid phase extraction: new sorbent media.* TrAC Trends in Analytical Chemistry, 2016. **77**: p. 23-43.
73. Gao, D., et al., *Microfluidic cell culture and metabolism detection with electrospray ionization quadrupole time-of-flight mass spectrometer.* Analytical chemistry, 2010. **82**(13): p. 5679-5685.
74. Luo, Y.-S., et al., *Chemical and biological assessments of environmental mixtures: A review of current trends, advances, and future perspectives.* Journal of Hazardous Materials, 2022. **432**: p. 128658.
75. Gao, D., et al., *Characterization of drug permeability in Caco-2 monolayers by mass spectrometry on a membrane-based microfluidic device.* Lab on a Chip, 2013. **13**(5): p. 978-985.
76. Gao, D., et al., *Evaluation of the absorption of methotrexate on cells and its cytotoxicity assay by using an integrated microfluidic device coupled to a mass spectrometer.* Analytical chemistry, 2012. **84**(21): p. 9230-9237.
77. Mao, S., et al., *Imitation of drug metabolism in human liver and cytotoxicity assay using a microfluidic device coupled to mass spectrometric detection.* Lab on a Chip, 2012. **12**(1): p. 219-226.
78. Mao, S., et al., *Strategy for Signaling Molecule Detection by Using an Integrated Microfluidic Device Coupled with Mass Spectrometry to Study Cell-to-Cell Communication.* Analytical Chemistry, 2013. **85**(2): p. 868-876.
79. Dugan, C.E., et al., *Monitoring cell secretions on microfluidic chips using solid-phase extraction with mass spectrometry.* Analytical and Bioanalytical Chemistry, 2017. **409**(1): p. 169-178.
80. Marasco, C.C., et al., *Real-time cellular exometabolome analysis with a microfluidic-mass spectrometry platform.* PLoS One, 2015. **10**(2): p. e0117685.
81. Shan, L. and B.R. Jones, *Nano-LC: An updated review.* Biomedical Chromatography, 2022. **36**(5): p. e5317.
82. Lin, A., et al., *3D cell culture models and organ-on-a-chip: Meet separation science and mass spectrometry.* Electrophoresis, 2020. **41**(1-2): p. 56-64.
83. Vehus, T., et al., *Versatile, sensitive liquid chromatography mass spectrometry - Implementation of 10 µm OT columns suitable for small molecules, peptides and proteins.* Sci Rep, 2016. **6**: p. 37507.
84. Bell, D.S., *Recent Developments in Open-Tubular Liquid Chromatography Columns.* LC-GC North America, 2021. **39**: p. 315+.
85. Oedit, A., et al., *Lab-on-a-Chip hyphenation with mass spectrometry: strategies for bioanalytical applications.* Current Opinion in Biotechnology, 2015. **31**: p. 79-85.
86. Tsunoda, M., *On-Chip Liquid Chromatography.* Encyclopedia, 2022. **2**(1): p. 617-624.
87. Yin, H., et al., *Microfluidic Chip for Peptide Analysis with an Integrated HPLC Column, Sample Enrichment Column, and Nanoelectrospray Tip.* Analytical Chemistry, 2005. **77**(2): p. 527-533.
88. Amirifar, L., et al., *Droplet-based microfluidics in biomedical applications.* Biofabrication, 2022. **14**(2): p. 022001.

89. Sohrabi, S., N. kassir, and M. Keshavarz Moraveji, *Droplet microfluidics: fundamentals and its advanced applications.* RSC Advances, 2020. **10**(46): p. 27560-27574.
90. Zhang, X.-C., et al., *Integrated Droplet-Based Microextraction with ESI-MS for Removal of Matrix Interference in Single-Cell Analysis.* Scientific Reports, 2016. **6**(1): p. 24730.
91. Su, Y., Y. Zhu, and Q. Fang, *A multifunctional microfluidic droplet-array chip for analysis by electrospray ionization mass spectrometry.* Lab on a Chip, 2013. **13**(10): p. 1876-1882.
92. Zhu, Y. and Q. Fang, *Integrated Droplet Analysis System with Electrospray Ionization-Mass Spectrometry Using a Hydrophilic Tongue-Based Droplet Extraction Interface.* Analytical Chemistry, 2010. **82**(19): p. 8361-8366.
93. Pei, J., et al., *Analysis of Samples Stored as Individual Plugs in a Capillary by Electrospray Ionization Mass Spectrometry.* Analytical Chemistry, 2009. **81**(15): p. 6558-6561.
94. Kelly, R.T., et al., *Dilution-Free Analysis from Picoliter Droplets by Nano-Electrospray Ionization Mass Spectrometry.* Angewandte Chemie International Edition, 2009. **48**(37): p. 6832-6835.
95. Vitorino, R., et al., *Microfluidics for Peptidomics, Proteomics, and Cell Analysis.* Nanomaterials, 2021. **11**(5): p. 1118.

Section 2 - Ion mobility spectrometry-tandem mass spectrometry strategies for the on-line monitoring of a continuous microflow reaction

Darya Hadavi*, Peiliang Han*, Maarten Honing

Maastricht Multimodal Molecular imaging (M4i) Institute, Division of Imaging Mass Spectrometry Maastricht University, Universiteitssingel 50, 6229ER, Maastricht, The Netherlands.

Based on

Hadavi, D., Han, P*., & Honing, M. (2021). Ion mobility spectrometry-tandem mass spectrometry strategies for the on-line monitoring of a continuous microflow reaction. Journal of Flow Chemistry. doi:10.1007/s41981-021-00209-7*

Abstract

Continuous flow chemistry is an efficient, sustainable and green approach for chemical synthesis that surpasses some of the limitations of the traditional batch chemistry. Along with the multiple advantages of a flow reactor, it could be directly connected to the analytical techniques for on-line monitoring of a chemical reaction and ensure the quality by design. Here, we aim to use ion mobility, mass and tandem mass spectrometry (IMS-MS and MS/MS) for the on-line analysis of a pharmaceutically relevant chemical reaction. We carried out a model hetero-Diels Alder reaction in a microflow reactor directly connected to the IMS-MS and MS/MS using either electrospray or atmospheric pressure photo ionization methods. We were able to monitor the reaction mechanism of the Diels Alder reaction and structurally characterize the reaction product and synthesis side-products. The chosen approach enabled identification of two isomers of the main reaction product. A new strategy to annotate the ion mobility spectrum in the absence of standard molecules was introduced and tested for its validity. This was achieved by determining the survival yield of each isomer upon ion mobility separation and density functional theory calculations. This approach was verified by comparing the theoretically driven collision cross section values to the experimental data. In this paper, we demonstrated the potential of combined IMS-MS and MS/MS on-line analysis platform to investigate, monitor and characterize structural isomers in the millisecond time scale.

Keywords: Hetero-Diels Alder reaction, ion mobility spectrometry, tandem mass spectrometry, atmospheric pressure photo ionization, flow reaction, annotating ion mobility spectrum.

Introduction

Over the last decades, flow chemistry has garnered much attention in the pharmaceutical industry as it facilitates the efficient synthesis of Active Pharmaceutical Ingredients (API)s. Running the chemical reactions via continuous flow stream through milli- or micro-sized channels has a plethora of advantages compared to batch chemistry [1, 2]. Most importantly, the narrow channels of a flow reactor provide a larger surface-to-volume ratio, which leads to the efficient transfer of energy, improved control over the reaction pressure and enhanced mixing efficiency [3-5]. These features of a flow reactor make it feasible to run reactions at high or low temperatures and promote sustainability by mitigating the risk of working with hazardous materials and reducing the costs and environmental footprints. Moreover, flow chemistry is considered as Green Analytical Chemistry (GAC) due to decreasing the use of energy and reagents and eliminating wastes [6, 7]. Meanwhile, precise control over the reaction conditions raises the consistency of manufacturing high-quality products and facilitates the upscaling process [8, 9].

Coupling of flow reactors with analytical detection technologies allows the real-time and on-line reaction monitoring, facilitating process control. However, application of process analytical techniques such as Liquid Chromatography (LC), UltraViolet-Visible (UV-Vis) spectroscopy and Nuclear Magnetic Resonance (NMR) poses many challenges. Techniques such as NMR and UV-Vis fall short to study complex reaction mixtures over a large concentration range. In addition, the selective detection of molecules lacking UV-Vis chromophores becomes a challenge. With regard to the separation techniques, such as LC, the whole analysis cycle is relatively long and the reaction mixture is at the risk of decomposing within the column [10]. More importantly, it is challenging and rather time consuming to separate isomers, in particular stereoisomers, without a chiral column on LC [11]. Therefore, for the on-line reaction monitoring, there is a need for universal analytical detectors being sensitive, selective, while requiring short (micro to millisecond) analysis time.

Mass Spectrometry (MS) coupled with tandem mass spectrometry (MS/MS) and Ion Mobility Spectrometry (IMS) outperform other technologies by meeting the majority of the requirements for high quality reaction monitoring [12]. Unlike NMR and UV-vis, MS simultaneously separates reagents, impurities, intermediates, and products of a complex reaction in microseconds based on their mass over charge ratio (*m/z*). The IMS can surpass the limitations of LC by rapid (millisecond timescale) separation of isomeric compounds with high selectivity and improved signal-to-noise ratio [13]. Moreover, the separation of molecular ions based on their Collision Cross Section (CCS), size, shape, and charge by IMS enables elucidating structural information [14, 15]. Combined with MS/MS, the fragmentation pathways add to the potential to unambiguously assign the molecular structure of unknowns. Collision Induced Dissociation (CID) is one of the commonly used approaches in tandem mass spectrometry for survival yield analysis [16]. Hence, connecting a continuous flow chemical reactor to the IMS-MS and MS/MS, as an analytical tool, provides the possibility to monitor a reaction in real-time without stalling the production to collect samples in different steps of a reaction. In addition, the real-time information improves the process control by reducing chemical waste,

measurement time and most importantly, leads to a new dimension to quality by design [17-19].

The (hetero) Diels-Alder (DA) cycloaddition reactions are frequently applied for the synthesis of medicinal drugs due to their relatively high stereo selectivity and efficiency [20]. Despite numerous benefits and the increased interest in utilizing flow reactors to run a (hetero-) DA reaction, pharma and chemical industries have been very slow in the transition from batch to flow processing. As mentioned, this is also due to the scarcity of suitable Process Analytical Technologies (PAT)s [18]. To accelerate this transition, a model hetero-DA reaction carried out in a microflow reactor and connected to the IMS-MS and MS/MS for the on-line monitoring of the reaction. Using this analytical technique, the reaction mechanism and structural isomers formed in the hetero-DA reaction were assessed and the potential of combined IMS-MS and MS/MS experimentation were profoundly investigated.

Experimental

Materials and sample preparations

Methyl-2,4-pentadienoate, 4-methyl-2-pentanone, nitrosobenzene, 4-chloropiperidine hydrochloride, Dichloromethane (DCM), Acetonitrile (ACN), toluene, chloroform-d, Methanol (MeOH), acetic acid and water (H_2O) with >98% purity, ESI-L low concentrations tuning mix, APPI/APCI tuning mix and polyalanine purchased from Sigma-Aldrich (Zwijndrecht, The Netherlands).

The reaction condition in batch and isolation process

To perform the hetero-DA reaction in 4-methyl-2-pentanone solvent, a solution of nitrosobenzene (53.2 mg, 0.497 mmol) and methyl 2,4-pentadienoate (58.1 µL, 0.499 mmol) in 20 ml of 4M2P was stirred at 60 ^{o}C for 25 hours. To study the impact of residence time on the production efficiency, 50 µl of the reaction mixture was collected after 0.39, 1.63, 4.65, 7.38, and 25.1 hours. Samples were diluted with 150µl of a dilution solvent mixture, including 1mM of internal standard and 0.1% acetic acid to make it comparable to the flow reaction. When acetonitrile was used as the reaction solvent instead of 4-methyl-2-pentanone, a solution of nitrosobenzene (80.1 mg, 0.748 mmol) and methyl 2,4-pentadienoate (87.0 µL, 0.749 mmol) in acetonitrile (10 ml) was stirred at 60 ^{o}C for 8 hours. The same method was applied for the reaction of nitrosobenzene (53.2 mg, 0.497 mmol) with 20 mL 4-methyl-2-pentanone for the specificity experiment. The outcome of each batch reaction either analysed as a complex sample or purified by TLC preparative plate (Sigma-Aldrich, Zwijndrecht, the Netherlands) prior to analysing. For the reaction in 4M2P, the reaction mixture diluted with water (20 ml) and extracted with ethyl acetate (3x15 ml). For the reaction in acetonitrile, 15 ml of water and 3x10 ml of ethyl acetate was used for dilution and extraction. Subsequently, the combined organic layer was washed with brine (10 ml) and dried with anhydrous Na_2SO_4. After filtration, the solution was concentrated under vacuum and purified using TLC (eluted

with 1:1 dichloromethane/ n-hexane) to afford the product as a white solid (32.9 mg, 30% for the reaction in 4M2P and 74 mg, 45% for the reaction in acetonitrile).

The microflow reactor platform and the reaction condition

The reaction was carried out in the Chemtrix Labtrix® microflow reactor set up (Fig.1 and online resource Fig. S8) consisted of 4 gas tight glass syringes with luer lock fitting (1ml-Hamilton, Amsterdam, The Netherlands), flow rate controllers (Chemyx Fusion 200 syringe pump- Stafford, TX, USA), temperature controller, Back Pressure Regulator (BPR), outer dilution inlet and a start unit, which accommodated the glass microreactor (Chemtrix R3227 type). The Chemtrix R3227 microflow reactor consisted of two main inlets, static mixer, residence time loop, a third inlet port to introduce a dilution solvent (inner dilution inlet), a second static mixer and an outlet port. This microreactor has the effective reaction volume of 19.5 µl and it provides the residence times from 0.78 to 97.5 minutes (for A+B reaction) with the (total) flow rate ranging between 0.2 and 25 µl/min. The outlet port directly connected to a BPR to keep the pressure at constant value of 2×10^6 Pa. Right after the BPR, a T-connector was placed to mix the reaction outcome with the dilution solvent mixture (Fig. 1 and online resource Fig. S8). The line coming out of the T-connector was directly connected to ESI or APPI ionization source, placed in front of the MS orifice.

The reaction was conducted by continuous injection of nitrosobenzene (50mM) and methyl-2,4-pentadienoate (50mM) solutions dissolved in 4M2P through main inlets. Dilution solvent mixture consisted of MeOH/ H_2O/ACN (2:1:1) and 0.1% acetic acid introduced to the reaction outcome through inner and outer dilution inlets. As an internal standard 1mM of 4-chloropiperidine hydrochloride added to the reaction outcome through the inner dilution inlet. To monitor the impact of residence time on hetero-DA reaction the temperature was set to the constant optimised value of 60ºC. The flow rate of each starting materials set to 2, 1, 0.5, 0.35, 0.25 and 0.12 µl/min to reach the residence times of approximately 5, 10, 20, 28, 40 and 80 minutes (respectively). The flow rate of the dilution solvent on inner dilution inlet always set as the sum flow rate of each starting material. The outer dilution inlet was used to further dilute the reaction outcome. Its flow rate was set to 8, 4, 2, 1.4, 1 and 0.5 µl/min respectively for shortest to longest residence time. To monitor the effect of temperature, the reaction residence time was set to the constant optimised value of 20 min. The reaction was monitored under increasing temperatures of 25, 40, 60, 80, 100 and 120 ºC. For APPI experiments, DCM was used instead of 4M2P as the reaction solvent. For this set of experiments, dopants including pure toluene and DCM/toluene (1:1) were respectively injected through the inner and outer dilution inlets.

ESI/APPI-IMS-MS/MS parameters

Synapt HDMS G2Si (Waters, Milford, MA, USA) equipped with a TWIMS, as well as a Trapped-Ion Mobility Spectrometry-Q-TOF (Bruker Daltonics Inc., Billerica, MA, USA) were used for the ion mobility and tandem mass spectrometry analysis. Table. S1 presents the set parameters for IMS measurements on each instrument. Nitrogen gas

was used in the ion mobility cell and helium gas was used before the ion mobility cell for collisional cooling. Argon was used as the collision gas in the trap and transfer cells. The ESI and APPI experiments performed in positive ion mode under the optimized ionization conditions listed in table. S1. The mass spectra acquisition range was set between *m/z* 50 and 300 Da. ESI-L low concentrations tuning mix and APPI/APCI tuning mix were used for the mass calibration and polyalanine was used to the IMS calibration. On the TIMS instrument, the massive ions with lower mobility (k) elute first compared to the lighter and compact ions, however the IMS graph is constructed based on 1/k ($V.s/cm^2$) values, making it comparable to the IMS generated by the TWIMS instrument.

For IMS-MS/MS experiments, the precursor ion was isolated in the quadrupole and fragmented via CID after the ion mobility cell in the transfer cell. The collision energy was increased from 5 to 30 eV in 5eV increments (total of 6 collision energies). The MS/MS results were the average of 2 minutes acquisition time per collision energy. To extract the CID spectrum of each isomer from its ion mobility, first the ion mobility of the precursor ion at *m/z* 220 was extracted. Next, the mobility range of interest were selected (e.g. from 4 until 4.5 ms). The peak picking then performed in the non-chromatic mode using the following parameters: min drift time peak width of 0.2 ms, MS resolution of 35000 and minimum intensity threshold of 1000 counts. The CID spectra were copied to excel for further analysis. Previously explained methods [21] were employed to plot the experimental and linear survival yield graphs. The experimental survival yield was plotted based on the ratio of the intensity of the Precursor ion (P) to the sum of the intensities of the precursor and Fragment ions (F) (Equation 1). This graph was transformed to linear form by equation 2 and 3.

$$\text{Experimental survival yield} = \frac{IntensityP}{IntensityP+\Sigma(IntensityF)}$$

Equation 1

$$\text{Sigmoidal survival yield} = \frac{1}{1+c*e^{-b.CE}}$$

Equation 2

Where b is the slope of the linear segment, and the intercept of the linear portion is the natural logarithm of c.

$$\ln\left(\frac{1-Survival\ yeild}{Survival\ yeild}\right) = \ln(c)\text{-b(CE)} \qquad \text{Equation 3}$$

NMR

The Bruker (Rheinstetten, Germany) Avance III HD NMR spectrometer operated at the ^1H frequency of 700 MHz and equipped with a cryogenically cooled triple channel [^1H,^{13}C,^{15}N] TCI probe. The ^1H and ^{13}C spectra were recorded as 250 mM in $CDCl_3$ solutions with 0.03% TMS as internal chemical shift reference standard. Spectra were processed using Topspin 3.2 softwareand analyzed by the program Sparky 3.114 (Goddard & Kneller) and MestReNova

Data evaluations

The acquired data by Synapt G2Si analysed by MassLynx v4.1. and DriftScope v2.8 software. The measured data by TIMS-TOF analysed by Compass DataAnalysis v5.0 software (Bruker). The extracted ion mobility spectra extracted and plotted in excel for further analysis. To correct for the ion suppression effects, the intensity of the reaction product ions normalised with the intensity of 4-chloropiperidin (the internal standard). For CCS calculations, the molecules structurally optimized by DFT on Spartan software (Wavefunction, Inc. & Q-Chem, Irvine, CA, USA). Conformer distribution calculations were performed to obtain the global energy minimum with Density Functional ωB97X-D and basis set 6-31G* using Molecular Force Field (MMFF) geometry. The software considered 100 conformers, while keeping the E≤40 kJ/mol and the energy of maximum 10 conformers calculated while keeping the E≤15 kJ/mol. The IMoS software used for theoretical CCS calculations with Trajectory Method (TM) with 300.000 N_2 gas molecules per orientation. Mulliken charges were used for partial atomic charges, they were automatically calculated by Spartan. Calculations performed for each conformer with Boltzmann weight above 1%.

Results and Discussion

A model hetero-DA reaction was carried out in the Chemtrix Labtrix® microflow reactor directly connected to the IMS-MS and MS/MS for the on-line monitoring of the reaction (Fig. 1). The molecular identifications and separations were studied by Trapped Ion Mobility Spectrometry (TIMS) and Traveling Wave Ion Mobility Spectrometry (TWIMS) incorporated in Quadrupole Time-Of-Flight (Q-TOF) mass spectrometer. The reagents and synthesized molecules were ionized by an Electrospray Ionization (ESI) and Atmospheric Pressure Photo Ionization (APPI). The reaction was monitored at different temperatures and residence times.

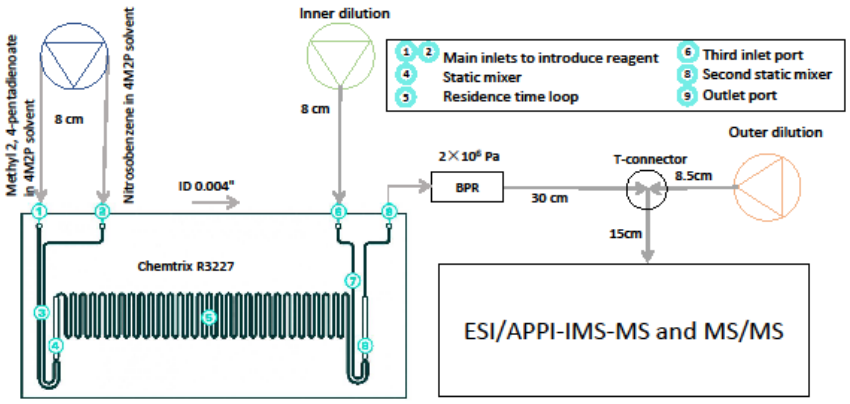

Figure 1. Schematic of the reaction set up to visualize the microreactor, main inlets, dilution inlets and connection to the MS analyzer.

Hetero-Diels alder reaction

In organic chemistry, a wide range of biologically active compounds are synthesised by (hetero-) DA reactions. In particular, the formation of 1,2-oxazine compounds is of

special interest to synthesise bioactive products or stabilize them and selectively functionalize natural products [22-24]. The 1,2-oxazine compounds are formed as a result of nitroso dienophile reaction with conjugated diene. Considering the importance of nitroso hetero-DA reactions in pharma [24], in this study, nitrosobenzene **1**, as a dienophile, was exposed to react with methyl 2, 4-pentadienoate **2**, as a diene, through a hetero-DA mechanism to form product **3** (methyl 2-phenyl-3,6-dihydro-2H-1,2-oxazine-6-carboxylate) (Fig. 2a). The reaction was performed in 4-methyl-2-pentanone (4M2P) solvent with high boiling point (116 ºC) to prevent over pressuring in the microflow reactor within the range of tested temperatures (25-120 ºC). The reaction efficiency in the microflow reactor was compared with the batch chemistry reaction.

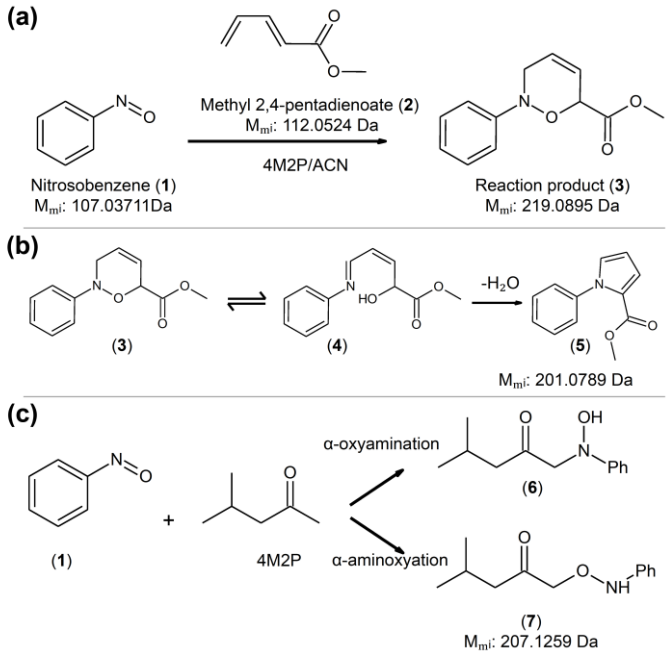

Figure 2. Hetero-DA reaction schematics. a Reaction schematic of reagent nitrosobenzene (1) with reagent Methyl 2,4-pentadienoate (2) in 4-methyl-2-pentanone (4M2P) or acetonitrile (ACN) solvent. b Ring opening of molecule (3) to form isomeric molecule (4) and its dehydrated molecular structure (5). c Two possible reaction mechanisms of α-oxyamination and α-aminoxyation for the reaction of nitrosobenzene (1) with the solvent molecules (4M2P).

The characterization of the reaction elements by ESI and APPI – MS and MS/MS

Connecting the microflow reactor to the IMS-MS and MS/MS enabled the tentative structural identification of the reaction products, including side-products. The mass spectrum of the reaction outcome generated after ionizing by ESI and APPI sources are depicted in online resource Fig. S1a, b. The ESI-MS contained the ions at *m/z* 220 and 242, being respectively assigned as the $[M+H]^+$ and $[M+Na]^+$ ions of the reaction product

3. Although the reaction outcome ionized under soft conditions (Table. S1), the reaction mass spectrum included several fragment ions caused by upfront CID processes [25]. According to the tandem mass spectrometry of product **3**, ions with *m/z* 202, 190, 170 160, 132 and 94 were being directly originated from the parent ion *m/z* 220 (online resource Fig. S1c).

To ensure regioselectivity of the hetero-DA reaction to form product **3**, the reagents were reacted in batch with acetonitrile solvent, similar to a previous study [26]. According to the ^{1}H and ^{13}C NMR spectra (online resource Fig. S1d and 1e) the outcome of this reaction was consistent with the outcome of the microflow reaction.

The (fragment) ion at *m/z* 202 was formed by the loss of H_2O from product **3.** The tandem mass spectrum of the precursor ion *m/z* 202 showed a base peak at *m/z* 170 (online resource Fig. S2a). This fragment ion was formed due to the loss of methanol. This fragmentation pathway indicated that the loss of H_2O from the molecule **3** did not occur from the ester group. The only remaining source of oxygen for water loss was in the oxazine ring. The oxazine could go through the ring opening process in the microflow reactor to form the molecule **4**, subsequently lose a water molecule through the cyclization reaction to form a compound **5** (Fig. 2b). To further confirm this mechanism, the reaction product in the liquid phase was isolated and purified using preparative Thin Layer Chromatography (TLC) and tested by NMR. The NMR spectrum of the peak at *m/z* 202 showed a methyl group at 3.7 ppm as well as three protons of the pyrrole ring with sp2 environment, unlike the molecule **3** that had only two sp2 protons (online resource Fig. S2b). In addition, the absence of a proton at 5 ppm close to the ester group indicated the pyrrole shape of the molecule (Fig. 2b). Hence, the peak at *m/z* 202 was annotated as the molecule **5**, which could be formed in the liquid phase due to the condensation reaction and/or in the gas phase due to the water loss from the molecule **4**. Consistent with this finding, the N-O bond energy of molecule **3** is 201 kJ/mol, which is a smaller value than other bonds in the ring (C-C 347 kJ/mol, C-N 305kJ/mol, C-O 358 kJ/mol) [27]. The relatively weak bond energy of N-O explains the position of ring-opening reaction to form molecule **4** from molecule **3**. These results indicated that the investigated hetero-DA reaction formed two structurally isomeric molecules (**3** and **4**).

The peak at *m/z* 225 was annotated as the protonated dimer ($[2M+H]^+$) of the reaction reagent **2**. The identity of this peak was confirmed by fragmenting the precursor ion (*m/z* 225) in collision cell and annotating the fragment peaks (online resource Fig. S3a). This reaction outcome was formed by self-dimerization of methyl 2,4-pentadienoate (**2**) and could be regarded as an impurity. It is because the dimer was already present in the commercial reagent prior to running the reaction. This observation was also verified by the impurities on NMR (online resource Fig. S3b).

The peaks at *m/z* 199 and 230 were identified as the side-products of hetero-DA reaction. Unlike the protonated ion of the main product (**3**), *m/z* 230 required higher collision energy (20eV) to yield 70% disassociation. This observation implies that this molecule is more stable compared to the main reaction product and likely having a different molecular structure. Merino et al., suggests that ketone groups tend to react with nitroso groups by either α-oxyamination or α-aminoxyation mechanism (Fig. 2c)

[28]. Hence, the nitrosobenzene reagent (**1**) could also react with the solvent 4M2P and form the side-products **6** and/or **7**. This reaction pathway was confirmed by running an additional batch reaction with reagent **1** and 4M2P (without reagent **2**) at 60 ˚C overnight. The mass spectrum of this overnight reaction was comparative to the spectrum of the hetero-DA reaction (online resource Fig. S4); in a way that both spectra included peaks at *m/z* 208 and 190. Based on the MS/MS analysis, these peaks were respectively $[M+H]^+$ and $[M+H-H_2O]^+$ ions of the side-products **6** and/or **7**. Consequently, the peak at *m/z* 230 is the sodium adduct of the side-products. The tendency of the side-product molecules to lose water suggested that the reaction occurred only through the α-oxyamination pathway to form side-product **6** rather than **7**. The sodium adduct formation of the side-product **6** in the gas phase explains the stability of the peak at *m/z* 230 owing to sharing the positive charge of Na^+ with oxygen of ketone and hydroxyl groups.

The identity of the low abundant peak at *m/z* 199 was also determined by MS/MS and verified by NMR analysis (online resource Fig. S5). As reported earlier [29], nitrosobenzene molecules can react with each other to form a dimer, which explains the peak at *m/z* 199 as the side-product of the reaction.

The APPI-MS data were comparative to the ESI-MS. The APPI source resulted in the formation of both $[M]^{\cdot+}$ and $[M+H]^+$ ions of the reaction products at *m/z* 219 and 220 respectively (online resource Fig. S1b). The APPI forms radical cations after being excited to high energic states or by electron transfer. In the latter case a neutral species such as toluene, known as Dopant (D), absorbs photon energy from the light source in the ionization chamber. The internally excited dopant (D^*) ionizes a neutral target Molecule (M) that has lower ionization energy by electron transfer. Consequently, the radical cations are formed (Equation 4).

$$D^* + M \rightarrow D + M^{+\cdot} + e^- \quad \text{Equation 4}$$

Since the hetero-DA reaction was performed in the 4M2P solvent, the reaction products were mainly protonated ($[M+H]^+$). This is due to the high proton affinity (≈832.7 kJ/mol at 300K) of the 4M2P solvent, which imposes the protonation of molecules through the equation 5.

$$[S_n + H]^+ + M \rightarrow [S_n + M + H]^+$$
$$[S_n + M + H]^+ \rightarrow nS + [M + H]^+$$
Equation 5

When the solvent of the reaction was exchanged with dichloromethane, having a lower proton affinity (628.0 kJ/mol at 300K) compared to 4M2P, the reaction products formed radical cations. This process demonstrated the versatility of the APPI source to utilize in a diverse range of organic synthesis with no restrictions on the solvent choice. Regardless of the solvent type, molecules are ionized either by proton or electron transfer. The ESI and APPI -MS-MS/MS data of the isolated batch reaction product were consistent with the acquired data from microflow reactor (online resource Fig. S6).

ESI and APPI-IMS-MS/MS

The ion mobility spectrometry of the reaction products was studied by TWIMS and TIMS instruments. Each technique has different separation mechanism as explained before [30]. Annotating the IMS of isomeric compounds becomes a challenge when there are no standard molecules for IMS comparison. This challenge is even more pronounced for the reactions leading to unknown isomeric forms of the main product. In such instances, even if each isomer is fragmented by MS/MS through a distinctive pathway, the tandem mass spectrum contains the fragment ions of all isomers, withholding the separation of isomers based on one/multiple unique product ion(s). The combination of ion mobility with tandem mass spectrometry brings another dimension to molecular ion identifications. By applying IMS-MS/MS approach, the generated fragment ions of each isomer will have the same arrival time as their parent isomer. Isomers could be separated and identified based on a unique daughter ion under different mobility peaks or unique Collision Energy (CE) that results in 50% survival yield (CE_{50}). Ion mobility spectrometry also provides additional information regarding the 3D structure of each ion. This is possible by experimentally measuring the ion-neutral gas CCS and comparing it to the theoretically calculated CCS values.

The extracted ion mobility (EIM) of the ion at *m/z* 220 was reconstructed to plot its ion mobility spectrum. The plotted IMS showed a bimodal peak (Fig. 3a). The bimodal peak indicated the presence of at least two compounds with the same mass but different 3D structures. Therefore, the hetero-DA reaction produced two isomeric compounds (molecules **3** and **4**) with the same *m/z* value but different mobility. This observation is in line with the represented mechanism for the reaction (Fig. 2b). The IMS of the radical cation at *m/*z 219, which was formed by APPI source, demonstrated better resolution than the protonated ion at *m/z* 220 (Fig. 3b). This could be due to the formation of intramolecular H bridges in protonated molecules, which increases structural similarity of **3** and **4**. The IMS of the reaction elements were consistent regardless of the type of ionization source (APPI or ESI) and the ion mobility instrument (TWIMS or TIMS), even though TIMS resulted in better resolution data.

Apart from the isomeric separation, it is also essential to annotate each ion mobility peak to a correct molecular structure. To this end, different methods were employed. One of the unique features of TWIMS-TOF is that a mass analyser quadrupole is placed before the ion mobility cell, which enables performing MS/MS on the isolated precursor ions after IMS (IMS-MS/MS). Since the internal energy of an ion and its decomposition reaction rate are structural dependent features, it is known that even isomeric chemical structures show unique stability and survival yield under CID [21]. Hence, for the first time, we employed IMS-MS/MS method to define the CE_{50} of the isomeric reaction products. The *m/z* 220 was first isolated in the quadrupole and then separated in the ion mobility cell followed by CID. When the precursor ions exposed to the increasing CE after IMS separation, isomeric ions' survival decreased in a sigmoidal form (Fig. 3c). This graph transformed to a linear survival yield (Fig. 3d) to find the CE_{50} as reported earlier [21]. The results identified unique CE_{50} of 14.89 and 15.82 eV for the isomer with the short drift time (td 4-4.5ms) and long drift time (td 4.5-5ms) respectively. The molecule **4** could have higher stability due to its lower Gibbs free energy after opening the ring, caused by the formation of stronger bond (smaller ΔH) and increased flexibility (larger

ΔS). To verify this assumption the minimum energy of both compounds was calculated by Density Functional Theory (DFT). Regardless of the protonation site, the molecular ion **4** always had lower global minimum energy than the protonated molecular ion **3** (Table. S2). These findings indicated the higher stability of the molecular ion **4** compared to **3**. Therefore, based on CE_{50} and DFT calculations the drift time td 4-4.5 ms and 4.5-5 ms were respectively annotated to the molecular ions **3** and **4**.

To further verify the identity of the annotated ion mobility peaks, the experimentally derived $^{TWIMS}CCS_{N2}$ was compared to the theoretically calculated CCS of the molecular ions **3** and **4**. Table. S3 shows the calculated CCS values of the molecules **3** and **4** that were protonated on nitrogen or ester group. Based on the theoretically calculated data, the CCS of the protonated ion **4**, regardless of the protonation site, was always higher than the protonated molecule **3**, which was in line with the open structure of **4**. Hence, the experimentally derived $^{TWIMS}CCS_{N2}$ value of 152.3177±0.80 $Å^2$ corresponds to the molecular ion **4** and the smaller $^{TWIMS}CCS_{N2}$ value of 147.044±0.79 $Å^2$ corresponds to the more compact molecular ion **3** (Fig. 3e). These molecules were more likely protonated on the ester group, as the theoretical and experimental CCS values are in less than 5% agreement upon protonation on the ester group. With these data, td 4-4.5 ms was again annotated to be the protonated molecule **3** and the td 4.5-5ms was related the protonated molecule **4**.

The drift time/mass-to-charge heatmap of the reaction outcome also gave a quick insight regarding the stability of the reaction. Online resource Fig. S7 presented the low stability of the reaction products in TWIMS-MS. The heatmap of the isolated *m/z* 220 in the quadrupole, demonstrated the presence of ions with the raising *m/z* and drift time values (white solid line ellipse- online resource Fig. S7). This trend showed the dissociation of the reaction products before the ion mobility cell, during the traverse from the quadrupole until the IMS cell. Ions with the identical drift time and increasing *m/z* value are related to fragment ions generated after the ion mobility cell, from the transfer cell till the detector (white dashed line ellipse- online resource Fig. S7).

All these findings highlighted the added value of IMS-MS and MS/MS experiments on providing in depth knowledge on the molecular structure (identity) of (un)known reaction products in the millisecond time scale. These process analytical technologies and reaction monitoring strategies not only enabled separation, but also enabled the tentative identification of isomeric compounds that are not distinguishable by MS or MS/MS. It also enabled annotation of IMS peaks without using a standard compound. Ionizing molecules with APPI combined with different IMS-MS/MS scanning strategies shed further light to characterize molecules. With the combination of ESI/APPI-IMS-MS/MS the reaction products and intermediates of the model hetero- DA reaction were characterised.

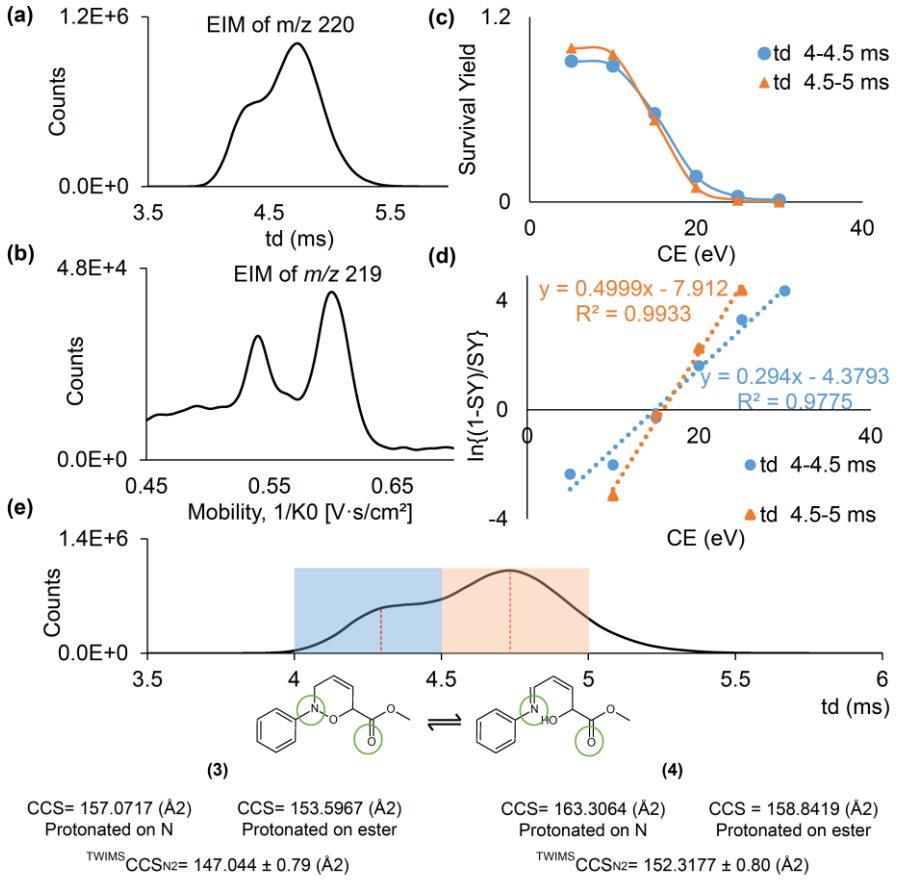

Figure 3. IMS and IMS-MS/MS analysis of the reaction products. a EIM of the protonated reaction products at m/z 220 analysed by ESI-TWIMS and ESI-TIMS. b EIM of the radical cation of reaction products at m/z 219 analysed by APPI-TIMS. c) Experimental survival yield of isomers upon ion mobility separation and CID at CE of 5, 10, 15, 20, 25, 30 eV. Filled blue circle corresponds to the isomer with short drift time (td 4-4.5ms) and filled orange triangle corresponds to the isomer with longer drift time (td 4.5-5ms). d Linear survival yield of the isomer at td 4-4.5 ms in filled blue circle and the isomer at td 4.5-5 ms in filled orange triangle. e Comparing the theoretically calculated CCS of the protonated molecules (3) and (4) on Nitrogen and ester groups with the experimentally derived TWIMSCCSN2 for the detected ion mobility peaks (dashed red lines).

Monitoring the microflow reaction by ESI-IMS-MS/MS

The reaction of nitrosobenzene with methyl 2, 4-pentadienoate was studied by directly connecting the Chemtrix Labtrix® microflow reactor to ESI/APPI-IMS-MS/MS analytical technique and compared to the batch chemistry results. The model hetero-DA reaction was investigated under various temperatures (25, 40, 60, 80, 100, 120 ºC) and residence times (5, 10, 20, 28, 40, 80 minutes) with constant pressure (2×10^6 Pa) and

concentrations (50mM methyl 2, 4-pentadienoate and nitrosobenzene (1:1)). The MS spectra were normalised to the intensity of the internal standard.

Fig. 4a and b presented the impact of residence time on the formation of reaction products (**3** and **4**) performed in the microflow versus batch reactor. The formation of the product molecules in both reactors were increased by raising the residence time. However, the reaction efficiency in the microflow reactor was higher than the batch reactor. In the batch reactor the abundance of the product ions increased 7 times after 7.38 hours of reaction, while in the microflow reactor this was done in only 40 minutes. The online monitoring of the reaction whilst raising the temperature indicated a systematic increase of the reaction products (Fig. 4c). These results demonstrated the potentials of microflow reactors and on-line measurements in increasing the reaction efficiency, improving reproducibility, reducing the number of experiments and lowering chemical consumptions compared to running multiple parallel experiments at different conditions required by batch chemistry.

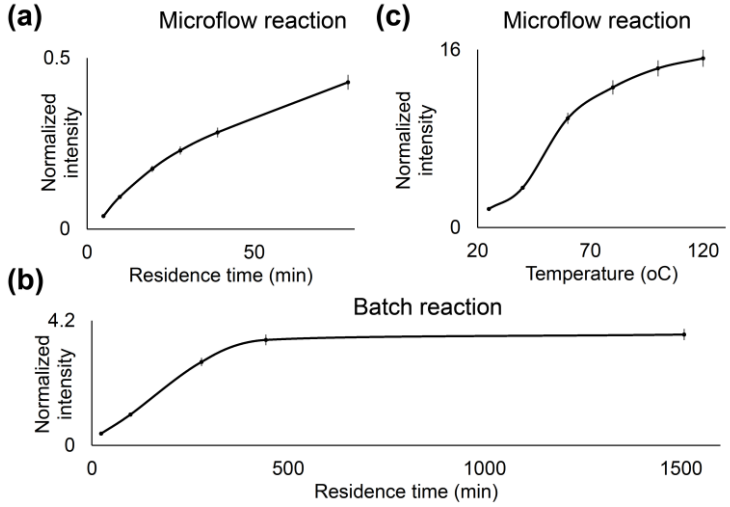

Figure 4.a Residence time effect on the formation of the reaction products after a) microflow reaction, b batch reaction. c Temperature effect on the formation of reaction products carried out in the microflow reactor.

Conclusion

The ion mobility-mass spectrometry and tandem mass spectrometry technique was used for the on-line monitoring the model hetero-DA reaction carried out in the microflow reactor and compared to batch reaction. When utilizing IMS-MS and MS/MS strategies, the elements of the reaction, including the isomeric reaction products, impurities and side-products were identified, characterized and separated. By systematically increasing the collision energy after the ion mobility separation, the survival yield of each isomer was calculated. The acquired survival yield was compared to the global minimum energy of ions calculated by DFT, which enabled annotating the ion mobility spectrum of isomers in the absence of standard molecules. The efficiency

of the reaction was higher when it was carried out in the microflow reactor compared to the batch reaction. The introduced strategies of hyphenating IMS-MS and MS/MS to a microflow reactor showed possible potentials to simultaneously detect different reaction products and above all their molecular structure (identity). The potential of APPI to act as a universal ionization technique, allowing the application of a wide variety of organic solvents, was introduced. The generation of radical ions through APPI and their specific fragment ions add another dimension to the structural identification process. It is anticipated that this approach be a valuable technology platform for the development of efficient and green chemical synthesis routes, readily linking reaction conditions to the presence of different reaction pathways.

Acknowledgements

We would like to thank Hans Ippel (CARIM, Maastricht University) for the execution and data interpretation of the NMR experiments and Yuandi Zhao (M4i, Maastricht University) for his artistic assistance.

Statements and Declarations

The authors declare that they have no financial or non-financial conflict of interest.

References

1. Bogdan, A.R. and A.W. Dombrowski, *Emerging Trends in Flow Chemistry and Applications to the Pharmaceutical Industry.* Journal of Medicinal Chemistry, 2019. **62**(14): p. 6422-6468.
2. Baumann, M., et al., *A Perspective on Continuous Flow Chemistry in the Pharmaceutical Industry.* Organic Process Research & Development, 2020.
3. Reckamp, J.M., et al., *Mixing Performance Evaluation for Commercially Available Micromixers Using Villermaux–Dushman Reaction Scheme with the Interaction by Exchange with the Mean Model.* Organic Process Research & Development, 2017. **21**(6): p. 816-820.
4. Schwolow, S., et al., *Application-Oriented Analysis of Mixing Performance in Microreactors.* Organic Process Research & Development, 2012. **16**(9): p. 1513-1522.
5. Schwolow, S., et al., *Design and application of a millistructured heat exchanger reactor for an energy-efficient process.* Chemical Engineering and Processing: Process Intensification, 2016. **108**: p. 109-116.
6. Elvira, K.S., et al., *The past, present and potential for microfluidic reactor technology in chemical synthesis.* Nature Chemistry, 2013. **5**(11): p. 905-915.
7. de la Guardia, M. and S. Garrigues, *Chapter 1 Past, Present and Future of Green Analytical Chemistry*, in *Challenges in Green Analytical Chemistry (2)*. 2020, The Royal Society of Chemistry. p. 1-18.
8. Campbell Brewer, A., et al., *Development and Scale-Up of a Continuous Aerobic Oxidative Chan–Lam Coupling.* Organic Process Research & Development, 2019. **23**(8): p. 1484-1498.
9. Schwolow, S., et al., *Kinetic and Scale-up Investigations of a Michael Addition in Microreactors.* Organic Process Research & Development, 2014. **18**(11): p. 1535-1544.
10. Fiers, T., et al., *Development of a highly sensitive method for the quantification of estrone and estradiol in serum by liquid chromatography tandem mass spectrometry without derivatization.* Journal of Chromatography B, 2012. **893-894**: p. 57-62.

11. Kuki, Á., et al., *Identification of Silymarin Constituents: An Improved HPLC–MS Method.* Chromatographia, 2012. **75**(3): p. 175-180.
12. Emwas, A.-H.M., *The Strengths and Weaknesses of NMR Spectroscopy and Mass Spectrometry with Particular Focus on Metabolomics Research*, in *Metabonomics: Methods and Protocols*, J.T. Bjerrum, Editor. 2015, Springer New York: New York, NY. p. 161-193.
13. Tadjimukhamedov, F.K., et al., *Liquid chromatography/electrospray ionization/ion mobility spectrometry of chlorophenols with full flow from large bore LC columns.* International Journal for Ion Mobility Spectrometry, 2008. **11**(1): p. 51-60.
14. Sorribes-Soriano, A., et al., *Trace analysis by ion mobility spectrometry: From conventional to smart sample preconcentration methods. A review.* Analytica Chimica Acta, 2018. **1026**: p. 37-50.
15. Hadavi, D., et al., *Adduct ion formation as a tool for the molecular structure assessment of ten isomers in Traveling Wave- and Trapped- Ion Mobility Spectrometry.* Rapid Communications in Mass Spectrometry, 2019. **33**.
16. Iacobucci, C., et al., *Insight into the Mechanisms of the Multicomponent Ugi and Ugi–Smiles Reactions by ESI-MS(/MS).* European Journal of Organic Chemistry, 2014. **2014**(32): p. 7087-7090.
17. Vargas, J.M., et al., *Process analytical technology in continuous manufacturing of a commercial pharmaceutical product.* International Journal of Pharmaceutics, 2018. **538**(1): p. 167-178.
18. Price, G.A., D. Mallik, and M.G. Organ, *Process Analytical Tools for Flow Analysis: A Perspective.* Journal of Flow Chemistry, 2017. **7**(3): p. 82-86.
19. Djuris, J., S. Ibric, and Z. Djuric, *1 - Quality-by-design in pharmaceutical development*, in *Computer-Aided Applications in Pharmaceutical Technology*, J. Djuris, Editor. 2013, Woodhead Publishing. p. 1-16.
20. Nicolaou, K.C., et al., *The Diels–Alder Reaction in Total Synthesis.* Angewandte Chemie International Edition, 2002. **41**(10): p. 1668-1698.
21. Kertesz, T.M., et al., *CE50: Quantifying Collision Induced Dissociation Energy for Small Molecule Characterization and Identification.* Journal of the American Society for Mass Spectrometry, 2009. **20**(9): p. 1759-1767.
22. Brulíková, L., et al., *Stereo- and regioselectivity of the hetero-Diels-Alder reaction of nitroso derivatives with conjugated dienes.* Beilstein journal of organic chemistry, 2016. **12**: p. 1949-1980.
23. Gamenara, D., *Hetero Diels-Alder adduct formation between nitrosobenzene and tetra-methyl purpurogallin and its retro-Diels-Alder reaction.* Journal of the Brazilian Chemical Society, 2001. **12**(4): p. 489.
24. Carosso, S. and M.J. Miller, *Nitroso Diels-Alder (NDA) reaction as an efficient tool for the functionalization of diene-containing natural products.* Organic & biomolecular chemistry, 2014. **12**(38): p. 7445-7468.
25. Oberacher, H., et al., *On the inter-instrument and the inter-laboratory transferability of a tandem mass spectral reference library. 3. Focus on ion trap and upfront CID.* Journal of Mass Spectrometry, 2012. **47**(2): p. 263-270.
26. Monbaliu, J.-C.M.R., et al., *Straightforward hetero Diels–Alder reactions of nitroso dienophiles by microreactor technology.* Tetrahedron Letters, 2010. **51**(44): p. 5830-5833.
27. Cottrell, T.L., *The strengths of chemical bonds*. 1958: Butterworths Scientific Publications.
28. Merino, P., et al., *Recent Advances on Asymmetric Nitroso Aldol Reaction.* Synthesis, 2016. **48**.

29. Taft, R.W., G. Klingensmith, and S. Ehrenson, *Multipolar complexes. I. The dimerization of nitrobenzene1*. Journal of the American Chemical Society, 1965. **87**(16): p. 3620-3626.
30. Cumeras, R., et al., *Review on ion mobility spectrometry. Part 1: current instrumentation.* The Analyst, 2015. **140**(5): p. 1376-1390.

General Discussion

General Discussion

Surface plasmon resonance, mass spectrometry, ion mobility, and tandem mass spectrometry are undoubtedly among the breakthrough discoveries in the field of analytics for understanding the molecular level dynamics. The beauty of these analytical tools is that they offer even more possibilities than what we have hinted at here. This thesis is certainly not a full disclosure of the capabilities of these techniques in answering real-world problems, but it has done its part by pushing their boundaries with respect to the unambiguous structural identification of molecules and complexes thereof.

Adduct ions, computational modeling, and their application on pathological samples

As thoroughly reported in this thesis, the separation of isomeric molecules is of particular importance in pharma and understanding (patho-) physiological processes. Depending on the separation resolution of ion mobility instruments, they give some degree of discrimination. However, relying solely on the resolution of an instrument is usually not sufficient. In order to find alternatives, the chapters of this thesis rely on hypothesis-driven science, addressing the scientific questions as explained in detail in the general introduction section.

Chapter 1- Section 1 brings new solution to ion mobility discrimination sciences by experimentally proving the benefit of using adduct salt ions as well as adducts with different sizes. Chapter 1 – Section 2, unlike other studies, uses the introduced approach in Chapter 1 - Section 1 to distinguish isomers in mixed solutions. Mixed solution samples are a better representative of complex biological samples, hence the introduced method opens a new door for analyzing (patho-) physiological samples. The immediate outlook is to apply these methods for direct analysis of human patient samples and biopsies for spatial localization of isomeric molecules on tissue by mass spectrometry imaging. However, there is a challenge when using the introduced methods in these two sections. It is that one adduct might have multiple preferential locations coordination in an isomer. This can eventually result in multiple mobility peaks or a very broad one for only one isomer, which might mask the signal of other isomers. Chapter 1- Section 2 offers a new solution for this challenge by indicating not to be limited to the experimentally generated data. This section practically brings a solution for a more rational interpretation of complex ion mobility results and to shed light on the behavior of ions in the gas phase. Chapter 1 – Section 2 elaborates in the method of extracting experimental collision cross sections (CCS) and comparing them to the theoretical molecular modeling CCS values. The introduced science in this section, the combination of computational modeling with experimental findings is advised for other ion mobility studies. However, the most important challenge in the introduced method is that the theoretical calculations could be computationally complex and expensive for large molecules (e.g. proteins). Besides this challenge, the benefits of using adduct ions for separation studies while performing theoretical calculations in parallel, are inevitable.

Tandem mass spectrometry before and after the ion mobility separation

Ion mobility cell positioned between two collision cells and a quadrupole located before them enabled us to introduce two new approaches for the separation of isomeric ions;

one is to perform MS/MS before the ion mobility separation (MS/MS-IMS) as discussed in Chapter 1, and the second is to do MS/MS after ion mobility separation (IMS-MS/MS) as experimented in Chapter 3 - Section 2. When IMS is positioned after the MS/MS, the CCS and thus the 3D conformation of the fragment ions can be assessed. Using this method, we introduced a new approach for the assessment of, sometimes selective, fragmentation pathway(s). Most importantly, this method enabled fragmenting away the identical parts of an ion and discriminating formerly indistinguishable isomers based on their small conformational differences. When performing IMS-MS/MS on mobility "separated" ions, the survival yield of each isomer becomes an important "property". It could be correlated to the global minimum energy of the ions (isomers), calculated by density functional theory. Eventually, this novel approach introduced in Chapter 3 – Section 2 enables annotating ion mobility peaks without requiring the standard molecule of each isomer. The introduced method in this chapter could now be implemented in on-line detection set ups, for instance for chemical reaction monitoring of chemical synthesis in a flow reactor connected to MS and IMS. Certainly one of the limiting factors in using the introduced techniques is that not all commercially available ion mobility instruments offer the possibility of performing MS/MS before the ion mobility cell. Even though this could be addressed by performing in-source fragmentation, still it is not possible to perform selective fragmentations. However, the introduced IMS-MS/MS can be used in many applications based on flow chemistry. As an example vitamin D3 flow chemistry analysis, as the precursor of this vitamin exists in multiple isomeric forms. This method also opens more doors for analyzing the isomeric content of organ-on-a-chip driven molecules.

Molecular interactions matter

Unraveling the (patho-) physiological processes is partly about the identification and physiochemical characterization of the involved molecules. The other important aspect is about understanding the interaction of molecules, particularly protein-protein interactions. Studying proteins' interactions with mass spectrometry and ion mobility requires the preservation of proteins' geometry throughout their journey from the ion source and vacuum to the detector. Chapter 2 – Section 1 addressed this requirement by introducing a buffer that has never been used for native-MS studies before. The introduced 4-ethyl morpholine/acetate buffer with pK_a close to the physiological pH outperformed the commonly applied solution of ammonium acetate in native mass spectrometry studies. Nonetheless, as commonly faced in sciences, these benefits are countered by significant disadvantages. In this case, the ideal buffer is both corrosive and toxic by nature. In addition, a new method was introduced to use arrival time distribution to study the compactness of proteins. The science of this section enables future studies on the protein-protein interaction of complex proteins with multiple subunits such as cardiac troponin. In addition, the introduced buffer and IMS-based calculation method enable the conformational studies of proteins to discover the changes imposed on proteins under different (patho-) physiological conditions. This section opens a new window in disease model's studies. Even though IMS and MS have been broadly used for intact protein studies, there is still no concrete evidence of whether proteins in the gas phase have the same 3D conformation as in their natural

liquid microenvironment. SPR gives an opportunity to study protein interactions in the liquid phase. In Chapter 2- Section 2 this technique was utilized to study the interaction of clinically important cardiac troponin subunits. Unlike other SPR studies, which investigate interactions of two proteins with each other, this section aimed to investigate the interactions of 3 protein subunits for the first time. Interestingly, as it was challenging to identify cardiac troponin I-cardiac troponin T (cTnI-cTnT) bicomplex with MS, we encounter the same challenge by SPR. There was no or a swift interaction between cTnI and cTnT. These findings emphasize the complexity of subunits I and T interactions as well as comparability of SPR and IMS-MS results. In addition, the findings of this chapter indicates the possibility of collecting unusual SPR signals for complex protein analysis. The main shortcoming of this study, alongside of all other SPR publications, is that the orientation of the immobilized proteins on the SPR sensor is not known. Future investigations should cover this important shortcoming. In addition, future work for complex protein analysis could include experiments with different orders of immobilization. Overall, this thesis expedited the potential of multiple analytical techniques to find an answer to fundamental questions and address application demands from multiple dimensions and various fields.

Valorization

Valorization

Creating impact has been the prime motivation and goal of my doctoral journey. Central was the creation of fundamental insight into principles of ion mobility spectrometry, new approaches in surface plasmon resonance, and even important the use of these technologies for in situ investigation of dynamic processes. The research described in this thesis, alongside other research and educational activities carried out during my PhD, was aimed at fulfilling this objective. As described below, some of the research outcomes had an immediate impact and some are anticipated to have a more long-term effect on academia, industry, and society.

Academic impact

One of the academic impacts, common to all chapters of this thesis, relates to the scientific breakthroughs in the field of drug discovery. Chapter 1 addresses this process from the small molecules' point of view. Chapter 1- Section 1 introduces an ion mobility-based methodology to discriminate structurally similar drug metabolites. The method is not exclusive to the test molecules, but rather a general approach applicable to a wide of range small molecules, enabling analytical chemists to implement a similar approach for the separation of isomeric compounds, which is necessary for pharmacokinetic and toxicological studies. In addition, this section discusses in detail the features of two types of ion mobility instruments. This can guide scientists to choose a suitable instrument for answering their research questions and improving their scientific impact.

Chapter 1- Section 2 evaluates a set of isomeric bile acids which are involved in a large variety of (patho)physiological conditions in the liver, kidney, intestine, lung, and even brain. Their diverse function on basis of small changes in their molecular structure, and therefore selective determination in biological materials, was the main rationale for studying their behavior in ion mobility spectrometry (IMS). The discussed science introduces different separation approaches by IMS and tandem mass spectrometry without chemically manipulating the molecules. The introduced methodology enables researchers to investigate the role and importance of structural isomers in the underlying molecular mechanisms of different diseases. These approaches were designed in a way to be translatable to complex biological samples, hence could be of use for clinical samples as well. In addition, this section aimed to fill one of the most important gaps in the field of IMS. Despite fast-growing progress in this field, there is limited knowledge on interpreting the actual mobility and collision cross section, while understanding the fate of molecules after ionization and throughout their trajectory in the mass spectrometer. This is essential for researchers to extract the correct information from their results and perform smart planning for (pre-) treatment of complex samples. The hyphenation of IMS with MS introduces the possibility of spatially resolving bile acids in a tissue by mass spectrometry-based imaging.

The scientific breakthroughs of Chapter 2 are related to the fast-developing area of native protein analysis. Chapter 2- Section 1 introduces a rediscovered buffer for studying proteins in their natural-like form by mass spectrometry. This opens a door for researchers to analyze a diverse range of proteins for target or biomarker identification

as well as structural and kinetic characterizations in relation to their biological activities. In addition, it provides the scientist with the possibility to elucidate molecular mechanisms involved in (phato)physiological conditions.

The initial results and observations from the previous section sparked the idea to further investigate the interaction of cardiac protein troponin subunits with surface plasmon resonance (SPR). For the SPR research project described in section 2, I was granted the competitive researcher fund of SWOL (University Fund Limburg). This section serves two main scientific impacts. One is suggesting a new approach for investigating the interaction kinetics of a complex protein's subunits. The other one is an attempt to study the kinetics of involved proteins in myocardial infarction. Myocardial infarction (MI) is one of the leading causes of death. The presented approach could ultimately unveil the proteins interaction mechanism, which can eventually aid in designing efficient diagnostic methods for discriminating MI from non-MI.

Chapter 3 is mainly focused on hyphenation sciences for studying small and large molecules. Chapter 3- Section 1 is a critical review of applied strategies to connect organ-on-a-chip with mass spectrometry. With this review, researchers can not only get an overview of previous attempts and discoveries but also, they can realize the shortcomings and focus on solving them.

The presented work in section 2 is adhering to the highly desired need for "flow chemistry", anticipated to be a more green and sustainable approach in the production of high-quality (purity) chemicals. The application of the specific design MS/MS -IMS scanning strategies and the use of fundamental insight into tandem mass spectrometry processes, allowed the in-situ detection of structural isomers, with even highly comparable MS/MS spectra. IMS served as a pre-separation step, before unraveling the structures by MS/MS. This approach is of special interest in the area of "Process Analytical technologies" as it enables chemists in a large variety of industrial applications to monitor chemical conversing processes, with high sensitivity and molecular structure resolved. The latter not being possible with the current and frequently applied IR and NMR technologies.

The majority of the findings and results presented in this thesis are published in open and peer-reviewed scientific journals. Hence, researchers with different scientific backgrounds can easily access the presented science and translate it to their research questions. The immediate academic impact of the published work in chapter 1- section 1 is reflected in the recognition by the journal of rapid communication in mass spectrometry (RCM). This article was recognized as one of the most read and downloaded papers in this journal between 2018 and 2019.

The PhD journey would not be complete without an impact on educating the next generation of scientists. Besides lecturing and tutoring that I carried out, one of the most effective approaches in transferring hard and soft professional skills as well as knowledge is to supervise undergraduates. The immediate academic impact of supervising 12 students (including HBO, bachelor, and master students) is reflected in their successful advancement in their following careers and education. In addition to

supervising students in STEM sciences, supervising honours+ students from social, political, and economic sciences added another dimension to the academic impact of my journey.

Industrial Impact

During my PhD journey, I had the unique opportunity to collaborate with multiple industrial partners active in the fields of polymer materials (DSM Materials Research Center), production of industrial enzymes (DSM Food), advanced chemical synthesis and biocatalysis (Innosyn), drug delivery and click chemistry (Cristal Therapeutics), pharmaceutical R&D (Janssen Pharmaceutica), synthetic biobased polymers (Be4Plastics), producer of flow-reactors (Chemtrix) and the manufacturer of advanced SPR technologies (Bionavis).

For instance, the performed projects together with DSM centers were focused on separation sciences for fast and effective analysis of low caloric sweeteners (steviol glycosides) and metabolites of a drug candidate for epilepsy disease. The results of these fruitful collaborations were a published paper (Chapter 1- Section 1) as well as the implementation of the introduced principle in their routing analysis.

The performed projects in collaboration with Janssen Pharmaceutica led to three different publications including Chapter 1 – Section 1, a just-published paper in RCM as the shared co-first author as well as a published paper in the journal of Analytical and bioanalytical chemistry. My contribution to the latest paper was to develop a novel 3D-printed mold for quantitative mass spectrometry imaging. This mold is now routinely used in the laboratories of Janssen Pharmaceutica.

The fruitful collaboration with Cristal Therapeutics resulted in a publication in the journal of Chemical science and the granting of a patent for the specific click chemistry discovered. The patented CliCr technology has been recently sold to Synaffix. In the project, MS was applied for the in-situ monitoring of cyclo addition reactions (Click Chemistry), once again proving the ability of MS and possibly IMS technologies for the accurate monitoring of (bio)chemical conversions. The industrial impact of the in-situ MS experimentation is eminent.

Industry 4.0 or the fourth industrial revolution centers around smart factories, where continuous manufacturing processes such as "flow-chemistry" will play a dominant role in the further electrification and green production of the chemical industry. The implementation of flow chemistry and online reaction monitoring are two of the important drivers toward Industry 4.0. With this goal in mind, and in collaboration with Chemtrix, a commercially available microflow reactor was hyphenated with IMS-MS for the online reaction monitoring by IMS and MS/MS. This work (chapter 3- Section 2) was published in the journal of Flow chemistry to reach out to academic and industrial researchers proving the tremendous potential of the discussed and combined IMS, MS/MS strategies.

The success of our collaboration with BioNavis is reflected in the presented work in Chapter 2- Section 2. Our fruitful collaboration ensured that the SPR community is

familiarised with the unique feature of BioNavis for easy monitoring of the full angel range, routine analysis, and easy implementation in the industry. In addition, the introduced approach provides insights for pharma R&D to develop novel diagnostic strategies to be able to discriminate myocardial infarction from other diseases.

Furthermore, in the pursuit of translating fundamental research to functional products and solutions, together with NWO (Dutch Research Council) and Lorentz center, we organised the "Life Sciences with Industry" workshops in 2020 and 2021. This workshop encouraged cooperation and the exchange of knowledge between academia and industry. In a stimulating setting, scientists and researchers from both academia and industry worked closely together to find innovative solutions to scientifically challenging and commercially important R&D problems of the invited industry partners. Participants were young and talented scientists (PhDs, postdocs, and more experienced researchers) from different sectors of the life sciences and physics, guided by senior researchers from industry and academia. Even though we had to cancel our workshop in 2020 due to Corona restrictions, the success of this workshop in 2021 allowed me and others to directly benefit from the impact of scientific research in the context of business and industry.

Societal impact

The research projects of which a considerable part forms the basis of this thesis were directed to a more fundamental understanding of analytical technologies, the design of novel approaches to detect selectively structural isomers, and research (bio) chemical processes including click chemistry, biocatalysis and the dynamic interaction of protein subunits in the formation of 3D structures. These projects were performed in collaboration and co-creation with both academic and industrial partners from M4i, Maastricht University, Brightlands Chemelot R&D campus, and abroad. Besides a diversity of small molecules, proteins, and synthetic polymers were investigated broadening my scope on sciences. Hence, an additional target group of this thesis was improving the life quality of society, which includes not only patients but also their families, caregivers, and the social security system. The offered approach in this thesis will affect society from different aspects of diagnosis, prevention, treatment, and economy. Chapter 1- Section 1 is examining the metabolites of a potential drug candidate, targeting the treatment of patients suffering from epilepsy disease. Chapter 1- Section 2 is analyzing bile acids that are involved in multiple pathological pathways including neurodegenerative diseases such as Alzheimer's and Parkinson's. This study can potentially serve diagnostic, prevention, and treatment purposes. The same applies to Chapter 2- Section 1. This study is introducing an approach to analyze and study proteins as key elements for identifying biomarkers or targets. Chapter 2- Section 2 is directly analyzing cardiac troponin complex for elucidation of the mechanism of myocardial infarction to eventually come up with a more efficient diagnostic method. Chapter 3- Section 1 is an opening towards constructing a more precise platform for understanding disease mechanisms and finding the most optimal treatment approaches, particularly personalized medicine. Chapter 3- Section 2 is in line with the call of the FDA (Food and Drug Administration) to switch from batch process to continuous flow chemistry. The presented work offers an efficient approach to drug

discovery that can eventually increase the speed of medicine available to patients, reduce waste to provide an environmentally clean production method, and use less material to alleviate economic burdens.

In addition, as scientists, we are also responsible to communicate our contemporary scientific developments to society. This way we can keep them well informed and aware of our findings and future steps, receive their insight and hear their discussions and needs. To this end, I used two platforms TEDx Maastricht (2018) and Pint of Science Maastricht (2022) to engage the public with my PhD research and findings.

Lastly, my interest in the socio-political topic of inequality led me to participate in the "Honours+ program challenge" organized by Maastricht University EDLAB in 2020-2021 and 2021-2022. The results of these works are the publicly available critical literature studies with the proposed solutions for two specific inequality problems. The immediate and futuristic academic and societal impacts of these efforts could be valorized by winning the "Honours+ program challenge" for two consecutive years.

Summary

Summary

Detecting, identifying, and characterizing molecules and structures as the substance of life are essential steps toward unveiling their role as a sole entity or more commonly as a part of a larger molecular assembly for specific biological functionalities. Next, it is of pivotal importance to translate the acquired knowledge of molecular structures and their activity to a more comprehensive understanding of the biological process, such as the biochemical foundations of diseases or metabolic disorders. The aim and ultimate outcomes of this thesis were to address these two aspects by offering new analytical strategies.

Chapter 1 is focused on the molecular structure assessment of small molecules, including drug metabolites and potential biomarkers, and drug targets.

Section 1 introduces strategies to differentiate 10 isomeric metabolites of a medicinal drug candidate, for the treatment of epilepsy. This was done by introducing ion mobility-based strategies and monitoring the mobility of the fragment ions. Next to this, the study investigated the analytical capabilities of two types of ion mobility instruments: traveling wave ion mobility (TWIMS) and trapped ion mobility spectrometry (TIMS). The results of this study indicated the influence of adduct(s) in the gas phase conformation of ions, which inevitably impacts their mobility.

Section 2 provides fundamental insights to assist in interpreting the ion mobility data (Collision Cross Section) and understanding the fate of ions in the gas phase. To this end, 14 clinically important bile acids, which included enantiomeric, diastereomeric, and structural isomers were studied. The outcome of this section enables extracting correct information from ion mobility spectrometry data and predicting the possibility of ion mobility separation. In addition, unlike previous studies, this section includes methodologies to separate isomers in a complex sample. These methodologies will enable scientists to directly examine and separate their complex (pre-) clinical samples.

The focus of Chapter 2 addresses challenges encountered in protein characterization and interactions studies. Section 1 introduces a rediscovered buffer, which has not been considered in the area of native mass spectrometry. Compared to the well-known and widely applied ammonium acetate it generates lower charge states opening a new research window in assessing the complex structures of proteins or assemblies thereof. The clinically important cardiac troponin complex was examined in native form for the first time using this buffer. In section 2, a follow-up study on the protein-protein interaction of three cardiac troponin subunits by surface plasmon resonance is described. The newly introduced methodology is likely to be of benefit for studying other complex protein complexes with more than two subunits.

Considering that life is dynamic in nature, we ought to perform our science in dynamic form as well, hence Chapter 3. The first section of this chapter provides an overview of coupling dynamic systems such as organ-on-a-chip to mass spectrometry for real-life monitoring, and selective, sensitive, and fast detections. Section 2 takes a step forward and analyses a dynamic chemical reaction in an on-line fashion by mass, tandem mass, and ion mobility spectrometry. This section discusses in detail the possibilities for on-

line monitoring of a microflow chemical reaction and the separation of structural isomers. In addition, it introduces a new strategy for annotating ion mobility spectra in the absence of standard molecules.

Samenvatting

Samenvatting

Het detecteren, identificeren en karakteriseren van moleculen en structuren als de bouwstenen van het leven zijn essentiele stappen richting het ontdekken van hun rol als unieke entiteit of, meer gebruikelijk, als onderdeel van een groter moleculaire geheel, voor specifieke biologische functies. Daarnaast is het van esentieel belang om de opgedane kennis van moleculaire structuren en hun activiteit te vertalen naar een meer alomvattend begrip van biologische processen, zoals de onderliggende biochemische fundamenten van ziekten en metabole aandoeningen. Het doel en de uiteindelijke uitkomst van deze thesis is het aampakken van deze twee aspecten door het aanbieden van nieuwe analytische strategiën.

Hoofdstuk 1 is gericht op de beoordeling van de moleculaire structuur van kleine moleculen, inclusief metabolieten van medicatie, potentiele biomarkers, en medicijn doelwitten. Deel 1 introduceert strategiën voor het differentieren van 10 isomere metabolieten van een kandidaat medicijn voor de behandeling van epilepsie. Dit werd gedaan door het introduceren van op ion mobiliteit-gebaseerde strategiën en door het observeren van de mobiliteit van fragment ionen. Daarnaast onderzoch deze studie de analytische mogelijkheden van 2 soorten ion mobiliteit instrumenten. De "Traveling Wave ion mobility spectroemtry" (TWIMS; reizende golf ion mobiliteit spectrometrie) en de "Trapped ion mobility spectrometry" (TIMS; gevangen ion mobiliteit spectrometrie). De resultaten van deze studie duidden op de invloed van adducten op vorm van moleculen in de gas fase , wat een onheroepelijke invloed heeft op hun mobiliteit.

Deel 2 geeft fundamentele inzichten die het interpreteren van ion mobiliteit data ("Collision Cross Section"; botsings-doorsnede) en het begrip van het lot van ionen in de gas fase ondersteunen. Hiervoor werden 14 klinisch relevante galzouten bestudeerd, die enantiomeren, diastomerenl, en structure isomeren bevatten. De uitkomst van dit deel biedt de mogelijkheid om de juiste informatie uit ion mobiliteit data te halen en om de mogelijkehid tot het gebruik van ion mobiliteit spectrometrie te voorspellen. Daarnaast, in tegenstelling tot voorgaande studies, bevat dit deel methodologiën om isomeren te scheiden in complexe monsters. Deze methodologiën laten wetenschappers toe om complexe (pre-)klinische monsters direct te bestuderen en te scheiden. De nadruk van hoofdstuk 2 ligt op het aanpakken van de uitdagingen met betrekking tot eiwit karakterisering and interactie studies. Deel 2 introduceert een herontdekte buffer welke niet eerder werd overwogen voor het gebruik in native massa spectrometrie. Vergeleken met het bekende en wijd-toegepaste ammonium accetaat genereert het een lagere lading staat die een nieuw onderzoeksdeel biedt voor het beoordelen van complexe eiwit structuren en eiwit samenstellingen. Het klinisch belangrijke "cardiac troponin" complex werd voor de eerste keer in de native vorm onderzocht met behulp van deze buffer. In deel 2, wordt een vervolg studie gericht op eiwit-eiwit interacties van die 3 cardiac troponin subdelen met begulp van oppervlakte plasmon resonantie beschreven.

Gezien het feit dat het leven van nature een dynamisch proces is, dienen we onze wetenschap ook in een dynamische vorm uit te voeren, vandaar hoofdstuk 3. Het eerste

deel van dit hoofdstuk geeft een overzicht van mogelijke koppelingen van dynamische systemen, zoals “organ-on-a-chip”, aan massa spectrometrie voor live, selectieve, gevoelige en snelle waarnemingen. Deel 2 neemt een stap voorwaarts en analyseert op een online manier een dynamische chemische reactie met massa, tandem massa, en ion mobiliteit spectrometrie. Dit deel bediscussieerd in detail de mogelijkheden voor het online monitoren van microflow chemische reacties en de scheiding van structurele isomeren. Daarnaast introduceert het een nieuwe strategie voor het annoteren van ion mobiliteits data (Collision cross sections & arrival time distributions) zonder gebruikt te maken van intern standaarden.

Appendix

Chapter 1 - Section 1

Adduct ion formation as a tool for the molecular structure assessment of ten isomers in traveling wave and trapped ion mobility spectrometry

Scan QR code for Supplementary information

Chapter 1 - Section 2

Uncovering the behaviour of ions in the gas-phase to predict the ion mobility separation of isomeric steroid compounds

Scan QR code for Supplementary information

Chapter 3 - Section 2

Ion mobility spectrometry-tandem mass spectrometry strategies for the on-line monitoring of a continuous microflow reaction

Scan QR code for Supplementary information

Chapter 2 - Section 1

Insulin - nano-ESI-TWIMS-TOF

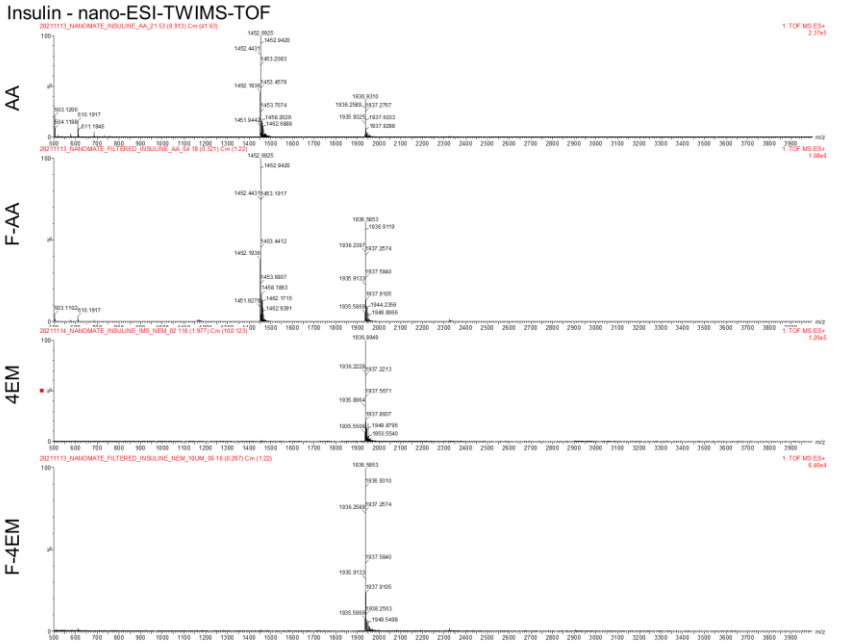

Ubiquitin - nano-ESI-TWIMS-TOF

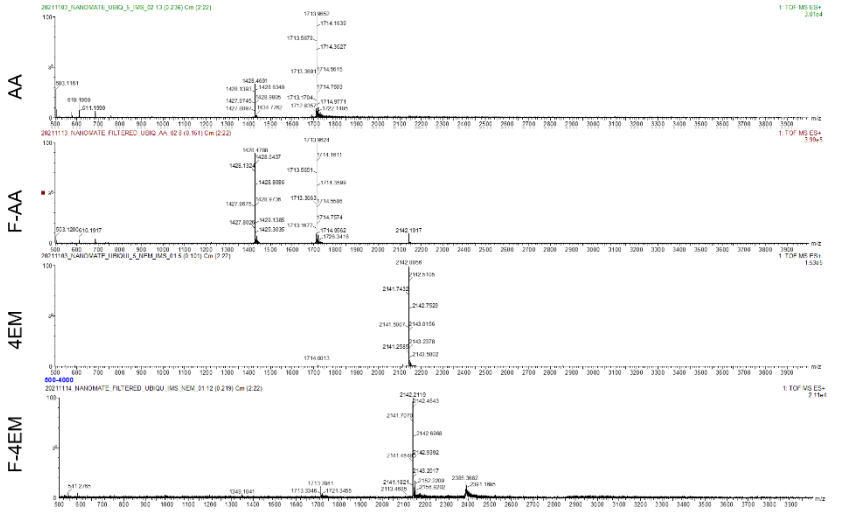

RNase - nano-ESI-TWIMS-TOF

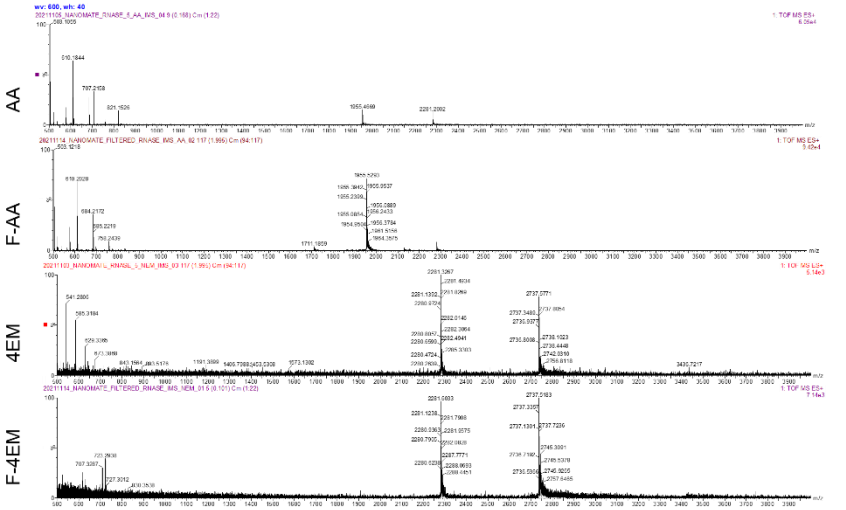

Lysozyme - nano-ESI-TWIMS-TOF

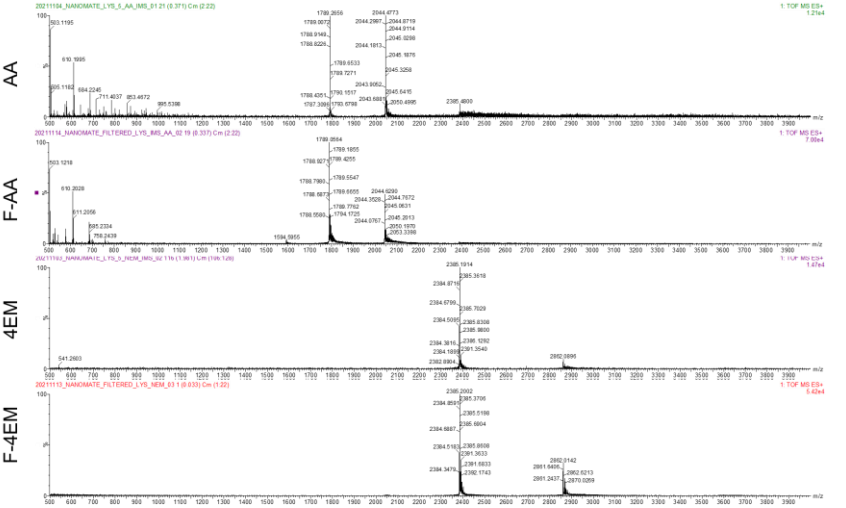

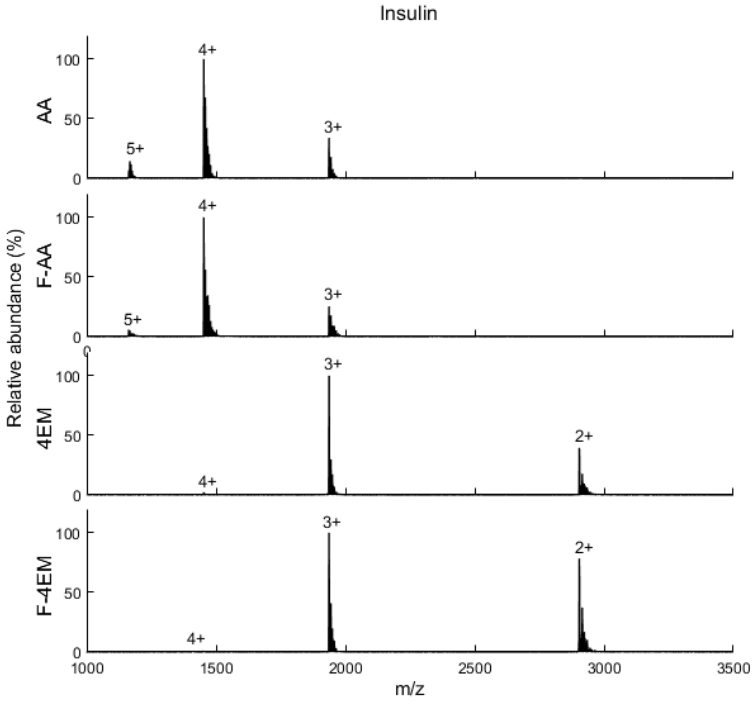
Insulin
AA
F-AA
4EM
F-4EM
Relative abundance (%)
m/z
4+
5+
3+
2+
1000
1500
2000
2500
3000
3500

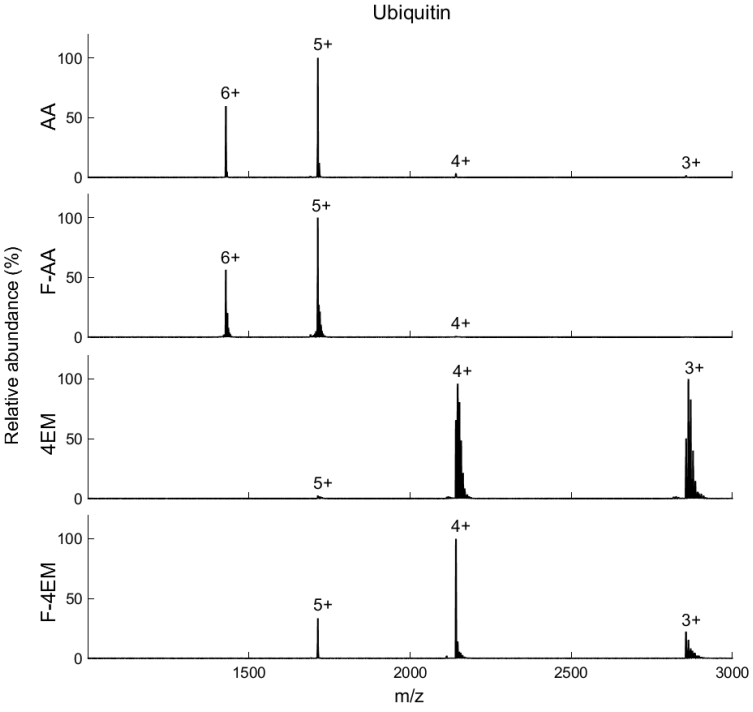
Ubiquitin
AA
F-AA
4EM
F-4EM
Relative abundance (%)
m/z
6+
5+
4+
3+
1500
2000
2500
3000

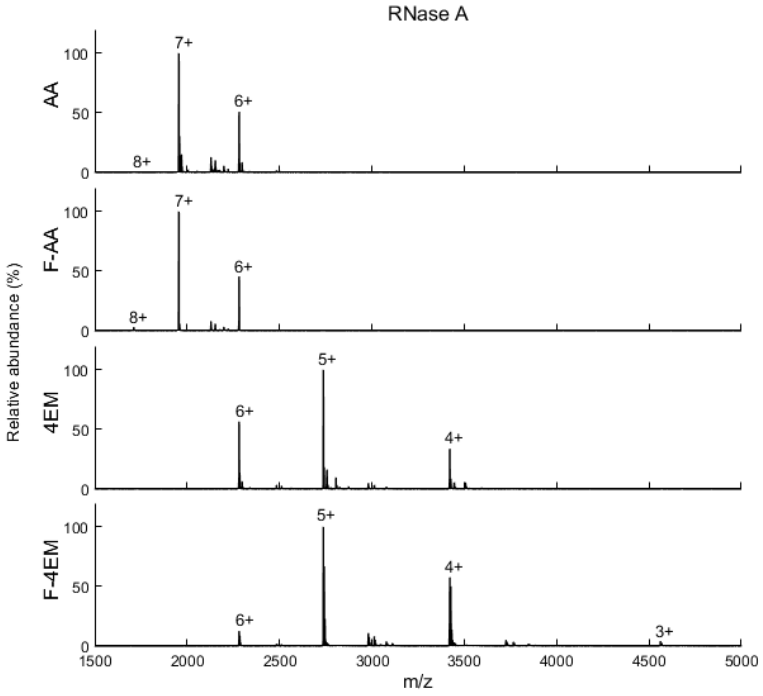
RNase A
AA
F-AA
4EM
F-4EM
Relative abundance (%)
m/z
7+
6+
8+
5+
4+
3+

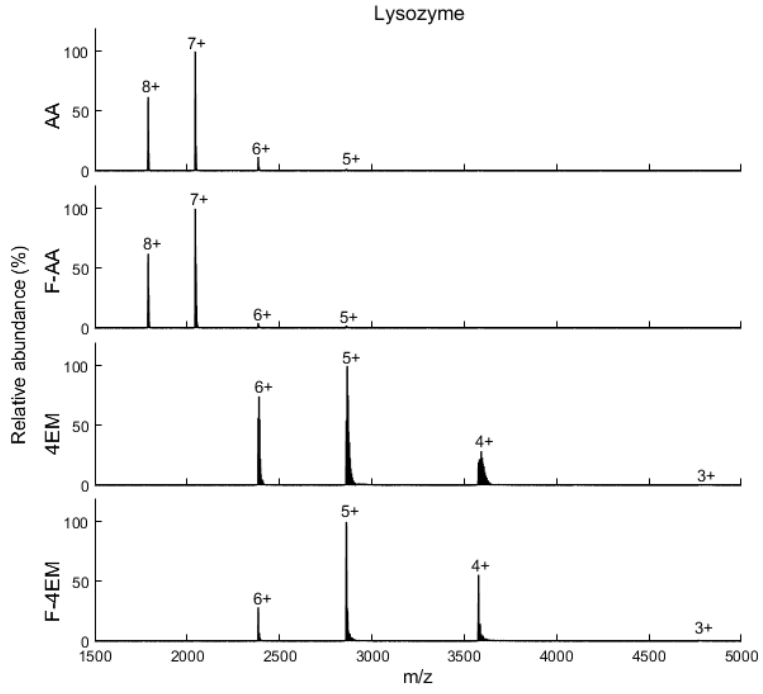
Lysozyme
AA
F-AA
4EM
F-4EM
Relative abundance (%)
m/z
7+
8+
6+
5+
4+
3+

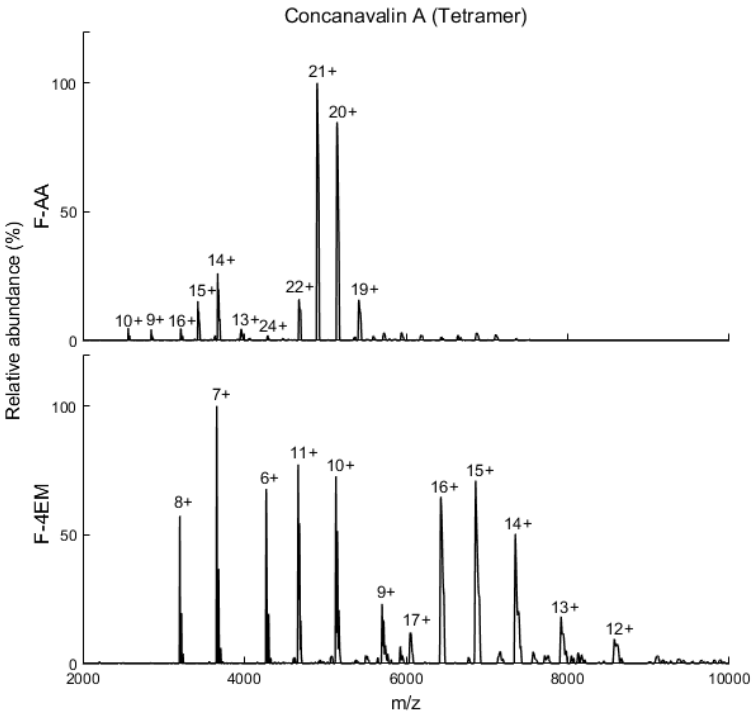

Figure S1.The nano-ESI-MS of proteins in AA, F-AA, 4EM and F-4EM analyzed by TWIMS-TOF and UHMR Q-Exactive orbitrap.

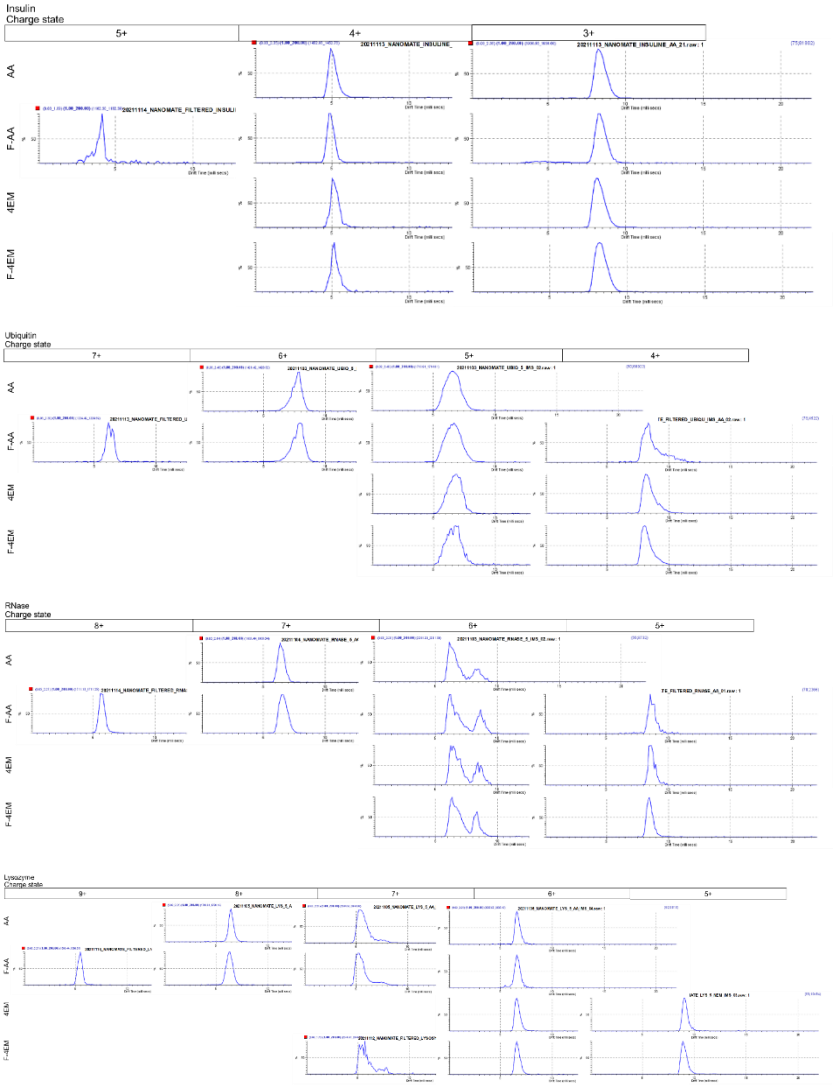

Figure S2. The ATD of each protein compared among charge states.

Abbreviations

3D	3-Dimensional
4EM	4-Ethylmorpholine
4M2P	4-Methyl-2-Pentanone
AcOH	Acetic Acid
AcOH	Acetic Acid
ACN	Acetonitrile
α-MCA	Alfa-Muricholic Acid
AlloCA	Allocholic Acid
AD	Alzheimer'S Disease
APCI	Atmospheric Pressure Chemical Ionisation
APPI	Atmospheric Pressure Photoionization
BPR	Back Pressure Regulator
β-MCA	Beta-Muricholic Acid
CE	Capillary Electrophoresis
Chip-LC	Chip Based Lc
CCS	Collision Cross Section
CE	Collision Energy
CID	Collision Induced Dissociation
DFT	Density Functional Theory
DCM	Dichloromethane
DA	Diels-Alder
EME	Electromembrane
ESI	Electrospray Ionization
ELISA	Enzyme-Linked Immunosorbent Assays
EHSS	Exact Hard-Sphere Scattering
EIM	Extracted Ion Mobilogram
FA	Formic Acid
F	Fragment Ions
FWHM	Full Width At Half-Maximum
γ-MCA	Gamma- Muricholic Acid
GC	Gas Chromatography
GCDCA	Glycochenodeoxycholic Acid-3-Sulfate Sodium Salt
GDCA	Glycodeoxycholic Acid-3-Sulfate Sodium Salt
GAC	Green Analytical Chemistry
HD	High-Definition
HPLC	High-Performance Liquid Chromatography
IR	Infrared
IMS	Ion Mobility Spectrometry
LC	Liquid Chromatography

MS	Mass Spectrometry
m/z	Mass-Over-Charge Ratio
MALDI	Matrix Assisted Laser Desorption/Ionization
MMFF	Merck Molecular Force Field
MeOH	Methanol
MI	Myocardial Infarction
NMR	Nuclear Magnetic Resonance
ω-MCA	Omega-Muricholic Acid
OOC	Organ-On-A-Chip
PD	Pharmacodynamic
PK	Pharmacokinetic
PDMS	Polydimethylsiloxane
PMMA	Polymethyl Methacrylate
P	Precursor Ion
PAT	Process Analytical Technologies
PA	Projection Approximation
Q-TOF	Quadrupole Time-Of-Flight
SPE	Solid Phase Extraction
SLM	Supported Liquid Membrane
SPR	Surface Plasmon Resonance
MS/MS	Tandem Mass Spectrometry
TCDCA	Taurine Conjugated Chenodeoxycholic Acid
TDCA	Taurine Conjugated Deoxycholic Acid
Tα-MCA	Taurine conjugated Alfa-MCA
Tβ-MCA	Taurine conjugated Beta-MCA
Tγ-MCA	Taurine conjugated Gamma-MCA
Tω-MCA	Taurine conjugated Omega-MCA
TLC	Thin Layer Chromatography
TOF	Time-Of-Flight
TM	Trajectory Method
TEER	Transepithelial Electrical Resistance
TIMS	Trapped Ion Mobility Spectrometry
TWIMS	Traveling Wave Ion Mobility Spectrometry
UV-Vis	Ultraviolet-Visible
H_2O	Water

Curriculum Vitae

Darya Hadavi

Curriculum Vitae

LinkedIn link

- [2023] • **Postdoctoral researcher on developing antimicrobial technologies on hard and soft tissue implants,** M4I institute, Faculty of Health, medicine and life science, Maastricht university, The Netherlands
  Supervisors: Dr. Berta Cillero Pastor and Prof. dr. Maarten Honing

- [2018-2022] • **PhD Candidate on strategies for molecular structure elucidation in static and dynamic systems**, M4I institute, Faculty of Health, medicine and life science, Maastricht university, The Netherlands
  Promotor: Prof. dr. Maarten Honing
  Co-promotors: Dr. Tiffany Porta Siegel and Dr. Eva Cuypers

- [2017-2018] • **Scientific researcher on Coccolithophores-on-a-chip**, MESA+ Institute for Nanotechnology, MIRA Institute for Biomedical Technology and Technical medicine, The university of Twente, The Netherlands.
  Supervisor: Prof. dr. ir. Albert van den Berg, Dr. ir. Wouter Olthuis

- [2016] • **Research Intern in 3D printing and vessel-on-a-chip,** Micronit Microtechnologies, Enschede, The Netherlands.

- [2015-2016] • **Honors master in leadership and management**, The University of Twente, The Netherlands.
  Supervisor: Prof. Celeste Wilderom

- [2014-2016] • **MSc in Biomedical engineering-Bionanotechnology**, The University of Twente, The Netherlands.
  Thesis: Towards an alveolar-capillary barrier on-a-chip platform for nanoparticle
  Supervisors: Dr. Séverine Le Gac, Dr. Adithya Sridhar

- [2012-2014] • **Laboratory supervisor and manager at bacteriology lab,** Tehran Province Water and Wastewater (TPWW) Company, Tehran, Iran.

- [2008-2012] • **BSc in Cellular and Molecular Biology**, Azad university of Tehran Medical science, Iran.

- [1989] • **Born in Ardebil, Iran**

Awards and grants

- 2022 - Honours+ program challenge winner, Maastricht University EDLAB
- 2021 - Workshop grant award by Lorentz Centre, Leiden University and NWO
- 2021 - University Fund Limburg (SWOL) grant, Maastricht university
- 2021 - Honours+ program challenge winner, Maastricht University EDLAB
- 2020 - Best poster award, ISIMS, Virtual Poster Symposium, USA
- 2020 - The most read and downloaded article of the RCMS journal
- 2019 - NVMS Travel award
- 2017 - Active board member award of IrNUT, university of Twente
- 2016 - First poster award, NanoCity national conference, Amsterdam
- 2015 - Henk Zijm award, University of Twente
- 2014 - University of Twente master program scholarship award (UTS), University of Twente
- 2013 - Excellent performance award in proficiency test, Water and Wastewater Company, Iran
- 2012 - Top 3% BSc student award, Azad university of Tehran Medical Science, Tehran, Iran.

Oral and poster presentations during the PhD

- Advances in ion mobility spectrometry strategies to go beyond separation, Oral presentation and parallel session chair, The International Mass Spectrometry Conference (IMSC). 2022. Maastricht, The Netherlands.
- Pint of Science talk to public audience, Oral presentation. 2022. Maastricht, The Netherlands.
- Multiple reaction monitoring and 3D printed mimetic tissue model for absolute quantitation in mass spectrometry imaging, Poster presentation and parallel session chair, NWO CHAINS . 2021. The Netherlands.
- Microflow reactor hyphenated with ion mobility -mass spectrometry for drug discovery, Poster presentation and parallel session chair, TERMIS world congress. 2021. The Netherlands.
- The molecular structure identification and separation of bile acids by experimental and theoretical investigation of their behaviour in Ion Mobility-Mass Spectrometry, Poster presentation, ISIMS. 2020. Virtual Poster Symposium.
- Bridge academia and industry with flow reactors coupled with IMS-MS, Invited speaker, NVMS fall conference. 2019. Leiden, The Netherlands.
- Ion mobility separation of structural and stereoisomers by adduct ion formation, Poster presentation, 4th NVMS-BSMS Conference on Mass Spectrometry. 2019. Rolduc, The Netherlands.
- TEDx, 2018. Maastricht, The Netherlands.

- Advancing ion mobility separation and MS/MS strategies using adduct ion formation: broadening the scope to structural and stereoisomers, Oral presentation, 6th Chemistry as innovating science (CHAINS) conference. 2018. Veldhoven, The Netherlands.

List of publications

This thesis is based on the following publications

Hadavi, D., de Lange, E., Jordens, J., Mengerink, Y., Cuyckens, F., & Honing, M. (2019). Adduct ion formation as a tool for the molecular structure assessment of ten isomers in traveling wave and trapped ion mobility spectrometry. Rapid Communications in Mass Spectrometry, 33(S2), 49-59. doi:https://doi.org/10.1002/rcm.8419

Hadavi, D., Borzova, M., Porta Siegel, T., & Honing, M. (2022). Uncovering the behaviour of ions in the gas-phase to predict the ion mobility separation of isomeric steroid compounds. Analytica Chimica Acta, 1200, 339617. doi:10.1016/j.aca.2022.339617

Hadavi, D., Ng, C. Y., Zhao, Y., Mathew A., Anthony I. G. M., Cuypers E., Porta Siegel, T., Honing, M. "Buffer 4-ethylmorpholine/acetate maintains solution phase folding for native mass spectrometry of proteins and proteins complexes". Submitted

Zhao, Y., Šimičić, N., Albers, M., Honing, M., **Hadavi, D.** "Investigating the protein-protein interactions of cardiac troponin subunits using surface plasmon resonance". In preparation

Hadavi,D., Tosheva, I., Porta Siegel, T., Cuypers, E., Honing, M. "Technological advances for analysing the content of organ-on-a-chip by mass spectrometry". Submitted

Hadavi, D*., Han, P*., & Honing, M. (2021). Ion mobility spectrometry-tandem mass spectrometry strategies for the on-line monitoring of a continuous microflow reaction. Journal of Flow Chemistry. doi:10.1007/s41981-021-00209-7

Other publications during the PhD

Lamont, L***., Hadavi, D***., Bowman, A. P., Flinders, B., Cooper-Shepherd, D., Palmer, M., . . . Heeren, R. M. A. High-Resolution Ion Mobility Spectrometry Mass Spectrometry for Isomeric Separation of Prostanoids after Girard's reagent T Derivatization. Rapid Communications in Mass Spectrometry, n/a(n/a), e9439. doi:https://doi.org/10.1002/rcm.9439.

Calore, A. R., **Hadavi, D**., Honing, M., Albillos-Sanchez, A., Mota, C., Bernaerts, K., . . . Moroni, L. (2022). Cholecalciferol as Bioactive Plasticizer of High Molecular Weight Poly(D,L-Lactic Acid) Scaffolds for Bone Regeneration. Tissue Eng Part C Methods, 28(7), 335-350. doi:10.1089/ten.TEC.2022.0041

van Slagmaat, C. A. M. R., Noordijk, J., Monsegue, L. G., Mogensen, S., **Hadavi, D**., Han, P., . . . De Wildeman, S. M. A. (2021). Bio-based synthesis of cyclopentane-1,3-diamine and its application in bifunctional monomers for poly-condensation. Green Chemistry. doi:10.1039/D1GC02372A

van Slagmaat, C. A. M. R., Faber, T., Chou, K. C., Schwalb Freire, A. J., **Hadavi, D**., Han, P., . . . De Wildeman, S. M. A. (2021). Chemoselective formation of cyclo-aliphatic and cyclo-olefinic 1,3-diols via pressure hydrogenation of potentially biobased platform molecules using Knölker-type catalysts. Dalton Transactions, 50(29), 10102-10112. doi:10.1039/D1DT01252E

Lamont, L., **Hadavi, D**., Viehmann, B., Flinders, B., Heeren, R. M. A., Vreeken, R. J., & Porta Siegel, T. (2021). Quantitative mass spectrometry imaging of drugs and metabolites: a multiplatform comparison. Analytical and Bioanalytical Chemistry, 413(10), 2779-2791. doi:10.1007/s00216-021-03210-0

Weterings, J., Rijcken, C. J. F., Veldhuis, H., Meulemans, T., **Hadavi, D**., Timmers, M., . . . Liskamp, R. M. J. (2020). TMTHSI, a superior 7-membered ring alkyne containing reagent for strain-promoted azide–alkyne cycloaddition reactions. Chemical Science, 11(33), 9011-9016. doi:10.1039/D0SC03477K

van Slagmaat, C. A. M. R., Chou, K. C., Morick, L., **Hadavi, D**., Blom, B., & De Wildeman, S. M. A. (2019). Synthesis and Catalytic Application of Knölker-Type Iron Complexes with a Novel Asymmetric Cyclopentadienone Ligand Design. Catalysts, 9(10), 790.

Han, P*., **Hadavi, D*.,** Zoidis, S., Honing, M. Investigating the effect of proton shift and its effect on tandem mass spectrometry; a combined tandem mass spectrometry, ion mobility, and density functional theory study. In preparation.

* Shared co-first authors

Acknowledgments

Human Beings are members of a whole	بنی آدم اعضای یک دیگرند
In creation of one essence and soul	که در آفرینش زیک گوهرند
If one member is inflected with pain	چو عضوی به درد آورد روزگار
Other members uneasy will remain	دگر عضوها را نماند قرار
If you have no sympathy for human pain	تو کز محنت دیگران بی غمی
The name of human you cannot pertain	نشاید که نامت نهند آدمی
Saadi Shirazi	سعدی شیرازی

As a part of a whole, I could not be in my current position without others. Who did not remain easy through my PhD journey and have been there for me, for a diverse range of reasons and I am sincerely grateful for every one of them.

Love of my life **Papa and Mama**, thanking you is the most difficult part of writing this thesis. How can I be grateful enough? How can I write about multiset of your support? You have been in each piece of my universe, with your love, support, encouragement, insightful discussion, guidance, strength, inspiration and and and. May my life path will return this much of goodness in action. I am wholeheartedly thankful for your lively existence. Words fail to express the gratitude in my heart for all you have given me.

Maarten, with full confidence I say that you are one of a kind promoter. The very first agreement we made was that you said, “I will push you to top, and you will have to jump” and we shook hands on it. This principle that is still going on, made me strive to perform my best. In this journey, despite all my shortcomings, you never doubted me, you never made me feel staying alone in the dark and you never became disappointed in me. Rather, you gave me constructive criticism, challenged me, instructed me to find a correct direction and constantly supported me. Our scientific discussions have always been the best source of knowledge for me, where I was also encouraged to think out of box. Apart from being an incredible PhD promotor, you have also been a life coach. You lead by example to learn leadership, management, communication, team working and critical thinking skills as well as being committed, responsible, understanding, humble, caring, selfless, and resilient. I can write pages about all I learnt from you. I am sincerely and wholeheartedly grateful for your constant support and all you have taught me.

Helen, for me you are the symbol of beauty, not only outside but also inside. I always loved your energy and positivity, and I enjoyed our conversations. You have always made my life easier. Thank you for all of that.

Eva and Tiff, I appreciate to take the responsibility of being my co-promoters and giving constructive feedbacks on my works. On top of all thanks for trusting my work.

Ron, working at M4i has been an inspiring experience both academically and in terms of following your challenges, successes, and evolutions as an open access lecture. I am very grateful to you for providing an environment where I could constantly learn and improve, and where I could make the best use of the facilities and infrastructure.

Dear assessment committee, **Prof. Dr. Edwin De Pauw, Prof. Dr. Lorenzo Moroni, Dr. Ingrid Dijkgraaf and Dr. Tim Causon**, I would like to express my gratitude for taking the time to read and evaluate my thesis. I am looking forward to closely collaborate with you and we push the limits of science together.

Dear collaborators**, Jan Jordens, Ynze Mengerink, Filip Cuyckens, Peter Quaedflieg, Martin Albers, Jimmy Weterings, Rob van der Hoeven, Samantha Hughes, Sabine van Rijt, Matt Baker, Douwe de Boer, Marc Escriba, Frank Schaap, Burgert Blom and Fred van Geenen,** one of the greatest honours during my PhD journey was to work with you. I am very grateful for giving me the opportunities. This thesis is not an end for our collaboration. I will always look for further opportunities to work with you and bring more to the able of both academia and industry.

Andrew and Lennart, when I began my PhD, you have been my go-to guys, who listened to me, explained, and guided me, without any judgment but very patiently. I always looked up to you and enjoyed our scientific and friendly conversations.

Kasper and Ben you guys have always been supportive and made time for me to listen and give me necessary advice. My sincere appreciation.

Yuandi, your kind and happy spirit has always been an inspiration for me. Thank you for irradiating positive energy.

Ronny, thank you very much for bearing with me and my students. You have always kept a smile on your face and made me feel very comfortable to approach you for help and advice. I appreciate it very much.

Berta, your career path has been an inspiration for me, and I am very glad to begin my Postdoc journey with you. I am sure working with you will bring many more dimension into my science career.

Rob, Shane, Benjamin, Ian and Sebastiaan, working in the same team as you and collaborating with you was an honour and the best approach to learn from you. Thanks for opportunities.

Britt, Sylvia, Anjusha, and Jian-Hua, we always had great chats together. We shared our worries and looked for solutions together and celebrated our achievements. I thank you for making my PhD journey a pleasant one.

Lieke, Nino, Jos, Kees, Lucia, Melissa, Florien, Lidia and Kimberly, my dearest officemates, I do admit that you made my working environment much more pleasant, happy, and joyful. Thank you for your positivity, sense of humour and all the smiles that you gave me.

Loes, Peiliang and Bo, I enjoyed working together with you within the team of Analytics in System Imaging. We explored together and learnt from each other. I thank you for giving these opportunities and I am glad that we had shared path.

Aljoscha, Layla, Ro Ro, Christel and Kim you guys made M4i fun again. Thank you for bringing more joy to the group. I cannot thank you enough for being supportive and caring.

P-Max, Frédéric, Florian, Nina, Anton, Maxime, Charles, Naomi, Stephanie, Brenda, Klara, Mudita, Tim, Michele, Fabian, Roel, Laura van Hese, Laura Kollau, Mirella, Joel, Navya, Bryn, Pieter, Chiara, Marta, Bea, Anton, Andrea, Christian, Ana Miguel, Anne, Philippe, Isabeau, Kasper, Michiel, Andrej, Abril, Hang, Annet, Ye, Annemarie, Hans, Gert and Frans, it was my pleasure to get to know you, work with you and make memories with you. Thank you for your contribution in the realization of my thesis.

My dearest students, **Erik, Edwin, Nhan, Alex, Nils, Rianne, Marina, Che Yee, Diana, Ilona, Jonah, Mariana, Robin, Nika, Atanas, Giulia, Hannah, Nele, Rob, Benedikt, Luca, Noemi, Clara and those who we worked together during student led projects.** I do admit that we learnt from each other and together, we experienced and experimented multiple topics of science together. I am very grateful for your contributions and for sharing this journey with me.

Vasilis, even though we did not get to finish our PhD journeys together, our past relationship was a school of life. I thank you for that.

My dearest **Iranian friends,** you guys have made living in The Netherlands a pleasant experience. You brought joy and fun to my life, and we could miss Iran together. You tolerated my hectic work schedule and always warmly supported and welcomed me. I love you all and I am very happy to share my Maastricht life with you.

My virtual friends from different parts of the world, meeting you and working with you has opened a whole new chapter in my life. It has been a great honour for me to meet **Iranian scholars fighting for liberty in the diaspora** and to know that each of you is doing an incredible work in your field. And yet, your sense of altruism has not allowed you to simply stay put when others are plagued by pain. Hats off to your sense of responsibility and the greatest appreciation. I am confident that hand in hand and with others we will overcome the darkness. Women, Life, Freedom.

And last but certainly not least, lovely **Elahe and Rashed**, my dearest sister and brother, all my life you have paved and smoothed the way for me. You have put yourselves in trouble to light my path. You have selflessly opened the way for me, even if it cost you. You have always stood up for me and constantly supported me. You changed your priorities for me. I do not know how I can ever be grateful to you for all you have done. I love you and I am deeply grateful for everything.